LIMB POSITION SENSE: ROLE OF LIMB POSTURE, VISUAL EXPERIENCE, AND INPUT FROM MUSCLE SPINDLE Ia AFFERENTS

A Dissertation
Presented to
The Academic Faculty

by

Kyunggeune Oh

In Partial Fulfillment
of the Requirements for the Degree
Doctor of Philosophy in the
School of Biological Sciences

Georgia Institute of Technology
May 2019

LIMB POSITION SENSE: ROLE OF LIMB POSTURE, VISUAL EXPERIENCE, AND INPUT FROM MUSCLE SPINDLE Ia AFFERENTS

Approved by:

Dr. Boris I. Prilutsky, Advisor
School of Biological Sciences
Georgia Institute of Technology

Dr. Young-Hui Chang
School of Biological Sciences
Georgia Institute of Technology

Dr. T. Richard Nichols
School of Biological Sciences
Georgia Institute of Technology

Dr. Aaron Young
School of Mechanical Engineering
Georgia Institute of Technology

Dr. Lewis A. Wheaton
School of Biological Sciences
Georgia Institute of Technology

Date Approved: [March 21, 2019]

I would like to dedicate my dissertation work to my loving wife Soyoung Park, my beloved children Olivia, Meredith, and Allison, my incredible parents, and my wonderful sister Mihyun who have been always supportive with love and understanding.

ACKNOWLEDGEMENTS

Firstly, I would like to express my sincere gratitude to my advisor Dr. Boris Prilutsky for his continuing support. His guidance and immense knowledge helped me conducting my research and writing this thesis. Beside my advisor, I would like to thank the rest of my thesis committee members for their insightful comments and encouragement. My sincere thanks also go to Dr. Alexander Klishko, Dr. Hangue Park, Dr. Ricky Metha, Dr. Joshua Jarrell, Dr. Teresa Snow, and Dr. Guay-haur Shue. I will always remember how they gladly helped me solve my many academic or non-academic problems.

TABLE OF CONTENTS

LIST OF TABLES

LIST OF FIGURES

LIST OF SYMBOLS AND ABBREVIATIONS

CNS	Central nervous system
CNV	Contingent negative variation
DC	Dorsal column(s)
DCN	Dorsal column nuclei
DDM	Direction and distance matching
DLF	Dorsolateral funiculus
EEG	Electroencephalography
EMG	Electromyography
ERP	Event-related potential
GTO	Golgi tendon organ(s)
HA	Hamstring muscle
JAM	Joint angle matching
LCN	Lateral cervical nuclei
MDDM	Mirrored direction and distance matching
RANK/LANK	Right/Left ankle joint
RELB/LELB	Right/Left elbow joint
REYE/LEYE	Right/Left eye
RF	Rectus femoris muscle
RFT/LFT	Right/Left forelimb toe
RHD/LHD	Right/Left head
RHIP/LHIP	Right/Left hip joint
RHT/LHT	Right/Left hindlimb toe

RIC/LIC	Right/Left iliac crest
RKNE/LKNE	Right/Left knee joint
RMCP/LMCP	Right/Left Metacarpophalangeal joint
RMTP/LMTP	Right/Left Metatarsophalangeal joint
RSCP/LSCP	Right/Left scapula
RSHL/LSHL	Right/Left shoulder joint
RWRT/LWRT	Right/Left wrist joint
SA	Satorious muscle
VA	Vasti muscle
VPL	Ventral posterolateral
$\dot{\theta}_s$, $\dot{\theta}_e$	Shoulder and elbow angular speeds in ^{o}/s
$\Delta X_H, \Delta Y_H$	Small changes in x and y coordinates of the hand
$\Delta\theta_s, \Delta\theta_e$	Small changes in shoulder and elbow joint angles
e_s, e_e	Physiologically relevant random angle errors at the shoulder and elbow
$\boldsymbol{J}^*$	Congjuate transpose of $\boldsymbol{J}$
J_m	Modified Jacobian
$\|\|\boldsymbol{J}\|\|$	Euclidean norm of $\boldsymbol{J}$
L_{fa}	Length of forearm with the hand
L_{ua}	Length of upper arm
X_E, Y_E	x and y coordinates of the elbow
X_H, Y_H	x and y coordinates of the hand
X_S, Y_S	x and y coordinates of the shoulder
θ_e	Elbow joint angle
θ_s	Shoulder joint angle

λ_i	i-th eigenvalue
$\boldsymbol{v_{max}}$	Eigenvector of the maximum eigenvalue
$\boldsymbol{v_{min}}$	Eigenvector of the minimum eigenvalue
$f(\theta_s, \theta_e)$	Forward kinematic equation
$\boldsymbol{J}$	Jacobian
Rot	Rotation matrix
$T(\theta_s, \theta_e)$	Transformation from joint angle coordinates to hand coordinates
$Trans$	Translation matrix
κ	Condition number
$\boldsymbol{v}$	Eigenvector

SUMMARY

Limb position sense is the ability to determine location and orientation of limb segments with respect to each other and with respect to the external environment without vision. Limb position sense is critical for accurate control of posture and movement. The lack of position sense due to illness has devastating consequences for the performance of even simplest motor tasks performed under visual control. Position sense of limb segments with respect to each other originates from joint angle-related sensory information provided by the muscle spindles, Golgi tendon organs and cutaneous afferents in skin overlying joints. Limb endpoint position sense with respect to external space can be derived by the nervous system through a transformation of joint-related coordinates to endpoint external coordinates using estimated dimensions of limb segments. This coordinate transformation and factors that can potentially affect accuracy and precision of endpoint position sense in external space are not fully understood, and many important questions remain unanswered. For example, it is not clear why people perceive hand position more precisely in the radial than in azimuth direction and closer to the body than farther away. Moreover, since vision contributes to forming somatosensory representations of body segment dimensions and to integration of somatosensory information encoded in joint-based and external coordinates, would long-term blindness differentially affect the limb position sense in joint and external space coordinates? Furthermore, what does happen to precision of limb endpoint positioning in external space if input from muscle spindle Ia afferents from a major limb joint is compromised? My work addressed all these questions.

Using a theoretical analysis of the transformation of random joint angle errors to random hand position errors for a two-joint kinematic arm model, I demonstrated that arm posture alone can explain the better precision of hand position sense in the radial than in azimuth direction and closer to the body than farther away. I confirmed the model predictions in experiments with healthy sighted individuals (n=11) who performed a hand position matching task. The fact that the predicted distributions of random hand position errors (precision ellipses) in the horizontal workspace were nearly orthogonal to the experimentally obtained arm stiffness ellipses reported in the literature, provides a mechanistic explanation for how the distribution of random hand position errors is shaped for any arm posture.

To investigate the role of visual experience in arm position sense in joint and external space coordinates, I investigated long-term blind (n=7) and age-matched sighted individuals (n=7) who performed three arm position matching tasks: joint angle matching (JAM), hand distance and direction matching (DDM), and hand distance and mirror direction matching (MDDM). The latter hand position matching task was kinematically identical to the joint angle matching task JAM. The blind participants generally had lower accuracy and precision of arm position sense in joint angle and hand position matching than the sighted. In addition, the blind had the same precision of arm position sense in the joint angle matching and hand position matching tasks. Measuring the Contingent Negative Variation-inspired EEG potential (CNV), an indicator of neurophysiological functions related to task complexity during the performance of arm matching tasks, revealed that the blind group had a higher EEG negative potential than the sighted group. Both subject groups demonstrated a higher EEG negative potential in the hand position matching DDM

task than in the joint angle JAM task or in another hand position matching MDDM. These results suggest that visual experience positively affects arm position sense possibly due to integration of visual and proprioceptive sensory information and the development of more accurate body schema. I suggest that similar precision of arm position sense in joint and external coordinates in the blind participants may result from a possible increase in perceptual acuity of other exteroceptors that could provide information about limb position in the peripersonal space. The lower accuracy and higher perceived task complexity in the DDM task, as judged from the EEG negative potential, may indicate more complex transformations from the joint coordinates to hand position coordinates required for this task.

In the last series of experiments, I investigated precision of hindpaw position control just before and right after the stance phase during walking in 4 cats after their major knee muscles were self-reinnervated unilaterally. This procedure compromises sensory input from Ia afferents (Cope at al. 1994), the main source of joint-related position information. Contrary to my expectations, the precision of paw position control at the late and mid-swing phase during walking significantly increased bilaterally. The animals achieved this by adopting a more extended hindlimb posture bilaterally during mid-swing and prior to stance onset. This extended limb posture reduces the radial random error, as follows from my theoretical analysis of precision of limb position sense.

These studies determined for the first time the contribution of limb posture, visual experience and proprioceptive input to accuracy and precision of limb position sense. This information will help design new diagnostic and therapeutic tools for people with visual and proprioceptive deficits. The gained understanding of random error distributions of

hand position sense can be used to design control panels for blind and sighted operators that increase precision and accuracy of control.

CHAPTER 1. INTRODUCTION

Limb position sense is the ability to determine location and orientation of limb segments with respect to each other and with respect to the external environment without vision. Limb position sense is a vital part of our daily life. We use it every day to control and maintain our body posture and react appropriately to changes in environment around us. The lack of position sense due to severe large-fiber sensory neuropathy has devastating consequences for the performance of even simplest motor tasks (Cole and Paillard 1995). The current consensus on the mechanisms responsible for limb position sense is that signals generated by the muscle spindle afferents, and to some extent by cutaneous receptors in skin overlying joints (Gardner et al. 2000), mechanoreceptors in the joint capsule (Gardner et al. 2000; Proske and Gandevia 2012), and Golgi tendon organs (Kistemaker et al. 2012), ascend via various brain structures to the primary somatosensory cortex. These afferent signals generate sensations of position of limb segments with respect to each other (joint-based representation of position sense). Sensations of position of the limb endpoint with respect to the body and external environment (Cartesian body-based representation) are likely obtained in the somatosensory association areas by integrating signals encoded in external coordinates and obtained via other sensory modalities, i.e. visual, auditory, and tactile (Naito et al. 2016; Proske and Gandevia 2018).

The limb endpoint perception in the external space requires the transformation from perceived joint angles to limb endpoint location. This transformation is limb posture-dependent and nonlinear. Obtaining limb endpoint by the transformation of joint angle coordinates requires the accurate estimation of body segment lengths, which is normally

obtained via vision. However, even the sighted people have inaccurate perception of their body schema (Longo and Haggard 2010). Therefore, people with no or limited visual experience may have impaired abilities to accurately estimate body dimensions and thus obtain accurate estimates of hand position sense in external space. In addition, for accurate transformations from joint angles to limb endpoint coordinates accurate perception of joint angular positions is also important. The joint angular positions are derived primarily from the input from the muscle spindles. Thus, precision and accuracy of limb endpoint position sense depends on the three factors discussed above: (i) limb posture, (ii) visual experience, and (iii) inputs from muscle spindle afferents.

Before considering possible effects of these factors on endpoint position sense, I review physiological bases of limb position sense.

1.1 Limb position sense

It is easy to confuse limb position sense with kinesthesia and proprioception. Whereas position sense refers to the sense of stationary positions of limb segments, proprioception encompasses wider range of the senses. In an extended and original meaning, proprioception includes the abilities to sense all stimuli occurred in our own body, as well as non-muscular stimuli such as the senses from internal organs and blood vessels (Sherrington 1907). However, typically, the meaning of proprioception has been limited to the muscular senses regarding limb position, movement, load, and balance (Proske and Gandevia 2012). Kinesthesia, on the other hand, has been used to refer to the senses for both position and movement (Proske and Gandevia 2018; Proske and Gandevia 2012) or

only the sense of movement (Gilman 2002; Naito et al. 2016). In this study, kinesthesia will be used to refer to the sense of movement.

1.2 Factors affecting limb position sense

Studies have found many factors affect limb position sense. First, intrinsic factors such as age (Goble 2010), movement type (active or passive) (Fuentes and Bastian 2010), limb preference (Sainburg and Schaefer 2004), and muscle contraction history (thixotropy) (Wise et al. 1998) can affect position sense. Second, extrinsic factors such as visual (Held and Rekosh 1963), audio (Cuppone et al. 2018), and tactile feedback (Tsay et al. 2016) affect limb position sense. Finally, methods of testing position sense also can affect the testing results. For example, unilateral vs bilateral (Goble 2010), target location (near vs far) (Goble 2010), and joint range (extreme vs midrange) (Fuentes and Bastian 2010) affect position sense.

1.3 Anatomical and physiological bases of joint position sense: receptors and central pathways

Spindle primary afferents (group Ia) are considered major contributors to position and movement senses since they transmit information about muscle length and rate of muscle stretch (Casey 1999; Proske and Gandevia 2012). On the other hand, spindle secondary afferents (group II) provide only muscle length information and are related to position sense (Nardone et al. 2000; Prochazka and Gorassini 1998). Mechanoreceptors in joint capsules and cutaneous tactile receptors are also thought to play some roles in mediating the sense of position and movement (Gardner et al. 2000). Specifically, all of four different types of mechanoreceptors – Meissner corpuscles (rapidly adapting type I),

Pacinian corpuscles (rapidly adapting type II), Merkel endings (slowly adapting type I), and Ruffini endings (slowly adapting type II) – are regarded as receptors for movement, whereas only slowly adapting type II skin stretch receptors are considered as potential position sensors (Proske and Gandevia 2012). It has been known that major function of joint receptors in most joints is detecting joint limits through activation of nociceptors at extreme joint positions (Gardner et al. 2000; Proske and Gandevia 2012). However, several studies have reported that joint receptor can mediate position sense and movement in the finger joints (Clark et al. 1989; Ferrell et al. 1987). Although role of Golgi tendon organs (GTO) in position sense has been underestimated, recent studies have suggested that GTOs contribute to position and movement senses by providing information of tendon length change that is dependent on force applied to the tendon (Kistemaker et al. 2012).

Figure 1.1 shows a representative pathway that mediates position and movement sensations of the upper limb. Signals from the receptors ascend through the dorsal column-medial lemniscus (DC-ML) pathway. Specifically, inputs from the proprioceptors directly synapse on neurons in the ipsilateral dorsal column (DC) and project to dorsal column nuclei (cuneate nuclei and gracile nuclei) in the medulla. Second order neurons reach ventral posterolateral (VPL) region of the thalamus through the medial lemniscus, and third order neurons project to the primary somatosensory cortex (Delhaye et al. 2018a; Proske and Gandevia 2018).

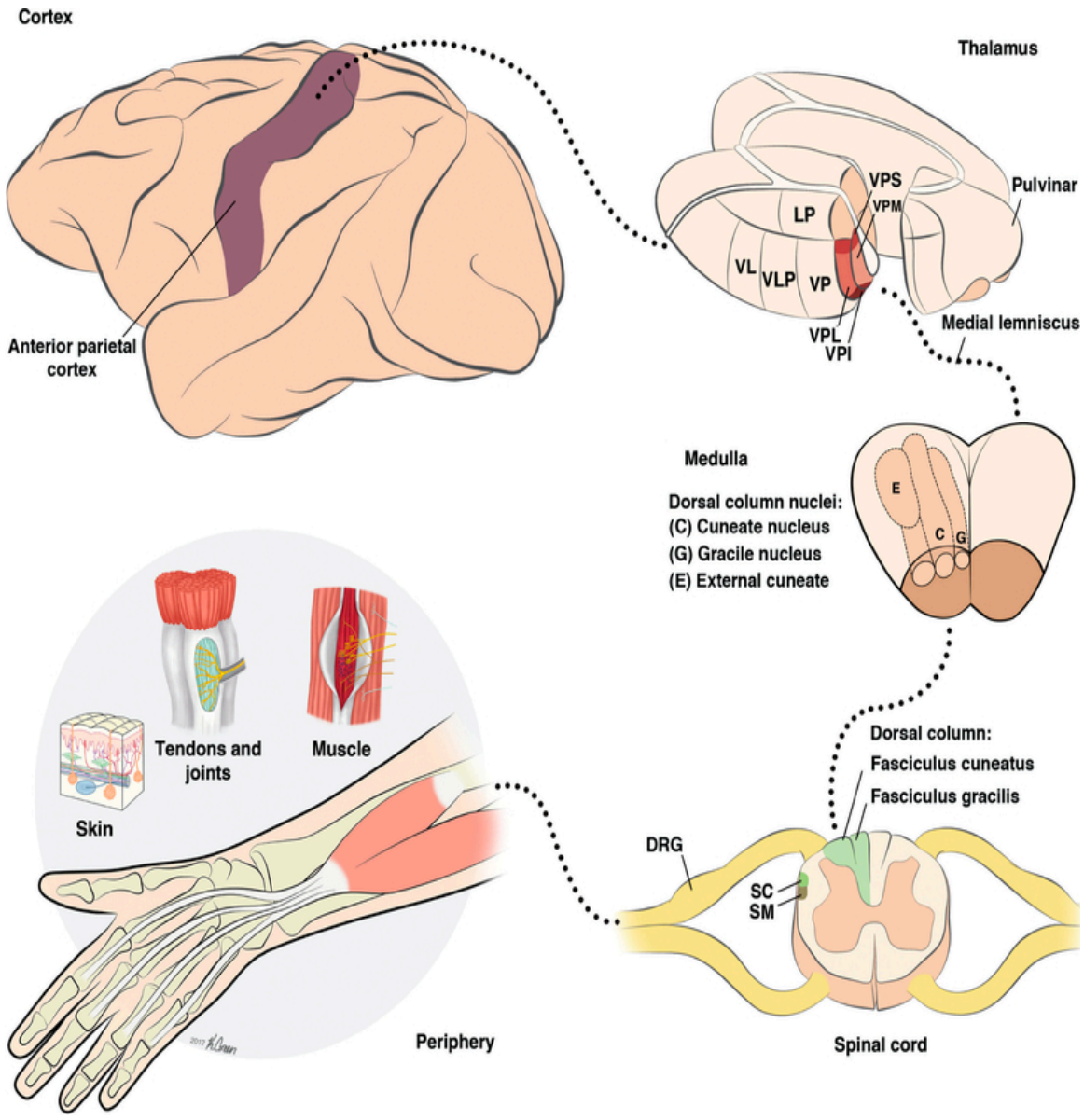

Figure 1. 1: Diagram of the peripheral receptors and central pathways mediating position sense, vibration sense, and tactile sensation. From (Delhaye et al. 2018a; Gilman 2002).

1.4 Position sense of limb endpoint in external space

The above-mentioned afferent signals generate sensations of position of limb segments with respect to each other (joint-based representation of position sense). We also can perceive position of the limb endpoint with respect to the body and external environment (Cartesian body-based representation) (Naito et al. 2016; Proske and Gandevia 2018). Since the brain perceives the limb endpoint position, it must somehow transform the joint-based information about relative positions of the body segments to the limb endpoint position. This transformation appears to be limb posture-dependent, nonlinear and requires an accurate estimation of the length of limb segments.

Studies have suggested that the posterior parietal cortex and dorsal premotor cortex are involved in the transformation between intrinsic (joint-based) and extrinsic (Cartesian body-based) coordinates (Fujiwara et al. 2017; Shadmehr and Wise 2005). For example, neural activities measured in dorsal premotor cortex during planning of reaching movement were affected by the location of target relative to the arm and the eye (Batista et al. 2007). In the case of the posterior parietal cortex, many its subregions, such as parietal reach region (Bhattacharyya et al. 2009; Pesaran et al. 2006) and V6A area (Galletti et al. 1999), were extensively investigated. As a result, it has been shown that different subregions are responsible for various coordinate transformations.

1.5 Non-uniform precision of hand position sense in the horizontal workspace

One of unresolved problems possibly related to coordinate transformations discussed above is the non-uniformity of hand position sense in the horizontal workspace. Specifically, hand position is perceived more precisely in the radial than in azimuth

direction and closer to the body than farther away (Rossetti et al. 1994; van Beers et al. 1998; Wilson et al. 2010). Although limb posture (Scott and Loeb 1994; van Beers et al. 1998; Wilson et al. 2010), muscle moment arms (Hall and McCloskey 1983), the biases of spindle (Honeycutt et al. 2012) and cutaneous (Aimonetti et al. 2012) afferent firing in specific movement directions, as well as the statistics of daily hand use (Howard et al. 2009) have been considered as possible explanations, there is no general consensus in the literature on the origin of the non-uniform hand position sense.

1.6 Role of visual experience in hand position sense in joint-based and Cartesian-based coordinate frames

Despite a long history of research in limb position sense, many important questions remain unanswered. For example, it is unclear why accuracy and precision of reproducing joint angles in the reference arm by the other, indicator arm without vision is typically lower than when the hand position or limb segment orientation with respect to the external space are reproduced by the indicator arm (Fuentes and Bastian 2010; Soechting 1982; Worringham et al. 1987). At first glance, it appears that the joint angle matching tasks should be more precise and accurate since the subject directly compares outputs from muscle spindle afferents from the two arms, which are directly related to the joint angles (Tsay et al. 2016). In the hand position matching, the nervous system needs to estimate the limb endpoint position from the joint angle-based information. An imperfect internal model of body segment dimensions would lead to lower accuracy and precision of the hand position matching performance. Yet, a number of studies reported the opposite results (Fuentes and Bastian 2010; Soechting 1982; Worringham et al. 1987).

Somatosensory signals from muscle spindle afferents enter the spinal cord and activate many interneurons and motoneurons (directly and indirectly). Some of spinal interneurons (i.e., interneurons in the dorsal spinocerebellar tract and in the dorsal-funiculus-medial-lemniscus system) relay the signals from these afferents to the primary somatosensory cortex via the cerebellum and thalamus (McIntyre et al. 1984; 1985; Oscarsson and Rosen 1963). Activation of the spindle afferents via muscle vibration in humans results in sensations of limb position changes (Goodwin et al. 1972; Lackner 1988) and in activation of the following brain areas as revealed in neuroimaging studies (Naito et al. 2016): somatosensory areas, including putative somatosensory area 3a and the spinocerebellum (Lobule VIIB, VIII), but also the motor network, including the primary motor cortex, dorsal premotor cortex, supplementary motor area, cingulate motor cortex, putamen/globus pallidas, and motor cerebellarhemisphere (Lobule V, dentate).

Studies of visually guided movements in nonhuman primates suggest that hand position is estimated based on visual and somatosensory information in the posterior parietal cortex in an eye-centered frame of reference (Buneo et al. 2002). In the premotor cortex that receives information from the parietal cortex, a neuronal population can encode the locations of reaching targets relative to the arm in arm-centered coordinates (Graziano 1999). The population activity of the majority of neurons in the primary somatosensory cortex that receive somatosensory input from the shoulder and elbow muscles appears to encode arm movement direction (Prud'homme and Kalaska 1994) in the arm-centered coordinate frame, as also reported for populations of cells in the parietal cortex (Kalaska et al. 1990) and primary motor cortex (Georgopoulos et al. 1982). Note, however, that the

movement direction encoding could also reflect encoding directions in the joint coordinate frame (Mussa-Ivaldi 1988).

1.7 Contingent negative variation (CNV) as an indicator of complexity of upcoming motor tasks

Visual experience is known to contribute to the formation of limb spatial sense (Thinus-Blanc and Gaunet 1997) via shaping the body schema that contributes to limb localization in extrapersonal space (Longo, Haggard, 2010). Loss of vision may affect accuracy of arm position sense because the lack of visual experience could affect remapping of the joint-based position information (proprioceptive and tactile) onto the limb location information in the external space (Crollen, Collignon 2012). Thus, visual experience may differentially affect the limb position sense in joint and external space coordinates, particularly because it might take more attention and cognitive effort for people with impaired vision to perform coordinate transformations from the joint to external space. On the other hand, the amount of information processing and task effort of the upcoming motor task can be evaluated using the EEG contingent negative variation potential (CNV, Walter et al. 1964). CNV is a classic event-related potential (ERP) that requires two stimuli: the first one is warning stimulus to let subject prepare for the task performance and the second one is an imperative stimulus, based on which the subject initiates the task. The stimuli are typically audio or visual signals, and the time gap between the stimuli is usually 0.5 -1.5 second. The time gap does not have to be the same across trials. CNV is known to arise between two stimuli and is a long-lasting negative potential of up to more than 10 seconds.

1.8 Effects of muscle self-reinnervation on somatosensation

Muscle self-reinnervation leads to permanent loss of stretch reflex (Cope et al. 1994; Cope and Clark 1993). Thus, self-reinnervation appears to disrupt the monosynaptic pathway from the spindle Ia afferents to motoneurons and that potentially could affect limb position sense. It is well established that complete loss of proprioception in people with large-fiber sensory neuropathy severely disrupts limb position sense and motor performance (Ghez et al. 1995; Rothwell et al. 1982; Sainburg et al. 1993). However, the effect of selected removal of monosynaptic input from the muscle spindle Ia afferents of muscles crossing a given joint on accuracy and precision of motor(Rossetti et al. 1994; van Beers et al. 1998; Wilson et al. 2010) performance are unknown. Given that input from the muscle spindles is the main contributor to limb position sense (Proske and Gandevia 2018), compromising this input by muscle self-reinnervation (Cope et al. 1994; Cope and Clark 1993; Lyle et al. 2016) may affect limb position sense and thus motor performance. Yet, removal of stretch reflex (monosynaptic input from spindle group Ia afferents) from ankle extensor muscles in the cat by self-reinnervation does not seem to dramatically change kinematics of level walking (Abelew et al. 2000; Gregor et al. 2018; Maas et al. 2007). Chang et al. (2009) also reported that patterns of hindlimb length and orientation is conserved after the ankle extensor self-reinnervation even though joint kinematics have changed significantly. This surprising result could be potentially explained by the fact that the compromised length dependent feedback in a distal joint (ankle) have a relatively minor contribution to the position of the hindlimb endpoint because of a short length of the distal limb segment (Goslow Jr et al. 1973; Hall and McCloskey 1983). Another contributing factor to relatively normal kinematics of level walking after self-reinnervation of ankle

extensors could be the presence of spindle afferent input from the intact ankle flexors. To address the above unresolved questions in the literature, monosynaptic input of spindle group Ia afferents from both major flexors and extensors of a more proximal knee joint will be removed by muscle self-reinnervation and the resulting kinematics of level walking will be analyzed. The expectation is that self-reinnervation of these muscles will lead to severe impairments of walking resembling those in a person with loss of proprioception (Lajoie et al. 1996).

The hindpaw position control during the swing phase of walking in the cat appears to be an appropriate model to investigate the role of the monosynaptic input of muscle spindle group Ia afferents in precision of paw position sense. According to the uncontrolled manifold analysis (Klishko et al. 2014), cats stabilize (control) their horizontal and vertical hindpaw positions during the swing phase of walking (especially immediately before and right after the stance phase) by coordinated changes of limb segment angles. Since cats cannot see their hindpaws, this stabilization must be based on hindlimb position sense. Therefore, analysis of hindpaw position immediately before and after the stance phase while the major muscles of the knee joint are self-reinnervated may reveal the effects of muscle spindle input disturbance on hindpaw position sense.

1.9 Specific aims

The above analysis of literature have revealed that the physiological mechanisms of perception of limb joint angles are generally well understood. However, the mechanisms responsible for position sense of the limb endpoint are less clear. My analysis of available literature and the transformation from joint to endpoint coordinates revealed three major

factors that might affect precision and accuracy of endpoint position sense. These factors are: (i) limb posture, (ii) visual experience, and (iii) input from muscle spindle afferents.

1.9.1 Specific Aim 1: Investigate contributions of arm posture to non-uniform precision of hand position sense in a horizontal workspace

Aim 1 investigated the role of limb posture in hand position sense. Studies have reported that precision of hand position sense is non-uniform in a horizontal workspace (Rossetti et al. 1994; van Beers et al. 1998; Wilson et al. 2010), however, no consistent explanation has been found in the literature. Since the transformation from the joint angles to hand position is nonlinear and depends on limb posture, one could expect a non-uniform precision of arm position sense and the dependence of precision of hand position sense on arm posture.

Hypothesis: I hypothesized that the non-uniform precision of hand position sense in a horizontal workspace originates from a nonlinear transformation of random errors of the arm joint angles to hand position random errors.

1.9.2 Specific Aim 2: Investigate precision and accuracy of arm position sense in the blind and sighted

Aim 2 addressed the role of visual experience in limb position sense in joint-based and Cartesian-based coordinate frames. According to the currently accepted view, limb position sense originates primarily from muscle spindle afferents, i.e. joint angle-related signals (Proske and Gandevia 2018). Therefore, position sense of the hand in the Cartesian coordinate frame should depend on sense of joint angle position and on a coordinate

transformation from joint angles to hand position. This transformation requires an accurate estimation of body segment dimensions, which is usually acquired by vision through visual experience. Therefore, people who lack visual experience may have an impaired abilities to accurately estimate body segment dimensions and thus accurately perceive hand position in external space.

Hypotheses: I hypothesized that individuals lacking visual experience would demonstrate lower accuracy and precision of the hand position sense in external space than normally sighted individuals; in addition, the blind would have better hand position sense in joint space than in external space.

1.9.3 Specific Aim 3: Investigate accuracy of hand position sense in cued movement paradigm based on negative EEG potentials in blind and sighted people during arm position matching in joint and external space.

Aim 3 investigated the effects of visual experience on accuracy of hand position sense and task complexity during hand matching tasks in joint and external space. Visual experience is known to contribute to the formation of the arm spatial sense (Thinus-Blanc and Gaunet 1997) via shaping the body schema that contributes to arm localization in the extrapersonal space (Longo, Haggard, 2010). Hand position sense may arise from the mapping of joint based, proprioceptive and tactile information onto visual information of hand location in extrapersonal space (Crollen, Collignon 2012). Visual information therefore calibrates joint-based sensory information to the extrapersonal space (Shadmehr and Wise, 2005). As such, no or little history of prior visual experience, common in long-term visually impaired individuals, could ultimately result in a poor mapping of joint-based

information onto the extrapersonal space. Thus, it might take more cognitive effort and larger errors for the visually impaired to perform coordinate transformations from the joint to external space compared to normally sighted blindfolded individuals.

Hypotheses: Two hypotheses were tested: (1) visual experience improves hand position sense (2) hand positioning in external space would be perceived as a more complex task and lead to lower accuracy.

1.9.4 Specific Aim 4: Investigate effects of self-reinnervation of hamstrings, quadriceps and sartorius on precision of hindpaw position control during the swing phase of level walking in the cat.

Aim 4 investigated effects of self-reinnervation of major knee muscles on precision of hindpaw position control during the swing phase of walking. Klishko et al. (2014) have found using the uncontrolled manifold analysis that cats stabilize (control) their horizontal and vertical hindpaw positions during the swing phase of walking (especially immediately before and after the stance phase) by coordinated changes of limb segment angles. Although it is well established that people with lack of proprioception loose limb position sense and the ability to perform coordinated movements without vision (Ghez et al. 1995; Rothwell et al. 1982; Sainburg et al. 1993), degrading muscle length feedback by removal of stretch reflex by muscle self-reinnervation (Cope et al. 1994) in cat ankle extensors does not seem to cause noticeable changes in kinematics of level walking (Gregor et al. 2018). Chang et al. (2009) also have reported that patterns of limb length and orientation were conserved in level walking of the cats with self-reinnervated ankle extensors, although joint angles changed. These surprising results could be potentially explained by the fact that the

compromised muscle length feedback in a distal joint (ankle) have a relatively minor contribution to the hindlimb kinematics because of a short length of the distal limb segment. In other words, the same amount of joint position error at the knee would cause a much greater error of paw positioning than the same error in the ankle would. Another contributing factor to relatively normal kinematics of level walking after self-reinnervation of ankle extensors could be the presence of spindle afferent input from the intact ankle flexors.

Hypotheses: I hypothesized that (1) self-reinnervation of knee muscles would reduce precision of hindpaw position control just before and after the stance phase and (2) self-reinnervation of knee muscles should disrupt the typical joint coordination that maintains invariant hindlimb orientation and length during walking.

CHAPTER 2. AIM 1: CONTRIBUTIONS OF ARM POSTURE TO NON-UNIFORM PRECISION OF HAND POSITION SENSE IN A HORIZONTAL WORKSPACE

2.1 Introduction

Position sense of the body limbs is critical for the accurate control of posture and movement and for the appropriate responses to sudden external perturbations. The lack of position sense due to illness has devastating consequences for the performance of even simplest motor tasks (Cole and Paillard 1995; Sainburg et al. 1993; Sarlegna et al. 2006). Although many sensory systems (visual, vestibular, tactile, proprioceptive) and voluntary motor commands contribute to limb position sense, the muscle spindle and cutaneous afferents appear to be the major contributors (Aimonetti et al. 2007; Collins et al. 2005; Feldman 2011; Matthews 1988; Plooy et al. 1998; Proske 2015; Proske and Gandevia 2012).

Hand position sense has been the focus of extensive studies. It has been shown experimentally that precision (random errors) of hand position sense is not uniform in a horizontal workspace. Specifically, the hand position is perceived more precisely in the radial than in azimuth direction and closer to the body than farther away (Rossetti et al. 1994; Slinger and Horsley 1906; van Beers et al. 1998; Wilson et al. 2010). Several explanations for the observed non-uniform precision of hand position sense have been put forward. Based on a qualitative graphic analysis of angle changes at shoulder and elbow joints in two arm postures, van Beers and colleagues (van Beers et al. 1998) suggested that

arm posture might be responsible for the non-uniform precision of hand position sense. This analysis provided some intuition for shape of the error distribution of the hand position at an extended and flexed arm posture. However, it has not provided a general mechanistic explanation for the non-uniform hand position precision, for the dependence of precision magnitude on the distance from the body, and could not be generalized to the entire horizontal plane. A later study (Howard et al. 2009) has proposed that the non-uniform precision of hand position sense in the arm workspace (i.e., higher precision near the body than farther away) results from the more frequent daily use of hands in close proximity to the body. Other possible explanations for the non-uniform precision of hand position sense proposed in the literature include arm posture comfort (Rossetti et al. 1994), spatial biases of muscle spindle and cutaneous afferent activity (Aimonetti et al. 2012; Ribot-Ciscar et al. 2003; Wilson et al. 2010) and muscle spindle distribution among one- and two-joint muscles (Scott and Loeb 1994; Sturnieks et al. 2007).

Since most of the above explanations are related to arm posture, and the non-uniformity appears to dependent on geometric limb parameters such as distance and direction of hand from the shoulder joint, I hypothesized that the non-uniform precision of hand position sense in a horizontal workspace might depend on an arm posture-related nonlinear transformation of random errors of the arm joint angles to hand position random errors. To test this hypothesis, we conducted a geometric analysis of this transformation using a two-segment arm model and compared model predictions with measured precision of hand position sense in hand position matching experiments.

2.2 Methods and materials

2.2.1 Jacobian-Based Geometric Analysis of Precision (Random Errors) of Hand Position

We conducted a Jacobian-based geometric analysis of a planar, two-segment kinematic chain representing the human arm (Fig. 2.1B). In this simplified geometric model, the relationship between the hand position $(X_H, Y_H)^T$ and the joint angles at the shoulder and the elbow (θ_s, θ_e) could be expressed as follows:

$$\begin{bmatrix} X_H \\ Y_H \end{bmatrix} = f(\theta_s, \theta_e) = \begin{bmatrix} f_x(\theta_s, \theta_e) \\ f_y(\theta_s, \theta_e) \end{bmatrix}, \quad (1)$$

where $f(\theta_s, \theta_e)$ is a forward kinematic transformation function that was computed using the four Denavit-Hartenberg parameters (Denavit and Hartenberg 1955; Spong and Vidyasagar 1989).

If the shoulder coordinate frame is set as shown in Fig. 2.1B (*Z* axis is perpendicular to the *XY* plane), the transformation from the shoulder coordinates to the hand coordinates $T(\theta_s, \theta_e)$ can be represented as the product of several rotation (Rot) and translation (Trans) matrices:

$$T(\theta_s, \theta_e) = Rot(Z_s, \theta_s)Trans(X_s, L_{ua})Rot(Z_e, -\pi + \theta_e)Trans\left(X_e, L_{fa}\right) =$$

$$\begin{bmatrix} \cos(\theta_s) & -\sin(\theta_s) & 0 & 0 \\ \sin(\theta_s) & \cos(\theta_s) & 0 & 0 \\ 0 & 0 & 1 & 0 \\ 0 & 0 & 0 & 1 \end{bmatrix} \begin{bmatrix} 1 & 0 & 0 & L_{ua} \\ 0 & 1 & 0 & 0 \\ 0 & 0 & 1 & 0 \\ 0 & 0 & 0 & 1 \end{bmatrix} \begin{bmatrix} \cos(-\pi + \theta_e) & -\sin(-\pi + \theta_e) & 0 & 0 \\ \sin(-\pi + \theta_e) & \cos(-\pi + \theta_e) & 0 & 0 \\ 0 & 0 & 1 & 0 \\ 0 & 0 & 0 & 1 \end{bmatrix} \begin{bmatrix} 1 & 0 & 0 & L_{fa} \\ 0 & 1 & 0 & 0 \\ 0 & 0 & 1 & 0 \\ 0 & 0 & 0 & 1 \end{bmatrix}$$

, (2)

where X_s and Z_s are the axes of the shoulder coordinate frame; X_e and Z_e are the axes of the elbow coordinate frame; L_{ua} and L_{fa} denote the lengths of the upper arm and forearm

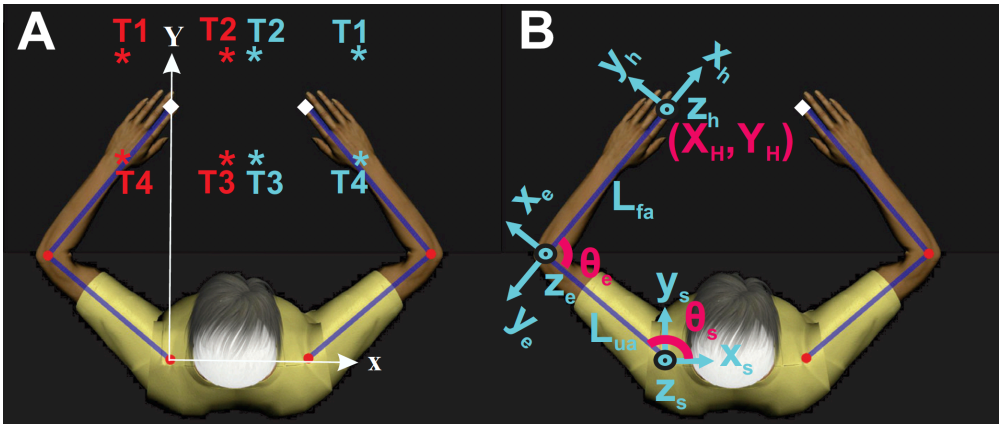

Figure 2. 1: Schematic of experimental setup and geometric arm model. A: Bimanual hand position matching experiment. The initial positions of the left and right index fingertips are marked as white diamonds. Red and cyan colored asterisks are the four targets for each arm (T1, T2, T3 and T4). Cyan asterisks indicate targets to which the robot moved the right hand; red asterisks correspond to the mirror images of the cyan asterisks and indicate the targets reached by the subject with the left hand to match the corresponding right targets. B: Coordinates of arm joints and parameters of the arm model for computing the forward kinematics using the Jacobian matrix (eq. 4). The origins of the shoulder, elbow and hand coordinate frames are at the shoulder, elbow and index fingertip, respectively. The positive directions of the corresponding x and y axes are indicated by the arrows; the direction of the z axes is perpendicular to the xy plane. θ_s and θ_e denote angles of the shoulder and elbow joints; L_{ua} and L_{fa} are the lengths of the upper arm and forearm+hand segments.

with hand, respectively. In 4x4-matrix $T(\theta_s, \theta_e)$, the first three elements of the fourth column are the *x*, *y*, and *z* coordinates of the hand position expressed as functions of the shoulder and elbow angles. Therefore, the position of the hand in the horizontal workspace can be expressed as

$$\begin{bmatrix} X_H \\ Y_H \end{bmatrix} = \begin{bmatrix} f_x(\theta_s, \theta_e) \\ f_y(\theta_s, \theta_e) \end{bmatrix} = \begin{bmatrix} T(\theta_s, \theta_e)_{(1,4)} \\ T(\theta_s, \theta_e)_{(2,4)} \end{bmatrix} =$$

$$= \begin{bmatrix} L_{fa}\cos(\theta_s)\cos(-\pi+\theta_e) - L_{fa}\sin(\theta_s)\sin(-\pi+\theta_e) + L_{ua}\cos(\theta_s) \\ L_{fa}\sin(\theta_s)\cos(-\pi+\theta_e) + L_{fa}\cos(\theta_s)\sin(-\pi+\theta_e) + L_{ua}\sin(\theta_s) \end{bmatrix}. \quad (3)$$

From equation 3 one can derive the relationship between small changes in joint angles $(\Delta\theta_s, \Delta\theta_e)^T$ and the corresponding changes in the hand position $(\Delta X_H, \Delta Y_H)^T$:

$$\begin{bmatrix}\Delta X_H \\ \Delta Y_H\end{bmatrix} = \boldsymbol{J}\begin{bmatrix}\Delta\theta_s \\ \Delta\theta_e\end{bmatrix}, \tag{4}$$

where $\boldsymbol{J}$ is the Jacobian:

$$\boldsymbol{J} = \begin{bmatrix}\frac{\partial f_x}{\partial\theta_s} & \frac{\partial f_x}{\partial\theta_e} \\ \frac{\partial f_y}{\partial\theta_s} & \frac{\partial f_y}{\partial\theta_e}\end{bmatrix}. \tag{5}$$

The changes in hand position caused by small changes in shoulder and elbow angles can be quantified by singular values of $\boldsymbol{J}$, which are square roots of eigenvalues of $\boldsymbol{J}^*\boldsymbol{J}$, where $\boldsymbol{J}^*$ is the conjugate transpose of $\boldsymbol{J}$ (Bretscher 2013). For example, the maximum singular value of $\boldsymbol{J}$, or the Euclidean norm of $\boldsymbol{J}$, is the maximum change that occurs in the hand position given small changes in the joint angles (see eq. 4):

$$\|\boldsymbol{J}\| = max_{i=1,n}\sqrt{\lambda_i(\boldsymbol{J}^*\boldsymbol{J})}. \tag{6}$$

where $\lambda_i(\boldsymbol{J}^*\boldsymbol{J})$ is the i-th eigenvalue of $\boldsymbol{J}^*\boldsymbol{J}$ and n is the rank of $\boldsymbol{J}$. In other words, the Euclidean norm of the Jacobian provides the measure of the maximum displacement of the hand caused by the combination of small joint angle displacements at the shoulder and elbow within a unit circle:

$$\sqrt{\Delta\theta_s^2 + \Delta\theta_e^2} < 1. \tag{7}$$

Similarly, the minimum hand displacement caused by small joint angle changes is determined as the square root of the minimum eigenvalue of $\boldsymbol{J}^*\boldsymbol{J}$ (Bretscher 2013). In

addition, eigenvectors $\boldsymbol{v}$ satisfying (8) were computed for given arm configurations. The eigenvectors corresponding to the maximum and minimum eigenvalues indicate the directions of the maximum and minimum displacements of the hand for given input of small joint angle deviations $(\Delta\theta_s, \Delta\theta_e)^T$:

$$\boldsymbol{J}^*\boldsymbol{J}\boldsymbol{v} = \lambda\boldsymbol{v}. \tag{8}$$

The computed eigenvectors were multiplied by $\boldsymbol{J}$, so that they expressed the directions of small displacements in the hand coordinates (Bretscher 2013). The eigenvalues and eigenvectors were used to construct a precision ellipse of hand position with the center at the left-hand location (X_H, Y_H), Fig. 2.1B. The length and direction of the semi-major axis of the ellipse corresponded to the maximum singular value of $\boldsymbol{J}$ and $\boldsymbol{J}\boldsymbol{v}_{\boldsymbol{max}}$, respectively ($\boldsymbol{v}_{\boldsymbol{max}}$ is the eigenvector of the maximum eigenvalue). The length and direction of the semi-minor axis corresponded to the minimum singular value of $\boldsymbol{J}$ and $\boldsymbol{J}\boldsymbol{v}_{\boldsymbol{min}}$, respectively ($\boldsymbol{v}_{\boldsymbol{min}}$ is the eigenvector of the minimum eigenvalue). With these ellipse parameters, precision ellipses were plotted for given arm configurations using Matlab function ellipse1 (Matlab R2016a, MathWorks Inc., Natick, MA, USA).

Another geometric parameter characterizing the relationship between small changes in joint angles and the corresponding changes in hand position (see eq. 4) is the condition number $\kappa(\boldsymbol{J})$, i.e., the square root of the ratio between the maximum and minimum eigenvalues of $(\boldsymbol{J}^*\boldsymbol{J})$. The condition number can be thought of as an error amplification factor since it reflects how errors in the joint angle space induce the errors in hand position (Merlet 2006):

$$\kappa(\boldsymbol{J}) = \|\boldsymbol{J}\|\|\boldsymbol{J}^{-1}\|. \quad (9)$$

Since the condition number is defined as the ratio of lengths of the major and minor axes of the precision ellipse, condition numbers that differ from a value of one indicate that there is a preferred error direction at a given arm posture, as opposed to equal errors in all directions.

To derive hand precision ellipses corresponding to physiologically relevant random angle errors at the shoulder and elbow, $(e_s, e_e)^T$, a modified Jacobian matrix was used:

$$J_m = J * \begin{bmatrix} e_s & 0 \\ 0 & e_e \end{bmatrix}. \quad (10)$$

This matrix scales joint angle errors and changes the unit circle input in the space of joint angle errors (see eq. 7) into an elliptical input:

$$\sqrt{\frac{\Delta\theta_s^2}{e_s^2} + \frac{\Delta\theta_e^2}{e_e^2}} < 1. \quad (11)$$

The deviations in the joint angle space in eq. 11, $(\Delta\theta_s, \Delta\theta_e)^T$, can be thought of as precision (random errors) of joint angle position sense within the detection thresholds of imposed joint rotations $(e_s, e_e)^T$. The detection threshold has been shown to depend on a joint, imposed joint rotation speed, and on whether joint movement is passive or active, i.e., imposed on the joint by external forces or produced voluntarily (Hall and McCloskey 1983). Hall and McCloskey (1983) measured detection thresholds for imposed rotations of elbow and shoulder joints as a function of the angular speed between 0.156 °/s and 80 °/s. Since our arm position matching tasks were static (see below), we evaluated the shoulder

and elbow detection thresholds at zero angular speed by extrapolating the data from Hall and McCloskey using the least-squares fit regressions:

$$e_s = 3.0145 \cdot e^{-4.8969 \cdot \dot{\theta}_s} + 0.1245 \quad (12a)$$

$$e_e = 3.8299 \cdot e^{-4.5809 \cdot \dot{\theta}_e} + 0.1414 \quad (12b)$$

where $\dot{\theta}_s$ and $\dot{\theta}_e$ are shoulder and elbow angular speeds in °/s. The computed angle detection thresholds for the shoulder and elbow at zero speed were $e_s = 3.14^o$ and $e_e = 3.97^o$, respectively. These values were used as the limits of random joint errors in derivations and plotting of hand precision ellipses (see eqs. 4, 10, and 11).

2.2.2 Hand Position Matching Experiment

We conducted a hand position matching experiment to determine precision of hand position sense at four locations of a horizontal space in front of the body (Fig. 2.1A) and compared the experimentally found precision with precision of hand position predicted by the model.

2.2.2.1 Subjects

All subjects of this study were right-handed (determined based on the Edinburgh Handedness Inventory (Oldfield 1971), over the age of 18 years and had no history of known neurological or musculoskeletal disorders. We recruited 11 individuals (7 males and 4 females; age 27.2±11.4 years; Table 2.1). The experimental procedures of this study were consistent with the Ethical Principles for Medical Research Involving Human Subjects described in the Declaration of Helsinki and were approved by the Institutional

Review Board of Georgia Institute of Technology. All subjects read and signed a written informed consent to participate in the study.

2.2.2.2 Experimental task

The subjects performed a bilateral hand position matching task while they were seated in the chair of the Kinarm exoskeleton robot (BKIN Technologies Ltd., Kingston ON, Canada) with both arms supported by the exoskeleton arms in a horizontal workspace. Before the task, subject's arms were secured in a pronated position in the Kinarm robotic arms, and the vertical axis of rotation of the shoulder and elbow joints of each arm was aligned with the corresponding joints of the Kinarm. No motion at the wrist joints was available. The Kinarm was calibrated in accordance with established procedures.

At the beginning of each trial, the Kinarm moved both hands of the subject to the initial positions in front of the corresponding shoulder to make the elbow angle 90^{o} (Fig. 2.1A). After a short delay (1 s), the Kinarm moved the right hand of the subject to one of the four target positions over the period of 1 sec in random order. The target locations for the right arm were: (1) at 45^{o} from the horizontal in the counterclockwise direction, T1; (2) at 135^{o}, T2; (3) at 225^{o}, T3; and (4) at 315^{o}, T4.

The subject had to match the distance and mirror direction of the right index finger motion from the initial position to the target with the left index fingertip. Fig. 2.1A demonstrates the corresponding targets for the left arm as mirror images of the right arm targets. For example, when the right index fingertip was moved to target T2 (cyan T2 target in Fig. 2.1A), the subject would match this right hand position by moving the left index fingertip in the mirror direction by the same distance (red T2 target in Fig. 2.1A). Note that

Table 2.1 Characteristics of subjects.

Subject	Age, years	Sex	Height, cm	Forearm + hand length, cm	Upper arm length, cm
1	21	F	155	38.9	29.9
2	23	F	152	37.5	25.0
3	19	M	165	39.8	29.3
4	47	M	178	43.7	31.9
5	25	M	181	46.7	31.5
6	19	F	168	41.1	28.8
7	29	F	156	38.9	32.1
8	20	M	175	43.7	29.1
9	22	M	170	47.7	33.1
10	22	M	170	41.3	27.3
11	52	M	188	47.2	26.3
Mean ± SD	27.2 ±11.4	-	168.9 ±11.4	42.41 ±3.62	29.48 ±2.56

for a two-joint arm in the horizontal plane, there is a one-to-one correspondence between the two joint angles and the respective two hand Cartesian coordinates. To account for differences in subjects' arm length, the target distance for each subject (D_T) was normalized based on the distance between the hand and shoulder at the initial hand position: $D_T = 0.10\sqrt{2(x/0.5272)}$. In the equation, x is the distance in m between the index fingertip initial position and the shoulder of a given subject; 0.5272 is the same distance in m for the subject from a preliminary study whose forearm+hand length and upper arm length were 40.86 cm and 30.01 cm, respectively. For that subject the distances

to the targets from the initial position were 10 cm. Because of this normalization, the absolute target distances from the initial hand position for all subjects ranged from 0.115 to 0.166 m.

When the right index fingertip being moved by the robot reached a target and stopped, the Kinarm generated a 200-ms beeping sound that indicated that the subject could start moving the left arm to perform hand matching. The assigned time for performing the matching task was 2.5 sec. The subjects were instructed to hold the position of the left arm when they reached the matching position until the Kinarm moved both arms back to the initial positions. Hand position matching was repeated 72 times (18 times for each target) with a 5-min break after every 24 repetitions. During the experiment, the arms and targets were hidden from subject's view by a non-transparent screen and cloth.

2.2.2.3 Analysis of experimental data

To evaluate precision (random errors) of the hand position matching, we analyzed position errors of the left index fingertip with respect to the mirror position of the corresponding right index fingertip, which was recorded in each trial. Random errors at each target of each subject were obtained by subtracting the mean horizontal and vertical coordinates of the left hand obtained across 18 trials for each target and subject from the left hand coordinates recorded in each trial. The obtained differences represented random errors of arm position matching for a given target and subject. The experimental distribution of these errors was fitted by the 95% confidence ellipse (Johnson and Wichern 2007).

Each ellipse was characterized by four parameters: the direction and length of the semi-major axis, size (area), and elongation (shape), i.e. the ratio of the lengths of the major and minor axes. The ellipse direction was defined as an angle between the ellipse major axis and the horizontal and had a range of 0^o– 90^o. Positive and negative orientation angles corresponded to the counterclockwise and clockwise rotations of the major axis from the horizontal, respectively.

We also computed the mean of absolute values of radial and azimuth random hand position errors from the projections of random errors on the line connecting the left shoulder and left hand and on the line perpendicular to the shoulder-hand line, respectively, for each subject across all targets and for distant targets (T1 and T2) and close targets (T3 and T4; Fig. 2.1A). Similarly, we computed the mean of absolute values of forward-backward and left-right random errors from the projections of random errors on the vertical and horizontal axes, respectively.

2.2.2.4 Statistical analysis

A two-way repeated measures ANOVA (IBM SPSS v21 software (Chicago, IL, USA)) was performed to compare the parameters of precision ellipses predicted by the model and obtained experimentally for each subject and target. Predicted precision ellipses for each subject were computed using the arm model described above and subject specific model parameters, i.e. segment lengths (Table 2.1) and the mean left hand position at each target determined experimentally. The two independent within-subject factors were Method (for determining hand precision ellipse: Model and Experiment) and Target (target locations T1, T2, T3, and T4; Fig. 2.1A). The dependent variables were the parameters of

the precision ellipses: the length of the ellipse semi-major axis, orientation of the semi-major axis, size of ellipse (ellipse area), and elongation of ellipse (shape). The repeated measures ANOVA was performed for each dependent variable. When significant effects of the independent factors or their interaction were detected, the Bonferroni post-hoc test was used for pairwise comparisons. We also computed the Pearson correlation coefficients between the predicted and measured ellipse parameters.

In addition, we compared the mean random errors between the radial and azimuth directions, forward-backward and left-right directions, and between distant (T1 and T2) and close (T3 and T4) targets. A two-way repeated measures ANOVA with two independent factors Method (Model and Experiment) and Target Distance was performed for each dependent variable (the mean random error computed in specific directions). The Bonferroni post-hoc test was used for pairwise comparisons.

Descriptive statistics values are reported as mean ± standard error, unless indicated otherwise. The significance level for all tests was set at an alpha level of 0.05.

2.3 Results

2.3.1 Jacobian-Based Geometric Analysis of Hand Position Precision

The results of Jacobian-based geometric analysis revealed how arm posture contributed to the non-uniform distribution of random hand position errors (precision). The computed maximum random error, represented as the norm of the Jacobian (eq. 6) and related to the length of the major axis of the precision ellipse, increased monotonically with the distance of the hand from the shoulder (Fig. 2.2A1, A2).

The condition number, indicating the precision ellipse shape and presence of a preferred error direction (eq. 9), was close to 2 at the intermediate distance from the body (between approximately 30 and 50 cm), whereas it was relatively high in the vicinity to the body (~15 cm) and extremely high in the most distant region where the elbow and shoulder angles were close to full extension (Fig. 2.2B1 and B2).

The orientation and shape of the precision ellipses varied with the hand position in the horizontal workspace (Fig. 2.2C1). The major axis of the ellipses was oriented almost vertically at extreme left and right hand positions, and nearly horizontal for hand positions of ~0–25 cm to the left of the shoulder and farther than ~20 cm from the shoulder.

The size of the precision ellipses also varied with the hand position. The ellipse area increased as a linear function of the distance from the shoulder except at the most distant hand position (Fig. 2.2C2).

2.3.2 Comparison between Measured and Predicted Hand Precision Ellipses

Hand precision ellipses obtained experimentally for each subject demonstrated target specific orientation and shape (Fig. 2.3). For example, the precision ellipses at distant targets (T1 and T2, Fig. 2.1A) had the tendency to be larger and more elongated than close targets (T3 and T4). The ellipses at right targets T2 and T3 typically had a greater negative orientation angle with respect to the horizontal, whereas the ellipses at left targets were either nearly horizontal (T1) or had the opposite orientation (T4). The predicted hand

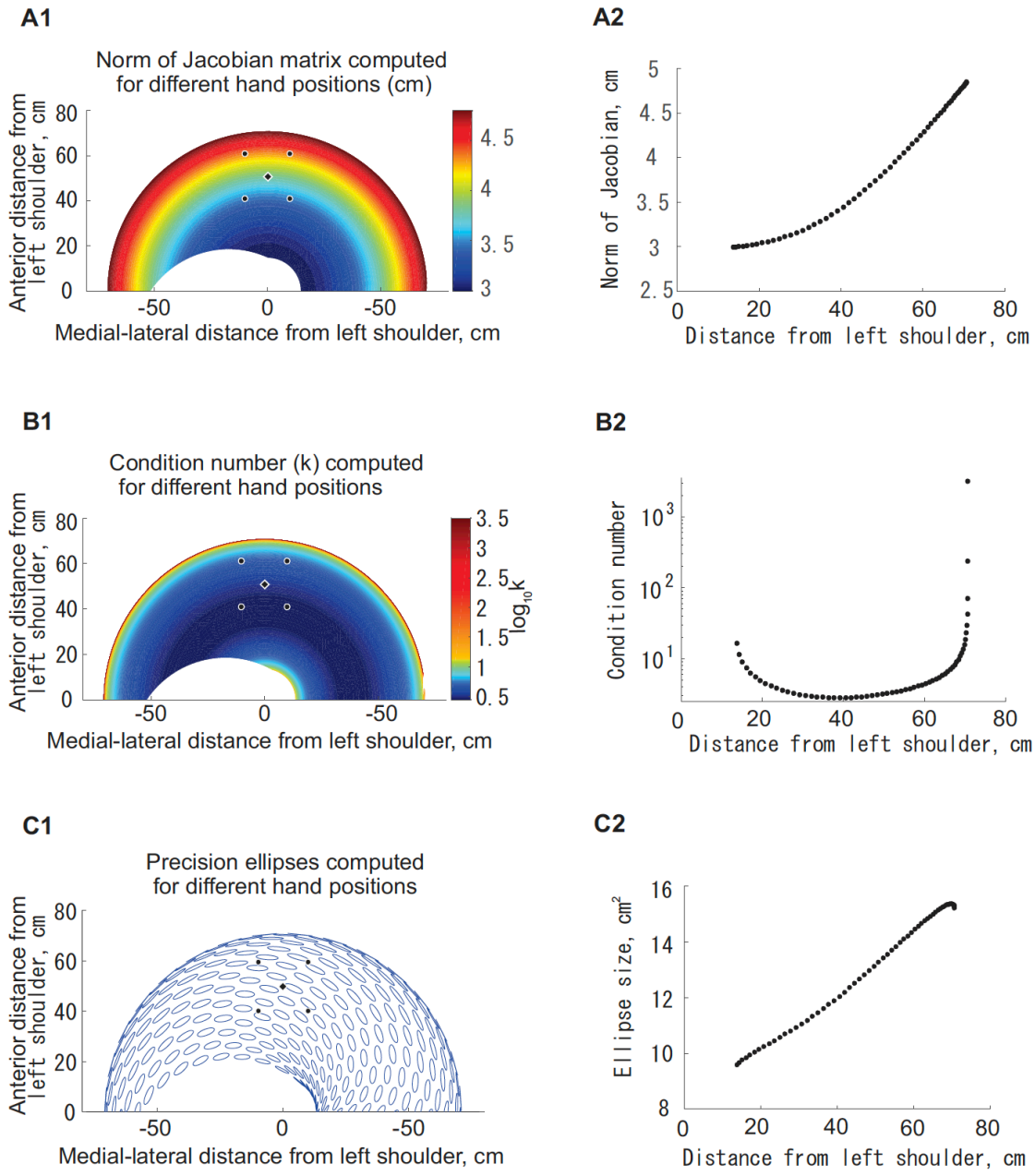

Figure 2.2: Results of geometric analysis of the transformation of random joint angle errors to random errors of hand position in a two-segment arm model. Arm segment lengths were set at L_{ua} = 30.01 cm and L_{fa} = 40.86 cm. In all left panels, the black circles indicate four target positions for the left arm (Fig. 2.1A); the black diamond is the initial position of the left index fingertip. A1: Color map of the norm of Jacobian matrix (or maximum random error) (eq. 6) in the horizontal workspace within the reach of the index fingertip. The coordinates (0,0) correspond to the location of the left shoulder. The norm was computed and plotted for arm configurations corresponding to the elbow and shoulder angles in the ranges of 0.1–3.14 and 0.1–4.08 radians, respectively, with a step of 0.2

radian. The white region in the vicinity of the shoulder indicates the region that could not be reached by the left index fingertip (color bar unit: cm). A2: The Jacobian norm as a function of the distance between the index fingertip and shoulder. B1: Color map of the condition number (ratio of lengths of the major and minor axes of precision ellipse) in the horizontal workspace in logarithmic scale. B2: The condition number as a function of the distance between the index fingertip and shoulder. C1: Precision ellipses computed for different hand locations in the horizontal workspace assuming the perception thresholds of 3.14° and 3.97° for the shoulder and elbow joints (see text for details). The center of each ellipse coincides with the corresponding index fingertip location. The ellipses were plotted in the ranges of 0.1–3.14 and 0.1–4.08 radians for elbow and shoulder joints, respectively, with a step of 0.2 radian. C2: Ellipse size (area) as a function of the distance between the index fingertip and shoulder.

precision ellipses demonstrated qualitatively similar trends (Fig. 2.3). The two-way repeated measures ANOVA revealed that only the ellipse orientation was unaffected by the method of ellipse determination (factor Method: experimental vs. theoretical), that is, the predicted orientation of the hand precision ellipse did not differ from the experimental orientation ($F(1, 10)=4.469$, $p=0.061$). The Pearson correlation coefficient calculated between the theoretical and experimental orientations across all targets and subjects was also rather high and significant ($r=0.683$, $p<0.001$). The ANOVA confirmed the qualitative observations above that the ellipse orientation dependent significantly on Target ($F(3, 30)=24.993$, $p<0.001$), as well as on the Method-Target interaction ($F(3, 30)=6.258$, $p=0.002$). Post hoc tests demonstrated that the predicted and experimented ellipse orientations were different only at target T4 ($p = 0.007$). The mean difference between predicted and experimental ellipse orientations across all four targets was $6.6 \pm 3.1°$.

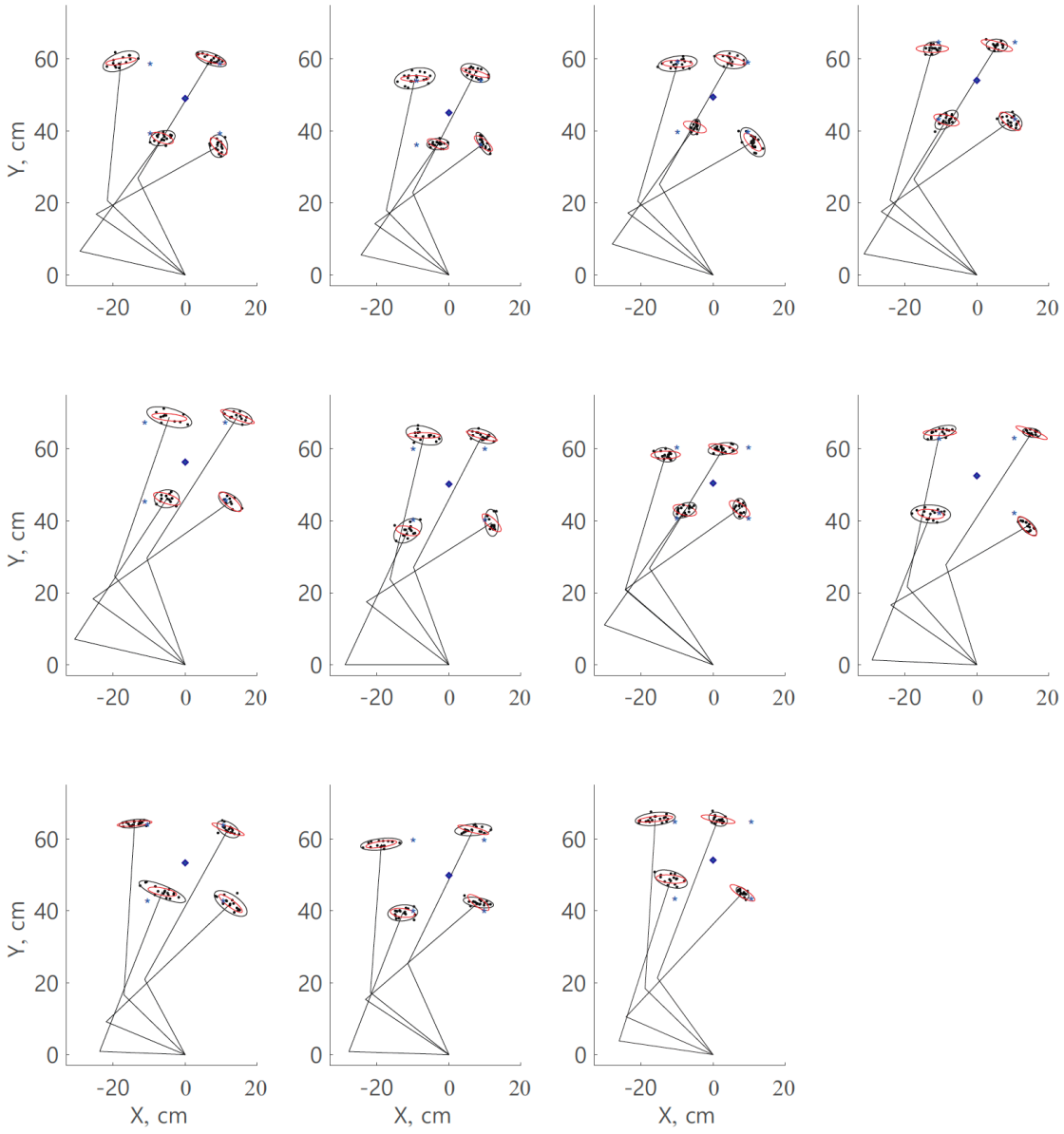

Figure 2.3: Measured (black lines) and predicted by the model (red lines) hand precision ellipses for four targets of all subjects. Small black circles demonstrate results of multiple trials. The upper arm and forearm+hand are displayed as black lines. The blue asterisks indicate target positions; the blue diamonds denote the initial hand position. The endpoint of the arm at each posture coincides with the mean hand position across multiple trials.

The second-best predicted parameter of the precision ellipse was the length of the semi-major axis (the maximum random error). Although factor Method ($F(1, 10)=12.754$, $p=0.005$) had a significant main effect on this variable, the post hoc tests revealed that the predicted maximum random errors were not significantly different from the experiment at targets T2 and T3 (Fig. 2.1A; $p = 0.879$ and $p = 0.104$, respectively). The mean difference in the maximum random errors between the predictions and experiment across all targets was 0.77 cm. The interaction between Method and Target was not significant ($F(3, 30)=2.245$, $p=0.103$). The Pearson correlation coefficient computed between the predicted and measured maximum precision error was relatively low but significant ($r=0.309$, $p=0.046$).

On the other hand, the shape and area of the hand precision ellipse were not well predicted by the arm geometric model. For example, factor Method had a strong significant effect on the ellipse shape and area ($F(1, 10)=143.610$, $p<0.001$ and $F(1, 10)=96.065$, $p<0.001$, respectively). Factor Target affected only the ellipse shape ($F(3, 30)=26.568$, $p<0.001$) but not the ellipse area ($F(3, 30)=1.565$, $p=0.218$). The Method-Target interaction was also significant for the ellipse shape only ($F(3, 30)=32.660$, $p<0.001$). The total random errors, defined as the precision ellipse area were underestimated by the model – the mean predicted and experimental ellipse areas across all targets were 13.0 ± 0.42 cm^2 vs 33.7 ± 6.8 cm^2. The shape of the predicted ellipses was more elongated compared to those of measured ellipses (3.82 ± 0.87 vs 2.23 ± 0.13). The predicted ellipse shape correlated weakly with the ellipse shape determined in the experiment ($r=0.398$, $p=0.008$), whereas there was no significant correlation for the ellipse area $r=-0.019$, $p=0.906$).

2.3.3 *Effects of Arm Posture on Precision of Hand Position Sense in the Horizontal Workspace*

The mean random error in the azimuth direction was greater at distant targets than at close targets for both the experiment ($p=0.018$) and model ($p<0.001$); $F(1, 21)=29.17$, $p=0.001$; Fig. 2.4A1. The experimental azimuth errors were significantly greater than the predicted azimuth errors ($F(1, 21)=60.30$, $p<0.001$) and there was no significant interaction between factors Method and Target Distance ($F(1, 21)=0.170$, $p=0.685$). Similar results were obtained for the random errors in the right-left direction (Fig. 2.4A3) – the errors were greater at distant targets than at close ones ($F(1, 21)=8.40$, $p=0.009$) and the experimental errors were greater than the predictions ($F(1, 21)=44.66$, $p<0.001$).

The mean error in the radial direction was smaller at distant targets compared to the close targets ($F(1, 21)=22.37$, $p<0.001$) and the experimental radial errors were greater than the errors predicted by the model ($F(1, 21)=164.72$, $p<0.001$) with no significant interactions between Target Distance and Method ($F(1, 21)=0.578$, $p=0.456$); Fig. 2.4A2. Similar results were obtained for the mean random error in the forward-backward direction (Fig. 2.4A4; Target Distance: $F(1, 21)=29.39$, $p<0.001$; Method: $F(1, 21)=142.58$, $p<0.001$; Target Distance-Method interaction: $F(1, 21)=0.105$, $p=0.750$).

The comparison between the mean precision errors in the azimuth and radial directions across all targets revealed similar results for the experiment and model predictions – in both cases, the azimuth random error was greater (Fig. 2.4B1; $F(1, 43)=80.57$, $p<0.001$ and $F(1, 43)=190.17$, $p<0.001$). Similarly, both the experimental and

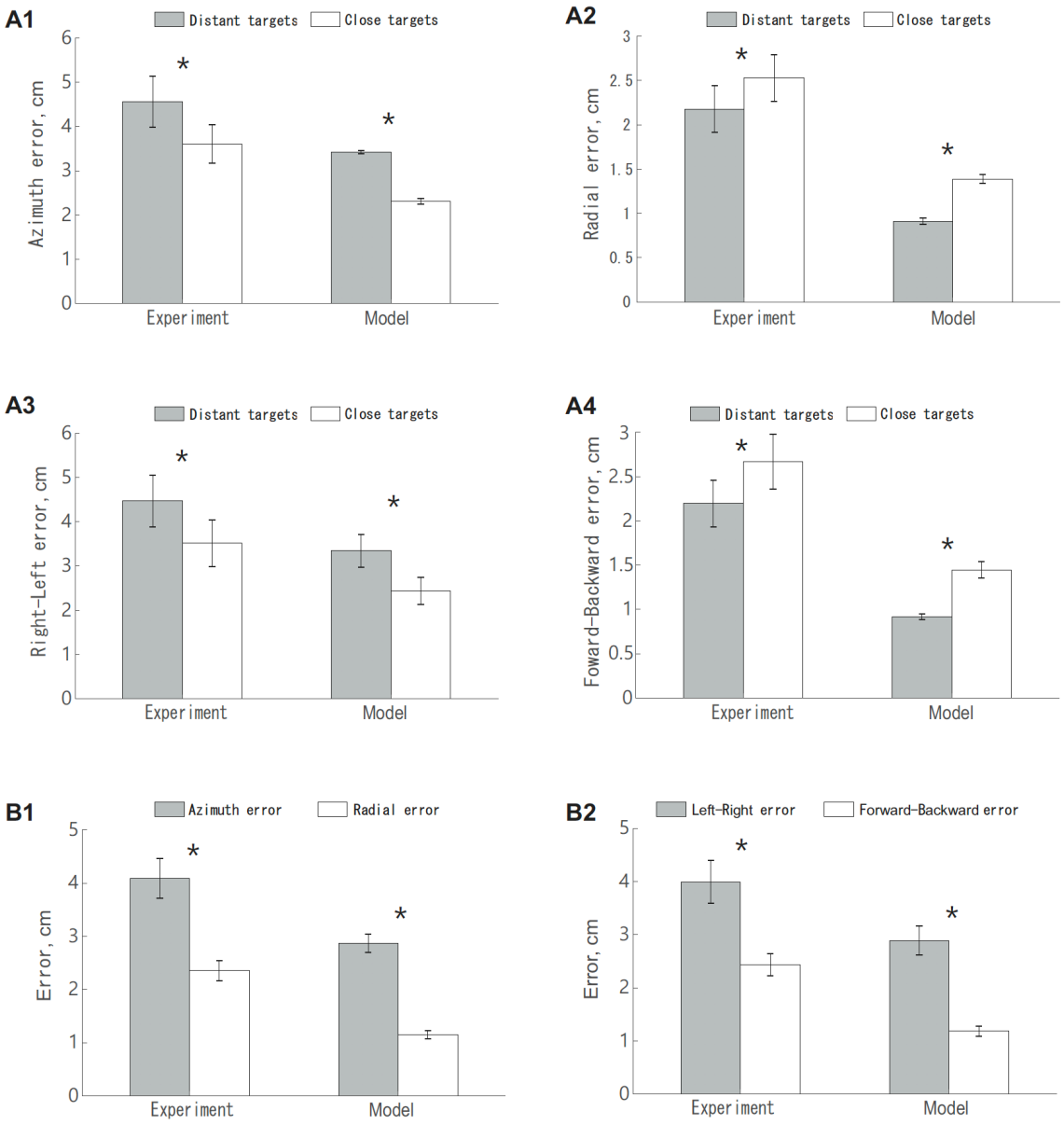

Figure 2.4: Comparisons of measured and predicted by the model mean random errors in different directions for distant (T1 and T2) and close (T3 and T4) targets (Fig. 2.1A). A1: Azimuth random errors for distant and close targets. A2: Radial random errors for distant and close targets. A3: Random errors in the right-left direction for distant and close targets. A4: Random errors in the forward-backward direction for distant and close targets. B1: Comparison of random errors between Azimuth and Radial directions across all targets. B2: Comparison of random errors between left-right and forward-backward directions across all targets.

predicted random errors in right-left direction were greater than those in the forward-backward direction (Fig. 2.4B2; $F(1, 43)=46.84$, $p<0.001$ and $F(1, 43)=100.33$, $p<0.001$).

2.4 Discussion

The goal of this study was to test the hypothesis that the non-uniform precision of hand position sense in a horizontal workspace depends on the arm posture-related transformation of random errors of the arm joint angles to hand position random errors. Geometric analysis of this transformation and precision of hand position sense determined experimentally in the hand position matching experiment supported the hypothesis.

2.4.1 Arm Posture Explains Non-Uniform Precision of Hand Position Sense in the Horizontal Workspace

The geometric model of the arm demonstrated an overall increase in the length of the major axis of the hand precision ellipse and in ellipse area with increasing distance from the shoulder to the hand (Fig. 2.2A1, A2, C2). This result explains the decrease in precision of hand position sense with increasing distance from the body reported in the literature (Rossetti et al. 1994; Slinger and Horsley 1906; van Beers et al. 1998; Wilson et al. 2010) and experimentally found in this study for azimuth and right-left errors (Fig. 2.4A1, A3). The model also predicted and could explain the known experimental fact that the precision of hand position is better in the radial and forward-backward directions than in the azimuth and right-left directions (van Beers et al. 1998; Wilson et al. 2010); see also experimental results of this study (Fig. 2.4B1, B2). This fact is explained by the elongated shape and orientation of the precision ellipses in the azimuth direction in most of the

horizontal workspace (Fig. 2.2C1). In the large workspace area lateral to the ipsilateral shoulder, in which precision of hand position sense is often measured, the precision ellipses are oriented close to the horizontal (Fig. 2.2C1), explaining greater precision in the forward-backward than in the right-left direction.

A few predictions of the arm geometric model were not supported by the experimental results in this study. Namely, the predicted hand precision ellipse size (major axis length of hand precision ellipse, ellipse area and mean random errors; Fig. 2.4) was substantially smaller than those of the ellipses obtained experimentally. There was low or no correlation between the predicted and measured ellipse shape and ellipse size. These discrepancies could be expected if other factors besides arm posture would affect precision of hand position sense (see Introduction). Nevertheless, our results suggest that arm posture alone can explain the non-uniform precision of hand position sense in the horizontal workspace.

2.4.2 Relationship between Predicted Precision of Hand Position and Measured Arm Stiffness

There is another property of the arm that strongly depends on arm posture – arm stiffness, which can be characterized in the horizontal workspace by the arm stiffness ellipse (Flash and Mussa-Ivaldi 1990; Mussa-Ivaldi et al. 1985). Arm stiffness is a relationship between externally applied hand displacements and the forces generated in response from the musculature with neural feedbacks (Flash and Mussa-Ivaldi 1990; Mussa-Ivaldi et al. 1985). (Mussa-Ivaldi et al. 1985) measured arm stiffness in human subjects and found that the shape and orientation of stiffness ellipses were practically

invariant over time and across subjects for given arm postures, whereas ellipse size was variable. To examine if the measured arm stiffness ellipses were related to the predicted hand precision ellipses that also depended on arm posture, we plotted them together (Fig. 2.5) for the same 15 hand locations, for which stiffness was measured by Flash and Mussa-Ivaldi (1990). Since subjects' arm segment lengths were not reported in that study, we used the following lengths of the forearm+hand and upper arm to compute the arm precision ellipses: L_{fa}= 32 cm and L_{ua} = 33 cm. These segment lengths were measured in one subject in the study of Mussa-Ivadi et al. (1985), in which the same method of measuring arm stiffness was used. We also approximated the arm stiffness ellipses for the four targets used in our study (Fig. 2.1A) by the linear surface interpolation (Sandwell 1987; Watson 2013) of the ellipse parameters reported by Flash and Mussa-Ivaldi (1990) (red thick ellipses in Fig. 2.5). It can be seen that the arm precision and stiffness ellipses are nearly orthogonal to each other across the workspace. The mean difference in the direction of the major axis between the stiffness and precision ellipses was 78.0^o ± 9.2^o. The circular correlation coefficient (Jammalamadaka et al. 2001) between the two directions was 0.979.

The nearly orthogonal orientations of the measured stiffness and predicted precision ellipses and high correlation between their orientations suggest that changes in arm stiffness orientation in the horizontal workspace depend on arm posture to a substantially larger degree than previously thought (Flash and Mussa-Ivaldi 1990; Mussa-Ivaldi et al. 1985); see also (Milner 2002; Perreault et al. 2002). The arm stiffness in turn can provide a mechanistic explanation for how the distribution of random errors of hand position sense is shaped in the workspace. For example, the greater precision of hand

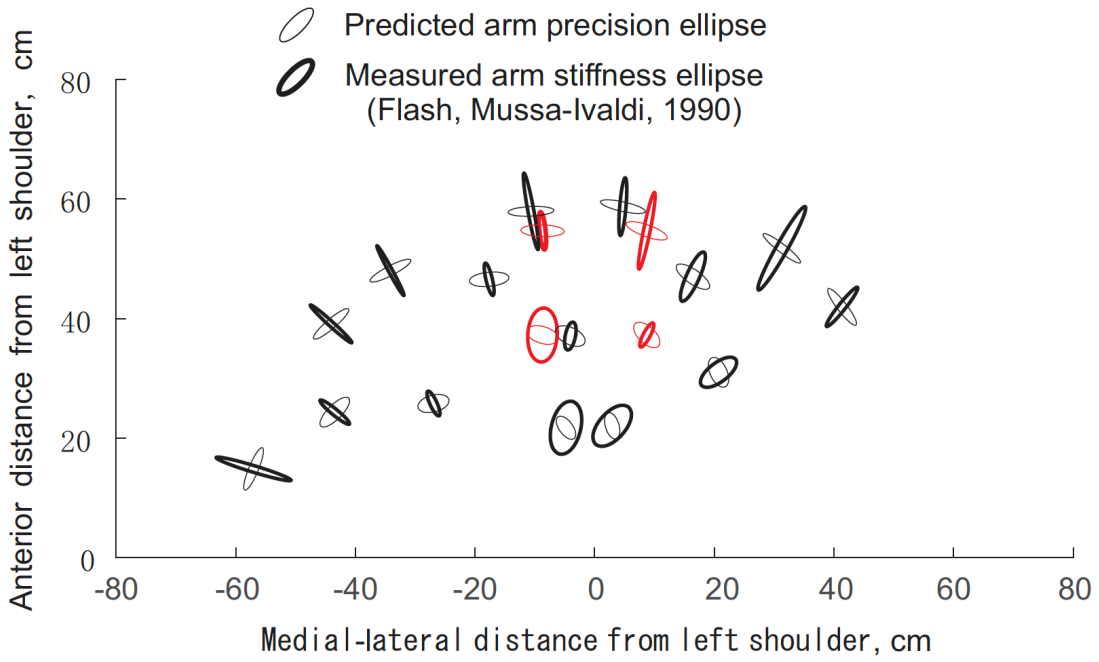

Figure 2.5: Predicted hand precision ellipses and experimentally measured hand stiffness ellipses for the left arm. Stiffness ellipses were measured at 15 hand locations by (Flash and Mussa-Ivaldi 1990). Red ellipses were obtained for the four targets used in this study (see text for details).

position sense in the radial directions compared to the azimuth directions (Fig. 2.4B1, B2; see also (van Beers et al. 1998; Wilson et al. 2010), could be explained by stronger restoring forces in the radial directions due to arm stiffness (Fig. 2.5) that prevent large hand deviations from the intended hand position due to internal and external noise. It should be kept in mind that the orientation, shape, and especially size of the arm stiffness ellipse does depend on muscle activity (Bottasso et al. 2006; Flash and Mussa-Ivaldi 1990; Franklin et al. 2007; Mussa-Ivaldi et al. 1985; Perreault et al. 2002; Prilutsky 2000), and people can modulate limb stiffness by changing muscle activity to improve precision of arm reaching

movements (Wong et al. 2009) or jaw movements during speech (Laboissiere et al. 2009). Our arm model, however, considers only the role of arm geometry in hand position sense. Similar results and conclusions about the relationship between precision of the hand position sense and arm stiffness were provided in (Itaguchi and Fukuzawa 2012; Lametti and Ostry 2010).

2.4.3 Underestimated precision errors by the geometric model

The geometric model reasonably predicted the experimental precision errors, however the magnitudes of predicted precision errors such as azimuth/radial errors and maximum/minimum errors were smaller than those measured in the hand position matching experiments (Fig. 2.3). First possible explanation for this result is that joint perception thresholds used in the model may be smaller than actual ones. For example, the estimated precision of elbow angle position reported in the literature can range from 0.6 – 1.1 degrees (van Beers et al. (1998) to 2.1 – 6.1 degrees (Fuentes and Bastian (2010). Another possibility is that additional sources of precision errors were not taken in to account by the model. Clark et al. (1995), for example, have suggested that precision errors of position sense may be affected by noise of information processing of sensory signals, inter-hemispheric transfer, or motor coordinate transformations. Therefore, additional sources of noise not included in the model might have contributed to smaller precision errors predicted by the model.

2.5 Conclusion

The results of this study demonstrated that arm posture contributes substantially to the non-uniform precision of hand position sense in the horizontal workspace. A two-

segment arm model predicted the orientation and shape of arm precision ellipses that were consistent with the experimentally found greater precision of hand position sense in the radial than in azimuth direction and in locations closer to the body than farther away. Since the theoretical precision ellipses were found to be nearly perpendicular to the arm stiffness ellipses measured in (Flash and Mussa-Ivaldi 1990), we suggest that the restoring forces, originating from the arm stiffness, shape the distribution of random errors of arm position sense and thus are partially responsible for the non-uniform random errors of position sense in different directions and locations of the workspace.

CHAPTER 3. AIM 2: PRECISION AND ACCURACY OF ARM POSITION SENSE ARE DIFFERENT IN THE BLIND AND NORMALLY SIGHTED

3.1 Introduction

Limb position sense is the ability to determine location and orientation of limb segments with respect to each other and to the external environment without vision. According to the current views, limb position sense originates from signals generated by the muscle spindles (Proske and Gandevia 2018) and cutaneous afferents overlying joints (Aimonetti et al. 2007; Cohen et al. 1994; Edin 2001). These signals ascend via the dorsal column and dorsolateral tracts through the medulla and thalamus to the primary somatosensory complex (Delhaye et al. 2018a; Delhaye et al. 2018b). This afferent input generates perception of limb segment positions with respect to each other (joint-based, intrinsic, representation of position sense) and also perception of position of the limb endpoint with respect to the body and external environment (Cartesian body-based representation, extrinsic). The latter representation requires a transformation from the joint-based representation of the limb segments and likely takes place in the posterior parietal cortex that integrates somatosensory, visual and auditory inputs via the multisensory neurons responding to different sensory modalities represented in different coordinate frames (Buneo et al. 2002; Delhaye et al. 2018a; Makin et al. 2007; Maravita et al. 2003).

The coordinate transformations from arm joint-based coordinates to coordinates of the hand in the Cartesian body-based representation is highly non-linear (Oh and Prilutsky

2019; Soechting and Terzuolo 1986) and depends on an accurate body schema and external representation of dimensions of arm segments (Longo et al. 2015; Medina and Coslett 2010). Vision and visual experience has been shown to play an important role in forming somatosensory representations of body segment dimensions and in automatic integration of somatosensory information encoded in intrinsic and extrinsic coordinates (Crollen and Collignon 2012; Thinus-Blanc and Gaunet 1997). For example, viewing a magnified image of one's own arm improves tactile acuity (Kennett et al. 2001). Vision dominates proprioception in perception of limb position in external space; however, with decreasing reliability of visual information, proprioception becomes dominant (Mon-Williams et al. 1997). The blind persons respond differently to an imposed sensory conflict between joint-based sensory signals and sensory information that determines limb location in the extrapersonal space (visual, tactile and auditory) than the normally sighted (Crollen and Collignon 2012; Nava et al. 2014). These results have led to the suggestion that the lack of visual experience, especially early in life, could affect automatic remapping of the joint-based position information (proprioceptive and tactile) onto the limb location information in the external space (Cappagli et al. 2017; Crollen and Collignon 2012; Fiehler et al. 2009). Thus, visual experience may differentially affect the limb position sense in joint and external space coordinates.

The goal of this study was to determine possible effects of visual experience on hand position sense in joint and external space. We hypothesized that individuals lacking visual experience would demonstrate lower accuracy and precision of the hand position sense in external space than normally sighted individuals. We also hypothesized that the blind would have better arm position sense in joint space than in external space.

3.2 Methods and materials

3.2.1 Subjects

All subjects of this study were right-handed (determined based on the Edinburgh Handedness Inventory (Oldfield 1971), over the age of 18 years and had no history of known neurological or musculoskeletal disorders. We recruited seven individuals with normal vision (5 males and 2 females; age = 31.4±12.7 years; mean±SD) and seven age-matched visually-impaired individuals (4 males and 3 females; age = 39.3±15.1 years; Table 3.1). The visually impaired subjects had best-corrected visual acuity at or below 20/200 in both eyes according to the Snellen acuity measure, i.e., they were legally blind. Four subjects from the visually impaired group were congenitally blind; one subject had been blind since the age of three; and the remaining two subjects became blind at the age of 15 and 25, respectively; Table 3.1. On average, the visually impaired subjects had been blind prior to the study for 33.1±10.7 years.

The experimental procedures of this study were consistent with the Ethical Principles for Medical Research Involving Human Subjects described in the Declaration of Helsinki and were approved by the Institutional Review Board of Georgia Institute of Technology. All subjects read (or were read to by the researchers) and signed an informed consent to participate in the study.

Table 3.1 Subject information.

Subject	Vision	Time without vision prior to study (years)	Cause of blindness	Age (years)	Sex	Height (cm)	Forearm + hand length (cm)	Upper arm length (cm)
Sighted Group								
1	Normal	-	-	23	F	152	37.5	25.0
2	Normal	-	-	47	M	178	43.7	31.9
3	Normal	-	-	25	M	181	46.7	31.5
4	Normal	-	-	29	F	156	38.9	32.1
5	Normal	-	-	22	M	170	47.7	33.1
6	Normal	-	-	22	M	170	41.3	27.3
7	Normal	-	-	52	M	188	47.2	26.3
Mean ± SD	-	-	-	31.4 ±12.7	-	168.9 ±11.4	42.41 ±3.62	29.48 ±2.56
Visually impaired group								
1	Impaired	38	Congenital malformation	38	M	160	45.5	25.4
2	Impaired	35	Congenital malformation	35	M	175	43.9	33.3
3	Impaired	43	Degenerative retinitis pigmentosa	58	M	180	49.3	33.5
4	Impaired	31	Diabetes	56	M	168	40.8	31.3
5	Impaired	46	Congenital malformation	46	F	152	37.3	23.8
6	Impaired	23	Optic nerve hypoplasia	23	F	152	39.1	26.4
7	Impaired	16	Retinoblastoma	19	F	150	34.2	22.9
Mean ± SD	-	33.1 ±10.7	-	39.3 ±15.1	-	162.4 ±12.1	41.44 ±5.16	28.09 ±4.51

3.2.2 Experimental tasks

The subjects performed bilateral arm matching tasks while they were seated in the chair of the Kinarm exoskeleton robot (BKIN Technologies Ltd., Kingston ON, Canada) with both arms supported by the robot arms in a horizontal workspace (Fig. 3.1). Prior to each experimental session, subject's arms were secured in a pronated position in the Kinarm robotic arms, and the vertical axis of rotation of the shoulder and elbow joints of each arm was aligned with the corresponding joints of the Kinarm. No motion at the wrist joints was available. The Kinarm was calibrated in accordance with established procedures.

Each subject performed three bilateral arm matching tasks. The three tasks were: (1) joint angle matching (JAM), in which the subject was instructed to match the shoulder and elbow angles of the reference right arm by the left arm (in joint coordinates); (2) hand distance and direction matching (DDM), in which the subject was instructed to match by the left hand the distance and direction of the reference right hand with respect to the initial hand position (in external space coordinates); and (3) hand distance and mirror direction matching (MDDM), in which the subject was to match by the left hand the distance and mirror direction of the reference right hand with respect to the initial hand position (in external space coordinates). As a result, JAM and MDDM had kinematically identical configuration though the instructions were based on either joint angle or distance/direction from the starting positions. The subjects were instructed that they could start their hand position matching with the left hand after they heard an audio cue that rang when the robot finished moving subjects' right hand to a target location. They were asked to stay still when they finished the hand position matching until their hands were moved back to starting points by robot or experimenters.

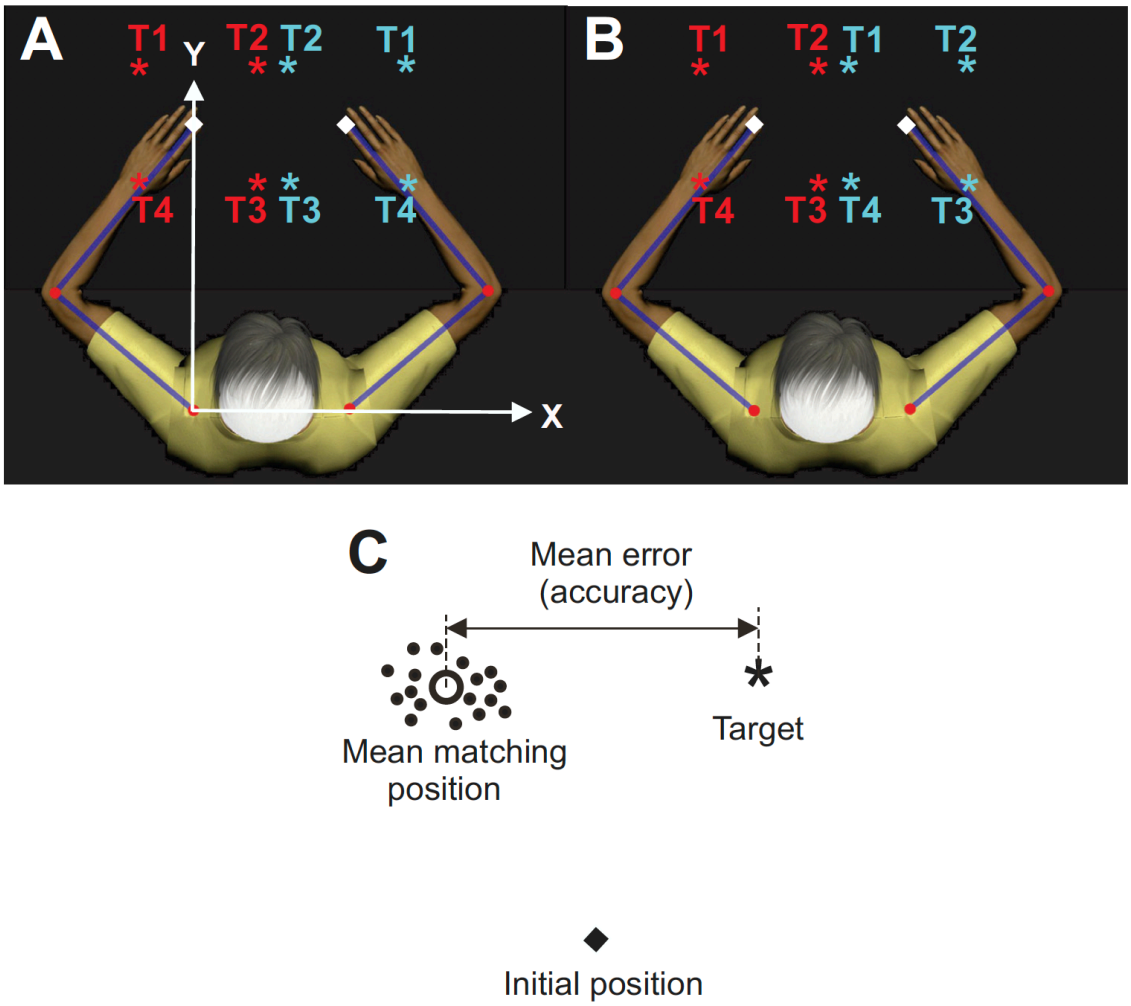

Figure 3.1: Schematic of experimental setup and geometric arm model. A: Bimanual joint angle matching (JAM) and hand distance and mirror direction matching (MDDM) tasks. The initial positions of the left and right index fingertips are marked as white diamonds. Cyan asterisks indicate target locations where the robot placed the right index fingertip. The corresponding red asterisks indicate target locations where the subject would place the left index fingertip if the JAM and MDDM arm matching tasks were accurately performed. B: Bimanual hand distance and direction matching task (DDM). Note different locations of the targets for the right hand. C: Definition of accuracy (mean error) of arm position matching.

At the beginning of each trial of JAM task, the Kinarm moved both hands of the subject to the initial positions in front of the corresponding shoulder; these hand positions corresponded to an elbow angle of each arm of 90^{o} (Fig. 3.1A). After a short delay (1 s), the Kinarm moved the right reference hand of the subject to one of the four target positions in random order over the period of 1 sec. The target locations for the right arm were: (1) at 45^{o} from the horizontal in the counterclockwise direction, T1; (2) at 135^{o}, T2; (3) at 225^{o}, T3; and (4) at 315^{o}, T4. When Kinarm robot placed the right index fingertip at a target and stopped, it generated a 200-ms beeping sound that indicated that the subject could start moving the left arm to perform joint angle matching. The assigned time for performing the matching task was 2.5 sec. The subjects were instructed to hold the position of the left arm when they reached the matching position until the Kinarm moved both arms back to the initial positions. Joint angle matching was repeated 72 times (18 times for each target in pseudo-random order) with a 5-min break after every 24 repetitions. During the experiment, the arms and targets were hidden from subject's view by a non-transparent screen and cloth. In the JAM task, the subject matched the shoulder and elbow angles of the right arm at each of arm configurations corresponding to the four targets (Fig. 3.1A) by the left arm. Since a two-joint arm in the horizontal plane is not kinematically redundant, there is a one-to-one correspondence between a given combination of shoulder and elbow angles and the corresponding horizontal and vertical hand coordinates. Thus, if the left and right joint angles were perfectly matched at each of four configurations of the right arm, the left hand position would be located at one of the four red targets in Fig. 3.1A. To account for subjects' arm length, the target distance was normalized based on the distance between the initial hand position and the shoulder: $D = 0.1\sqrt{2(x/0.5272)}$, where x is the

distance in m between the initial index fingertip position and the shoulder of a given subject; 0.5272 is the same distance in m for the subject from a preliminary study (her forearm+hand length and upper arm length were 40.86 cm and 30.01 cm, respectively). For that subject the distances to the targets were 10 cm from the initial position. After normalization, the absolute target distances from the initial hand position for all subjects ranged from 0.115 to 0.166 m.

After completing the JAM task and taking a 5-min rest, the hand direction and distance matching (DDM) task was performed by each subject using the same experimental protocol (18 matching for each target with a 5-min break after every 24 repetitions; 72 trials in total). In this task, the subject was instructed to match the distance and direction of the right index finger tip with respect to the initial fingertip position. For example, when the robot moved the right index fingertip to target T2 (cyan T2 target in Fig. 3.1B), the subject would match this right hand position by moving the left index fingertip from its initial position in the same direction by the same distance (red T2 target in Fig. 3.1B). The rest of the right hand targets T1, T3 and T4 corresponded to the left hand targets as shown in Fig. 3.1B.

The last arm position matching task performed by the subjects was the hand mirror direction and distance matching (MDDM) task. For example, when the robot moved the right index fingertip to target T1 (cyan T1 target in Fig. 3.1A), the subject was instructed to match the distance and the mirror direction of the right index finger tip with respect to the initial position with the left fingertip (red T1 target in Fig. 3.1A). The subjects in all tasks did not see their arms or targets.

3.2.3 Data analysis

As mentioned above, for a two-joint arm in a two-dimensional horizontal plane, a given combination of shoulder and elbow angles corresponds to the unique position of the index fingertip. Therefore, to evaluate accuracy and precision (random errors) of the joint angle matching performance, we analyzed the position errors of the left index fingertip with respect to the mirror position of the corresponding right index fingertip (red targets in Fig. 3.1A). The performance of hand position matching in the DDM and MDDM tasks was evaluated by comparing the matching position of the left index fingertip with the corresponding target positions of the left fingertip (red targets on Fig. 3.1B and Fig. 3.1A, respectively).

The accuracy of position sense (mean error) was computed for each subject, task and target as the mean distance between the patching position of the left index fingertip and the corresponding target position (Fig. 3.1C). To compute the random error (precision) of hand position sense, the mean x and y coordinates of the left fingertip obtained across 18 trials for each subject, target and task were subtracted from the matching left fingertip coordinates obtained for a given subject and target. The obtained differences represented random errors of arm position sense. The experimental distribution of these errors was fitted by the 95% confidence ellipse (Johnson and Wichern 2007). Each ellipse was characterized by four parameters: the direction and length of the semi-major axis, size (area), and elongation (shape), i.e. the ratio of the lengths of the major and minor axes. The ellipse direction was defined as an angle of 0^o to 90^o between the ellipse major axis and the horizontal. Positive and negative orientation angles of the precision ellipse corresponded

to the counterclockwise and clockwise rotations of the major axis from the horizontal, respectively.

3.2.4 Statistical analysis

To test the effects of vision, arm matching task and target location on accuracy of hand position sense, a linear mixed model analysis (West et al. 2015) was performed using statistical software IBM SPSS v20 (Chicago, IL, USA). In this analysis, Vision (normal sight, blindness), Task (JAM, DDM, MDDM), and Target (target locations T1 – T4, Fig. 3.1A, B) were within-subject independent fixed factors, whereas Subject and Trial were random factors. The dependent variable was the mean error (Fig. 3.1C). The Bonferroni post-hoc test was used for pairwise comparisons.

The same linear mixed model analysis was performed to evaluate the effects of the within-subject independent fixed factors – Vision, Task, and Target, on precision of arm position sense. The dependent variable was the area of the precision ellipse. The Bonferroni post-hoc test was used for pairwise comparisons. The significance level for all tests was set at an alpha level of 0.05.

3.3 Results

Although the target distances for each subject were normalized in accordance with the arm length, for display purposes, the target locations, locations of measured fingertip positions and the arm segment lengths were scaled such that the four target locations were at the horizontal and vertical distance of ± 10 cm from the initial position.

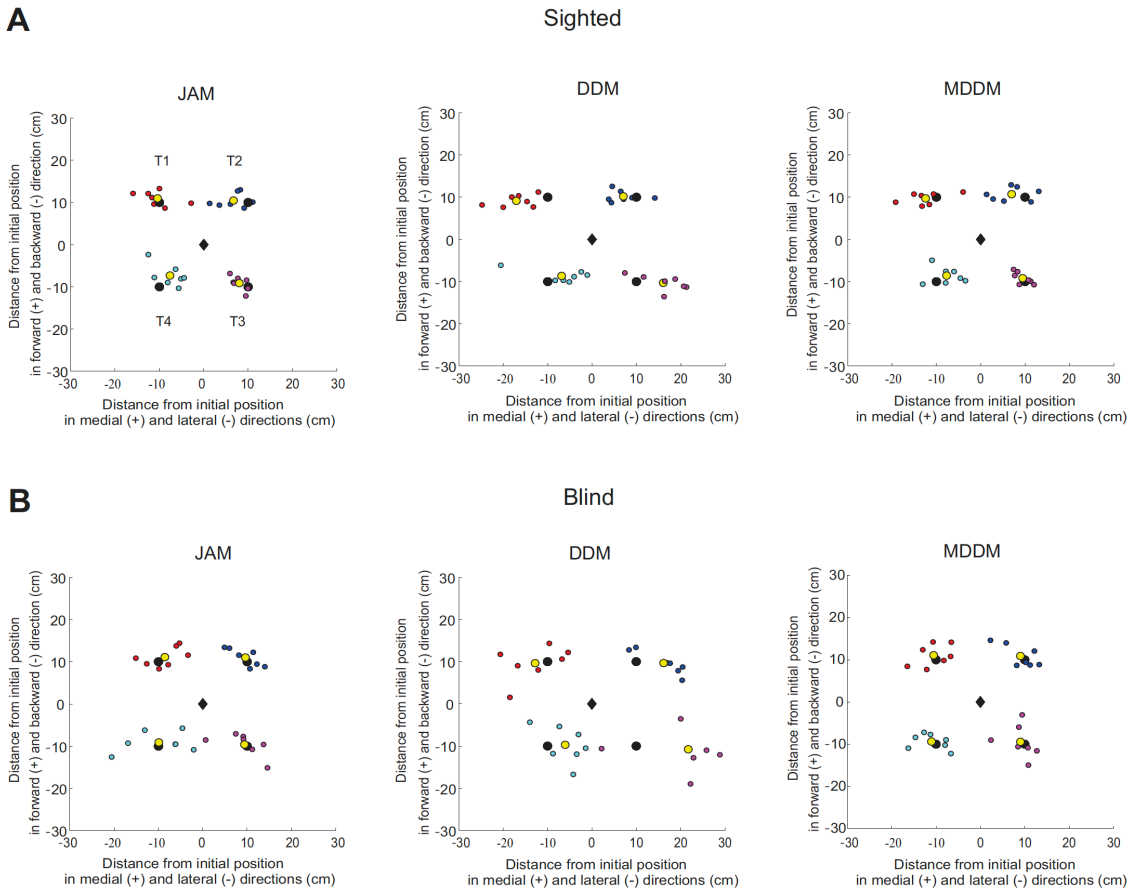

Figure 3.2: Matching positions of the left hand of individual subjects with respect to four targets (T1 – T4). Target position are indicated by black circles (correspond to the red asterisks in Fig. 3.1A, B). Black diamond indicates the initial hand position. Small color dots correspond to the mean matching hand position of individual subjects for a given target. Yellow circles indicate the mean hand matching positions across all subjects for a given target. JAM, DDM and MDDM denote the joint angle matching, hand distance and direction matching, and hand distance and mirror direction matching tasks, respectively (see text for more details). For presentation purposes, the location of hand matching positions and targets, as well as arm segment lengths of each subject were scaled to make the targets be located at the horizontal and vertical distances of ± 10 cm from the initial left hand position. A: Left hand matching positions of the sighted subjects in three arm position matching tasks. B: Left hand matching positions of the blind subjects in three arm position matching tasks.

3.3.1 Accuracy of hand position sense

The mean matching positions of the left index fingertip of individual normally sighted and blind subjects with respect to the target positions are shown in Fig. 3.2. Qualitatively, accuracy (the distance between the left hand matching position (yellowcircles) and the targets (black circles) appear to be markedly better for the tasks JAM and MDDM than for the task DDM for both groups of subjects. The accuracy of hand position sense, i.e., the mean error between the matching position of the left fingertip and the corresponding target location, was significantly affected by all three fixed factors: Vision $F(1, 16)=4.133$, $p=0.059$), Task ($F(2, 2597)=368.925$, $p<0.001$) and Target location ($F(3, 2597)=19.785$, $p<0.001$). All interactions between two or three factors were significant (Vision*Target ($F(3, 2597)=45.339$, $p<0.001$), Vision*Task ($F(2, 2597)=31.036$, $p<0.001$), Target*Task ($F(6, 2597)=81.723$, $p<0.001$), and Target*Vision*Task ($F(6, 2597)=23.522$, $p<0.001$). Post-hoc analysis revealed that the accuracy errors of arm matching in all three tasks were lower in the sighted group compared to the blind subjects across all targets ($F(1, 2597)=169.193$, $p<0.001$, Fig 3.3A). Another post-hoc analysis for task comparisons revealed that both subject groups had significantly lower accuracy in the DDM matching tasks ($F(2, 2597)=99.952$, $p<0.001$ and $F(2, 2597)=289.438$, $p<0.001$, respectively), whereas the accuracy of JAM and MDDM matching tasks did not differ significantly in sighted (($F(1, 2597)=0.1$, $p=0.752$) and blind ($F(1, 2597)=1.1$, $p=0.294$) subjects (Fig 3.3B).

3.3.2 Precision of hand position sense

The precision (random error) of arm position sense, as measured by the area of precision ellipse, was significantly affected by all fixed factors: Vision ($F(1,192)=13.994$,

$p<0.001$), Task ($F(2,192)=7.195$, $p=0.001$) and Target ($F(1,192)=4.583$, $p=0.004$). One significant interaction was found between Target and Task ($F(6,192)=3.083$, $p=0.007$). Precision ellipses of individual subjects for each matching tasks are shown in Fig. 3.4. Qualitatively, the shape (elongation) and orientation of precision ellipses were similar at a given target across subjects and tasks. For example, precision ellipses located farther away (T1 and T2, Fig. 3.1A) were more elongated and larger than targets closer to the body (T3 and T4). Precision ellipses at target T3 typically had negative orientations as opposed to ellipses at targets T1 and T4 that had either positive or horizontal orientations. Two congenitally blind subjects S1 and S2, as well as blind subject S3 who was blind for 43 years (Table 3.1), demonstrated especially poor precision of hand position sense in all tasks (ellipse areas ranged from 22.0 to 244.5 cm^2; Fig. 3.4B). Sighted subjects S3 and S6 demonstrated relatively low precision of arm position sense in task DDM (ellipse areas were between 20.6 and 169 cm^2; Fig. 3.4A).

Precision ellipses combined for all subjects within the sighted and blind groups are shown for each task in Fig. 3.5. For plotting purposes, the means of the matching left index finger position of each subject were placed to corresponding target locations. Precision ellipses of the blind subjects appeared to be much larger than those of the sighted subjects, especially for tasks JAM and MDDM. Ellipse orientation for a given target was generally consistent across tasks for both groups of subjects with few exceptions. For example, in blind subjects, ellipse orientation at target T3 was positive in task MDDM but negative in

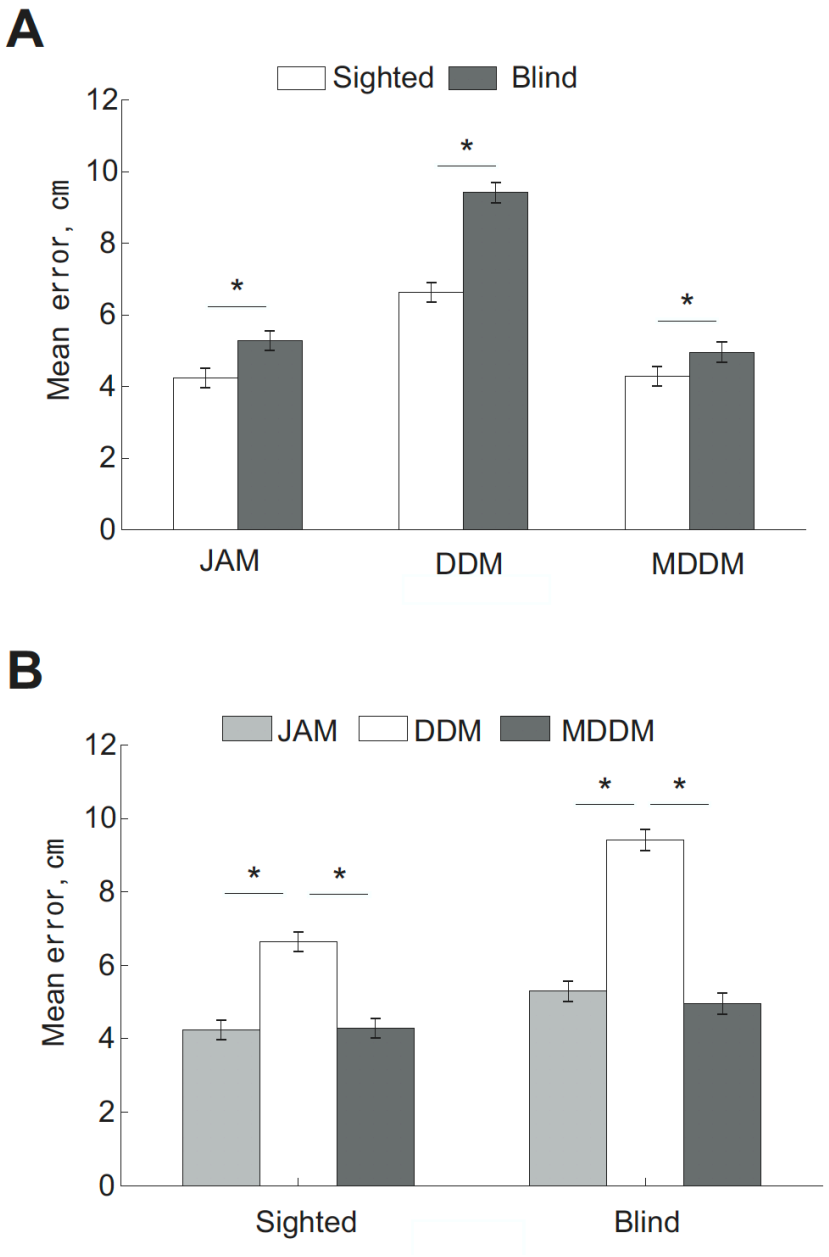

Figure 3.3: Accuracy (mean error) of arm position matching of the sighted and blind subjects for three arm position matching tasks across all targets. JAM, DDM and MDDM denote the joint angle matching, hand distance and direction matching, and hand distance and mirror direction matching tasks, respectively. Error bars represent 95%-confidence intervals. The horizontal lines with asterisks indicate significant differences ($p<0.05$) between the tasks or subject groups. A: Comparison of accuracy between the sighted and blind groups in three tasks. B: Comparison of accuracy among tasks for the sighted and blind subject groups.

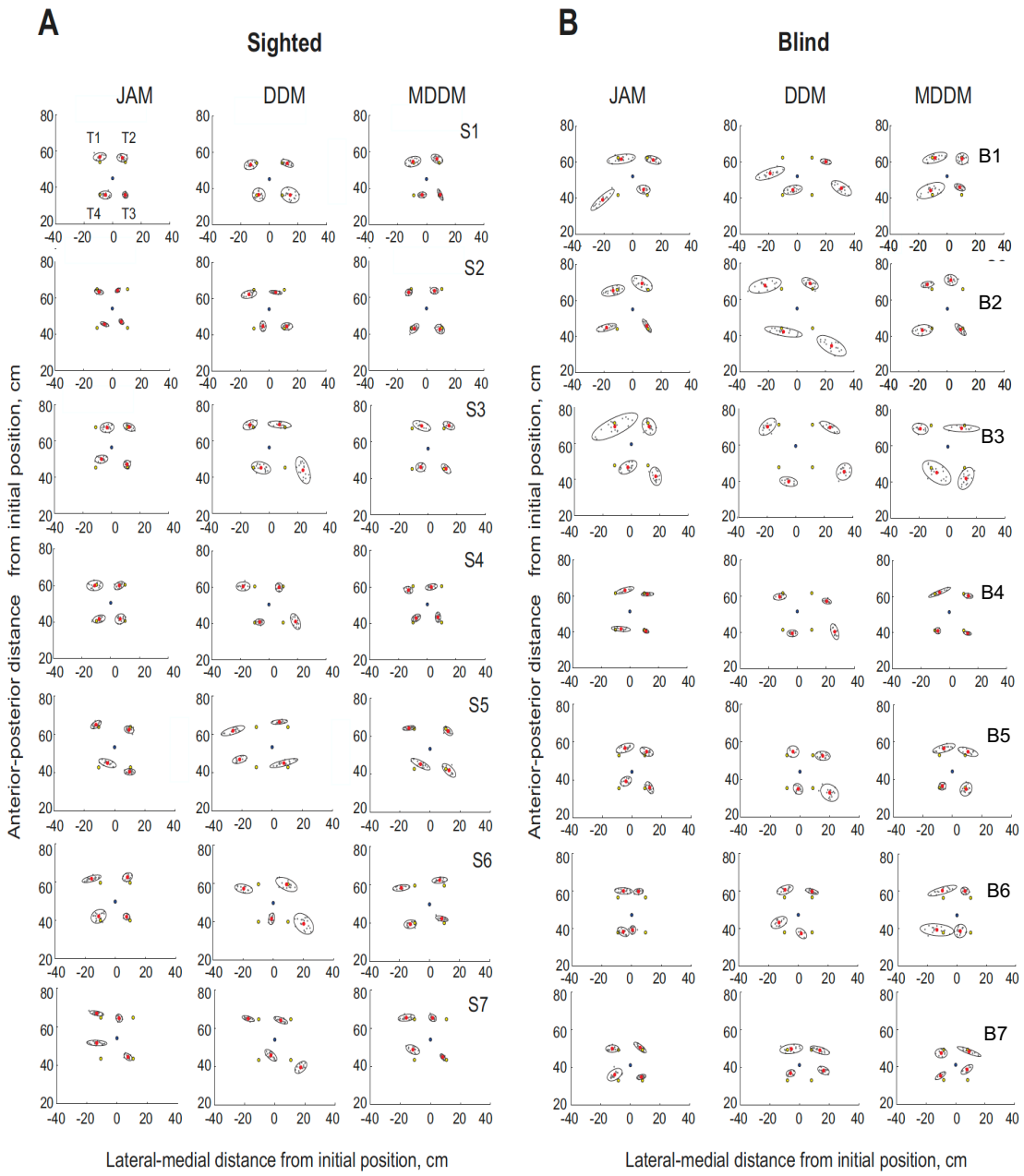

Figure 3.4: Distributions of random errors (precision ellipses) for each subject (S1, S1, …, S7), target and task. The ellipses correspond to 95%-confidential interval. Yellow circuits are target locations; gray dots are the mean left hand matching positions of individual subjects for a given target; red circles are the mean left hand matching positions across subjects for a given target; blue circles are initial left hand position. JAM, DDM and MDDM denote the joint angle matching, hand distance and direction matching, and hand distance and mirror direction matching tasks, respectively. A: Sighted subjects. B: Blind subjects.

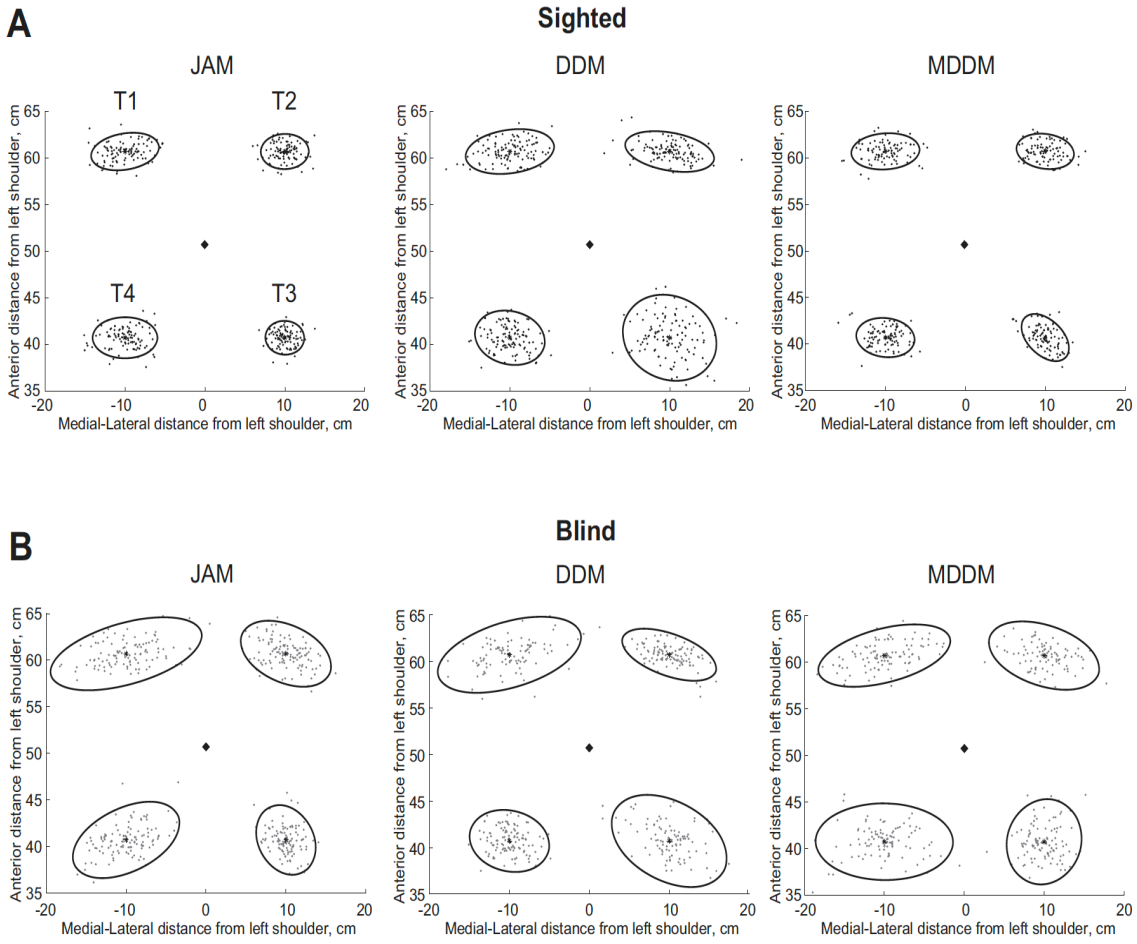

Figure 3.5: Combined precision ellipses of all subjects within each subject group. For display purposes, the mean left hand matching position of each subject was placed at the corresponding target location. Data were scaled to make the targets be located at the horizontal and vertical distances of $\pm$10 cm from the initial left hand position. JAM, DDM and MDDM denote the joint angle matching, hand distance and direction matching, and hand distance and mirror direction matching tasks, respectively. A: Sighted subjects. B: Blind subjects.

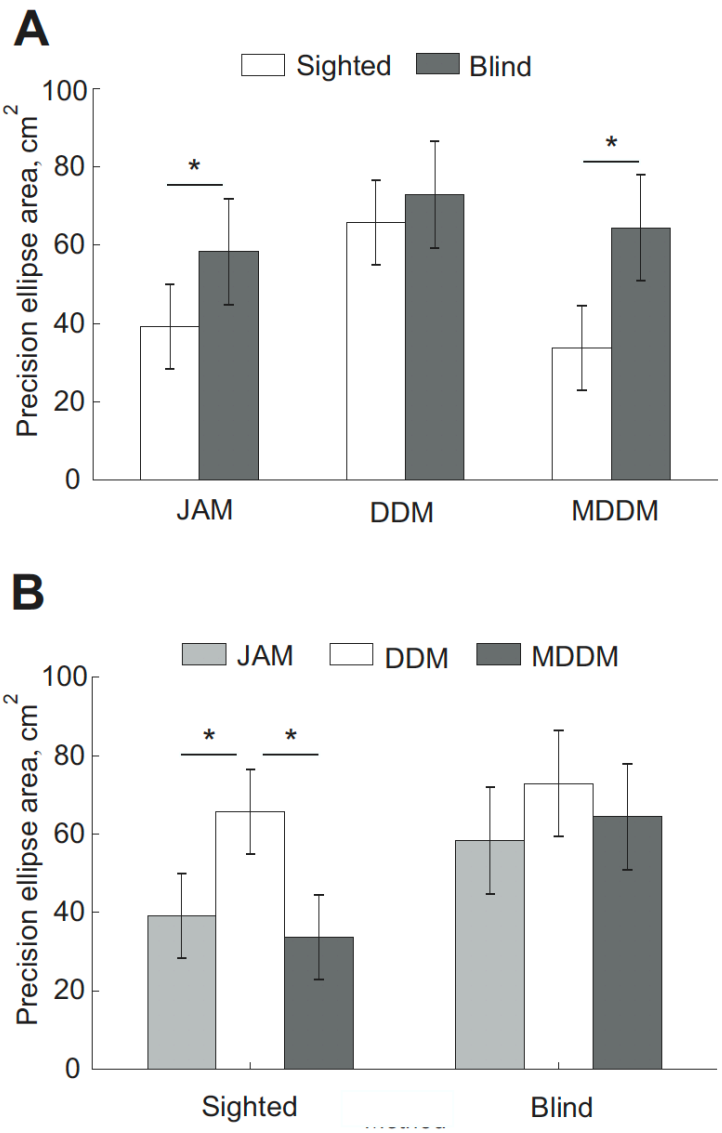

Figure 3.6: Mean of the precision ellipse area of arm position matching of the sighted and blind subjects for three arm position matching tasks across all targets. JAM, DDM and MDDM denote the joint angle matching, hand distance and direction matching, and hand distance and mirror direction matching tasks, respectively. Error bars represent 95%-confidence intervals. The horizontal lines with asterisks indicate significant differences ($p<0.05$) between the tasks or subject groups. A: Comparison of the precision ellipse area between the sighted and blind groups in three tasks. B: Comparison of the precision ellipse area among tasks for the sighted and blind subject groups.

tasks JAM and DDM (Fig. 3.5B). Post-hoc analysis revealed higher precision of arm position sense (lower area of the precision ellipse) of the sighted group compared to the blind subjects in tasks JAM ($F(1, 192)=4.734$, $p=0.031$) and MDDM ($F(1, 192)=12.233$, $p<0.001$). However, there was no difference in precision between the two groups of subjects in the DDM task ($F(1, 192)=0.650$, $p=0.421$; Fig. 3.6A). When the area of precision ellipses was compared among tasks for both groups of subjects, the sighted group demonstrated lower precision of position sense in the DDM task compared to the tasks JAM ($p<0.002$) and MDDM ($p<0.001$). There was no difference in precision ellipse area between the latter two tasks ($p=1.000$; Fig. 3.6B). The precision ellipse areas in the blind subject group did not differ significantly among the three tasks ($F(2, 192)=1.128$, $p<0.326$; Fig. 3.6B).

3.4 Discussion

The goal of this study was to determine possible effects of visual experience on hand position sense in joint and external space. We tested the hypotheses that individuals lacking visual experience would demonstrate lower accuracy and precision of the hand position sense in the external space than normally sighted individuals, and that the blind would have better arm position sense in joint space than in external space. The results of this study generally supported the first hypothesis, as the sighted subjects had higher accuracy of arm position sense than the blind in the two hand position matching tasks in external space, DDM and MDDM (Fig. 3.3A). However, precision of arm position sense was better in the sighted group in only one of the two hand matching tasks in external space, MDDM; whereas there was no difference in precision of hand position sense between the sighted and blind groups in the hand position matching task DDM (Fig. 3.6A). The second

hypothesis was only partially supported. Although accuracy of joint angle matching (task JAM) was better than accuracy of hand position matching in external coordinates (task DDM) in the blind group, there was no difference in accuracy of the joint angle matching and another hand position matching task in external coordinates, MDDM (Fig. 3.3B). In addition, the blind subjects demonstrated the same precision of arm position matching in joint and external coordinates (Fig. 3.6B).

3.4.1 Arm Position Matching Tasks and their Coordinate Systems

Assuming that that subjects followed the given instructions to perform the arm position matching tasks, the joint angle matching (task JAM) should involve evaluation of shoulder and elbow angles of the right reference arm and matching these angles by the left arm. Arm positions in this task are represented in joint-based coordinates, which are encoded by activity of the muscle spindles (Proske and Gandevia 2018) and skin afferents overlaying the joints (Aimonetti et al. 2007). The hand positions and directions in the tasks DDM and MDDM are, on the contrary, represented in external body-centered Cartisian coordinates that provide information about hand location with respect to the body in the horizontal plane. To derive hand position information without vision, the nervous system presumably transforms the joint-based sensory information to the hand location information using estimated dimensions of arm segments (Longo and Haggard 2010). Since evaluations of shape and dimensions of body segments are not precise and depend on previous experience and integration with other sensory modalities that modify perceived body image (Gandevia and Phegan 1999; Kennett et al. 2001), one could expect that joint angle matching between the two arms would be more accurate and precise than matching hand location in external space. In accordance with this expectation, arm position sense

was more accurate in the joint angle matching tasks than in the hand position matching DDM task in both groups of subjects (Fig. 3.3B); however, the hand position matching performance in the other hand position matching tasks MDDM had the same accuracy and precision as observed in the angle matching task in the sighted and blind subjects (Fig. 3.6B). Note that the second hand position matching task MDDM was kinematically identical to the joint angle matching task JAM (Fig. 3.1A). Thus, we cannot exclude the possibility that the subjects performing the hand matching MDDM task used joint angle matching instead even though these two tasks were separated during the course of testing by the hand matching DDM task (see METODS). The possibility that the subjects used joint angle matching in the MDDM task could explain the same matching performance in the JAM and MDDM tasks.

Another possible reason for the greater errors in asymmetric (DDM) task is that different muscle groups were recruited in the right and left arms when the subjects conducted DDM tasks. However, Iandolo et al. (2015) have reported that matching accuracy of asymmetric task in external coordinates was higher than that of symmetric task in joint coordinates during bimanual matching. Therefore, greater error in the asymmetric task cannot be explained by just recruitment of different muscle groups. Interestingly, in the asymmetric task of Iandolo et al. (2015), both hands had to be located at the same location in horizontal workspace even though they did not touch each other due to a vertical gap between them. This might have provided an additional perceptional cue and could explain a better hand position matching performance in that study.

The joint angle matching strategy was impossible to implement to perform the hand position matching in the DDM task because the joint angles of the referent right arm were

different from those of the indicator left arm (Fig. 3.1B). Therefore, the subjects had to derive hand position information from the joint-based sensory information of the two arms. Several previous studies have demonstrated that limb position sense evaluated in external coordinates of the peripersonal space may be more accurate than the same limb position judged in joint-based coordinates (Fuentes and Bastian 2010; Soechting 1982). These authors and others have explained these results by suggesting that the brain might better perceive limb positions in external peripersonal space because of integration of sensory information from multiple sensory modalities (i.e., proprioceptive, visiual, tactile and auditory) during the development and everyday sensory experiences. This idea was not supported by our results – accuracy and precision of joint angle matching was either better than or not different from the hand position matching in external coordinates (tasks DDM and MDDM, respectively; Fig. 3.3B and 3.6B). These discrepancies with previous studies could be caused by the fact that the previous studies examined relatively simple one-joint limb matching tasks (Fuentes and Bastian 2010; Soechting 1982), whereas we investigated two-joint arm position matching. Although configurations of a two-joint arm in a horizontal plane are not kinematically redundant (i.e., a given combination of shoulder and elbow angles correspond to a unique hand position), the geometric transformation from noisy joint angles to hand horizontal coordinates is still complex, ie., nonlinear and arm posture-related (Oh and Prilutsky 2019). Therefore, integration of multimodular sensory information about limb position during everyday tasks might not be able to improve limb position sense in the external peripersonal space for a multi-joint tasks as opposed a one-joint task.

3.4.2 Role of visual experience in hand position sense

The fact that the blind subjects in general had lower accuracy (Fig. 3.3A) and precision of hand position sense (in tasks JAM and MDDM; Fig. 3.6A) than the normally sighted suggests that visual experience improves arm position sense. Less accurate and precise position sense in the blind subjects cannot be explained by their older age compared to the sighted subjects (by 6.2 years or 16%; Table 3.1) and the fact that proprioceptive function degrades with age (Goble et al. 2009). First, ages of two subject groups were not statistically different (2-tailed independent t test, $p=0.651$). Second, we repeated the linear mixed analysis to test the effects of Vision, Task and Target of accuracy and precision of arm position sense using age of the subjects as a covariate. Inclusion age as a covariate did not change the results. Thus, the findings of this study are consistent with the notion that visual experience is important for the formation of accurate representation of external space by the nervous system (Thinus-Blanc and Gaunet 1997).

Although the auditory (Kellogg 1962) and tactile (Postma et al. 2007) sensory modalities contribute importantly to the development of the spatial sense, individuals deprived of visual experience early in life might not be able to form an exact representation of the peripersonal space. This might affect the joint angle and hand position matching tasks in blind persons differently. The former task relies on the comparison of joint angle-related proprioceptive and tactile information from the left and right limbs, which does not require the knowledge of arm location in the external space (Proske 2015). Although hand positions in external space can be derived from the joint angle-related information, this derivation requires estimations of arm segment dimensions from body schema (Longo and Haggard 2010), which might be compromised in the blind because of the importance of visual experience for forming an accurate body schema (Cattaneo et al. 2008; Gross et al.

1974) and automatic remapping between hand position in joint and external space (Crollen and Collignon 2012).

Nevertheless, accuracy of arm position sense in joint-based coordinates (task JAM) and hand external coordinates (task MDDM) was the same in the blind group. Precision of arm position sense was likewise the same in the above two tasks and the second hand position matching task DDM. The fact that position sense of the blind subjects was for the most part not worse in hand position matching than in joint angle matching task could be explained by the fact that 5 of 7 blind subjects (71%) lost sight at early age (≤3 years, Table 3.1). Congenital and early blind persons may substantially compensate effects of no or reduced visual experience on perception of external space by enhanced acuity in other sensory modalities, i.e. tactile (Alary et al. 2008; Stevens et al. 1996) and auditory (Lessard et al. 1998).

3.5 Conclusion

We found that the blind subjects generally had lower accuracy and precision of arm position sense in joint angle and hand position matching tasks than normally sighted individuals. Thus, visual experience positively affects arm position sense possibly due to integration of visual and proprioceptive sensory information and the development of more accurate body schema. We also found that the blind subjects had the same precision of arm position sense in the joint angle matching and hand position matching tasks. This unexpected result could be explained by a possible increase in perceptual acuity of other exteroceptors, e.g. tactile, that can provide information about limb position in the peripersonal space.

CHAPTER 4. AIM 3: INVESTIGATE ACCURACY OF HAND POSITION SENSE IN CUED MOVEMENT PARADIGM BASED ON NEGATIVE EEG POTENTIALS IN BLIND AND SIGHTED PEOPLE DURING ARM POSITION MATCHING IN JOINT AND EXTERNAL SPACE

4.1 Introduction

Visual experience is known to contribute to the formation of the hand position sense (Thinus-Blanc and Gaunet 1997) via shaping the body schema that contributes to perception of arm localization in the extrapersonal space (Longo and Haggard 2010). Specifically, hand position sense may arise from the mapping of joint-based, proprioceptive and tactile information onto visual information of hand location in extrapersonal space (Crollen and Collignon 2012). Visual information therefore calibrates joint-based sensory information to the extrapersonal space (Shadmehr and Wise 2005). As such, lack of visual experience, common in long-term visually impaired individuals, could ultimately result in a poor mapping of joint-based information onto the extrapersonal space. Thus, it might take more cognitive effort and greater errors for a visually impaired person to perform coordinate transformations from the joint to external space compared to blindfolded normally sighted people.

In the case of upper limb, information related to joint position from sensory receptors such as muscle spindles, tactile cutaneous receptors, mechanoreceptors in joint capsule area, and Golgi tendon organs reach the primary somatosensory cortex through the

dorsal column-medial lemniscus pathway (Delhaye et al. 2018a; Proske and Gandevia 2018). On the other hand, the posterior parietal cortex is known to be related to various coordinate transformations (Bhattacharyya et al. 2009; Galletti et al. 1999; Pesaran et al. 2006) and multisensory representation in peripersonal space (Buneo et al. 2002; Makin et al. 2007). Therefore, to perceive a limb endpoint position such as the hand, joint-based information from the primary somatosensory cortex needs to be transformed presumably in the posterior parietal cortex to limb endpoint position in the external space.

It has been suggested that task complexity expected to perform an upcoming motor task can be evaluated using the EEG contingent negative variation (CNV) potential (Cui et al. 2000; Walter et al. 1964). This potential can be measured between two stimuli: (i) a cue warning stimulus indicating an upcoming task and an imperative stimulus to initiate the task. Since the CNV potential has been reported to reflect complexity of an upcoming task, it can be used to distinguish between joint position matching and hand position matching tasks. One can assume that hand position matching tasks would be more complex compared to joint angle matching tasks, even if the two tasks have the same kinematics, because the former requires a transformation from joint angular positions to hand positions.

The goal these experiments was to compare complexity of joint position matching and hand position matching tasks using a CNV-inspired EEG potential. The hypothesis was tested that hand position matching tasks would be more complex, i.e. they would have more negative CNV-inspired potentials than those in the joint angle matching tasks.

4.2 Methods and materials

4.2.1 Subjects

All subjects of this study were right-handed (determined based on the Edinburgh Handedness Inventory (Oldfield 1971), over the age of 18 years and had no history of known neurological or musculoskeletal disorders. EEG data was collected from all participants, however, based on quality of EEG, seven individuals with normal vision (5 males and 2 females; age = 30.1±13.7 years (mean±SD) and seven visually-impaired individuals (4 males and 3 females; age = 39.3±15.1 years (Table 4.1) were selected and analyzed in Aim 3. The majority of the participants in this study also participated in the experiments of Aim 3. The visually impaired subjects had best-corrected visual acuity at or below 20/200 in both eyes according to the Snellen acuity measure, i.e., they were legally blind. Four subjects from the visually impaired group were congenitally blind; one subject had been blind since age of three; and the remaining two subjects became blind at the age of 15 and 25, respectively; Table 4.1. On average, the visually impaired subjects had been blind prior to the study for 33.1±10.7 years (mean±SD).

The experimental procedures of this study were consistent with the Ethical Principles for Medical Research Involving Human Subjects described in the Declaration of Helsinki and were approved by the Institutional Review Board of Georgia Institute of Technology. All subjects read (or were read to by the researchers) and signed an informed consent that was approved by the Institutional Review Board.

4.2.2 Experimental tasks

We measured accuracy of hand position sense and EEG activity in right-handed individuals with normal (n=7) and impaired (n=7) vision during hand position matching tasks.

Table 4.1 Subject information.

Subject	Vision	Time without vision (years)	Cause of blindness	Age (years)	Sex	Height (cm)	Forearm + hand length (cm)	Upper arm length (cm)
Sighted Group								
1	Normal	-	-	19	M	165	39.83	29.25
2	Normal	-	-	47	M	178	43.69	31.88
3	Normal	-	-	29	F	156	38.94	32.12
4	Normal	-	-	20	M	175	29.08	43.74
5	Normal	-	-	22	M	170	23.76	47.7
6	Normal	-	-	22	M	170	41.34	27.28
7	Normal	-	-	52	M	188	47.22	26.33
Mean ± SD	-	-	-	30.1 ±13.7	-	171.7 ±10.1	37.7 ±8.31	34.0 ±8.34
Visually impaired group								
1	Impaired	38	Congenital malformation	38	M	160	45.5	25.4
2	Impaired	35	Congenital malformation	35	M	175	43.9	33.3
3	Impaired	43	Degenerative retinitis pigmentosa	58	M	180	49.3	33.5
4	Impaired	31	Diabetes	56	M	168	40.8	31.3
5	Impaired	46	Congenital malformation	46	F	152	37.3	23.8
6	Impaired	23	Optic nerve hypoplasia	23	F	152	39.1	26.4
7	Impaired	16	Retinoblastoma	19	F	150	34.2	22.9
Mean ± SD	-	33.1 ±10.7	-	39.3 ±15.1	-	162.4 ±12.1	41.44 ±5.16	28.09 ±4.51

4.2.2.1 Hand position matching experiment

Gaunet and Rossetti (2006) and Rossetti et al. (1996) have reported that deprivation of early visual experience decreased the ability for memorizing proprioceptive targets. Therefore, bilateral hand position matching tasks, during which the subjects do not need to remember target locations, allow to avoid influences of memorizing proprioceptive targets.

Subjects performed three bilateral hand position matching tasks while they were seated in the chair of the Kinarm exoskeleton robot (BKIN Technologies Ltd., Kingston ON, Canada) with both arms supported by the robot arms in a horizontal workspace (Fig. 4.1). Before initiation of each task, subject's arms were secured in a pronated position in the Kinarm robotic arms, and the vertical axis of rotation of the shoulder and elbow joints of each arm was aligned with the corresponding joints of the Kinarm. No motion at the wrist joints was available. The Kinarm was calibrated in accordance with established procedures.

The three arm matching tasks: (1) joint angle matching (JAM), (2) Distance and dirction matching (DDM), and (3) Mirror direction and distance matching (MDDM) were the same as those described in Chapter 3 (see also Fig. 4.1). The analysis of accuracy was also the same.

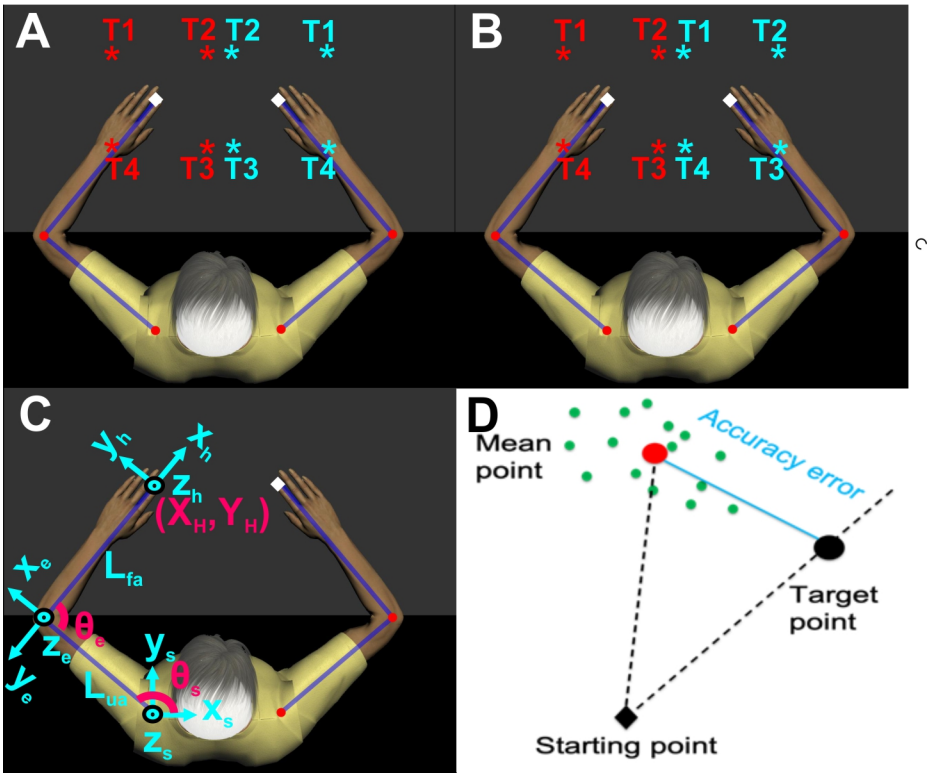

Figure 4.1: Schematic of experimental setup and geometric arm model. A: Bimanual arm-matching experiment (Tasks JAM, DDM and MDDM, see text for details). The initial positions of the left and right index fingertips are marked as white diamond. Red and cyan colored asterisks are the four targets for each arm. Cyan asterisks indicate targets reached by the robot with the right arm; red asterisks show targets reached by the subject with the left arm to match the corresponding right targets. B: Bimanual arm-matching experiment (asymmetric task: Task DDM). C: Coordinates of arm joints and parameters of the arm model for computing the forward kinematics using the Jacobian matrix. The origins of the shoulder, elbow and hand coordinate frames are at the shoulder, elbow and index fingertip, respectively. The positive directions of the corresponding x and y axes are indicated by the arrows; the direction of the z axes is perpendicular to the xy plane. θ_s and θ_e denote angles of the shoulder and elbow joints; L_{ua} and L_{fa} are the length of the upper arm and forearm+hand segments. D: Definitions of different accuracy error.

4.2.2.2 EEG recordings and cued movement paradigm for evoking negative potentials

EEG was recorded while the subjects were performing the hand position matching experiments. A standard 64 channel tin electrode cap (Electro cap, Eaton, OH) was used, and EEG was recorded with Synamps 2 system (Neuroscan, Charlotte, NC) (Fig. 4.2). Two electrodes were placed around the left eye to measure the electrooculographic activity, and one electrode was attached at each ear as a reference. The recording sampling rate was 1000 Hz.

As a pre-processing, the raw EEG data were epoched based on the onset of audio beep, that informed the subject that they need to initiate their position matching with the left hand; the beep was assigned the zero time point. Time period from -1500 msec to -1000 msec was assigned as a baseline where both of subject's hands were located at initial points (Fig. 4.3). The first time mark, a warning signal was the onset of the passive right-hand movement by the robot (-1000 msec) and second time mark, an imperative stimulus, was the audio beep at 0 msec.

4.2.3 Analysis of experimental data

The distances from the left shoulder to the initial point and the target distances from the initial point were differently set for each subject according to the arm segment lengths in the experiment, however, for display purposes, the location of actual data points and target locations from the initial point, the distance from the left shoulder and the initial point, and the arm segment lengths were scaled to make the four target locations be at ($\pm$10, $\pm$10) cm from the initial point.

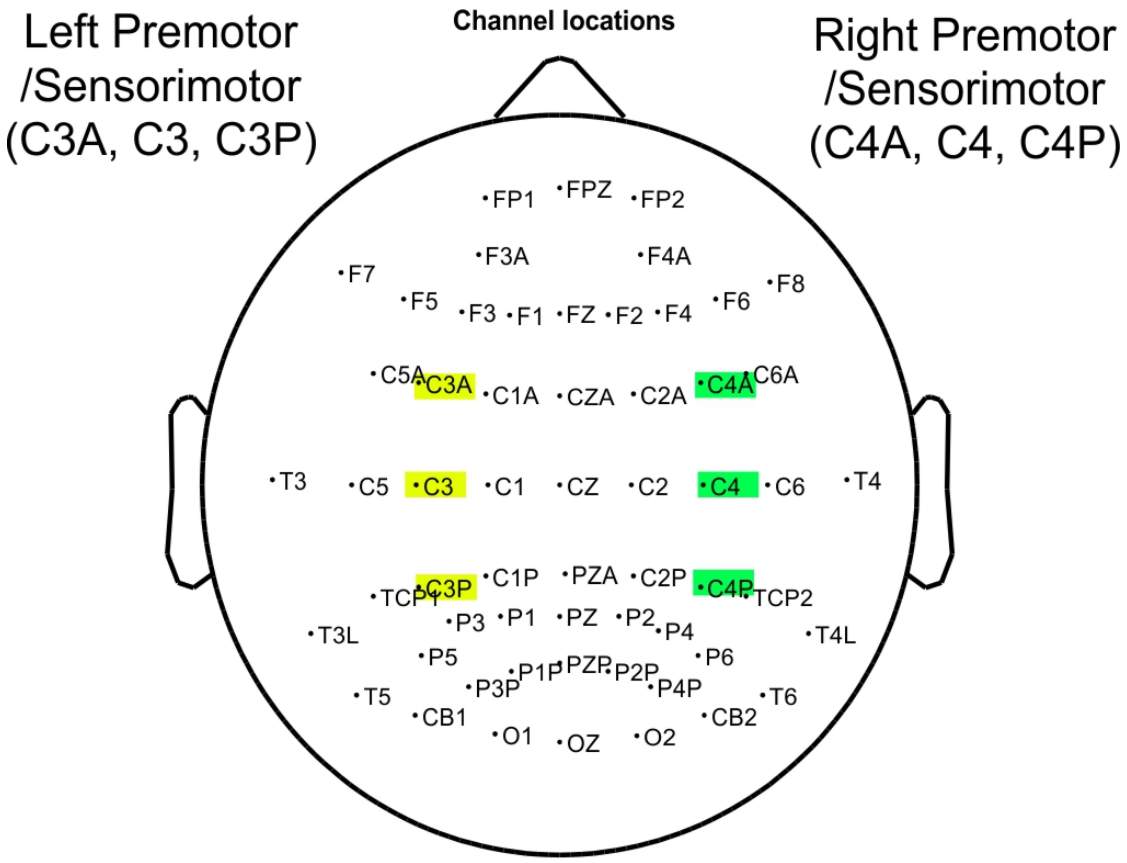

Figure 4.2: Channel locations. All 64 channels used for EEG record are presented. Only yellow (Left premotor/sensory motor: C3A, C3, and C3P) and green (Right premotor/sensory motor: C4A, C4, and C4P) colored channels were used for data analysis in this study.

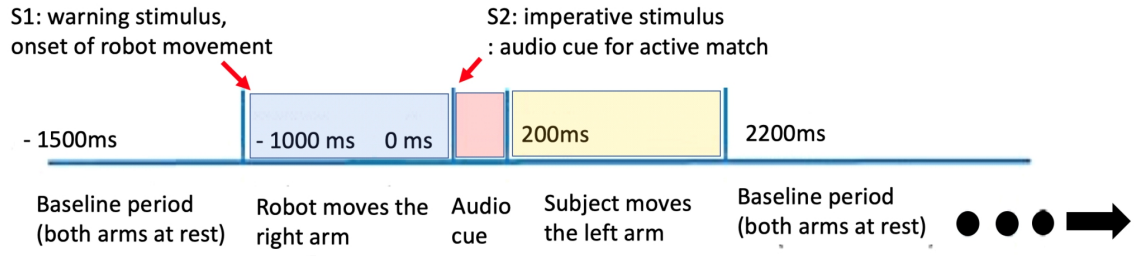

Figure 4.3: Time epochs for EEG analysis.

The mean x and y coordinates of the left index fingertip with respect to the mirror position of the right index fingertip were computed to evaluate the accuracy of hand position sense. The accuracy error was computed for each subject, task and target as the mean distance between the left index finger tip and the mirror position of the right index fingertip (target position, Fig. 4.1D).

EEG data were filtered by a bandpass filter (0.5-50 Hz). Eye blink and movement artifact were corrected via recursive least squares, and the residual artifacts were corrected with independent component analyses. Each single EEG trial was divided into two epochs: (1) passive movement of the right arm by the robot (-1000 - 0 msec) and (2) active movement of the left arm by the subject (0 – 2200 msec) (Fig. 4.3). Except for audio beep artifact duration (0~1000 msec), all the other time periods were separated by 500 ms time windows, and the average potentials of each time window were used for statistical analyses.

4.2.4 Statistical analysis

To test accuracy of hand position sense (Fig. 4.1D), a linear mixed model analysis (West et al. 2015) was performed. In this analysis, Vision (normal sight, blindness), Task (joint angle matching, hand position matching), and Target (target locations T1 – T4, Fig. 4.1A and 1B) were considered as fixed factors, whereas Subject and Trial were considered random factors. The Bonferroni post-hoc test was used for pairwise comparisons.

For comparisons of EEG potentials, one-way ANOVA were performed for averaged EEG potential values in each 500 msec time window with a fixed factor Vision or Task. All statistical tests were performed using IBM SPSS v21 software (Chicago, IL,

USA). The significance level for all tests was set at an alpha level of 0.05, and the Bonferroni post-hoc test was used for pairwise comparisons.

4.3 Results

4.3.1 Accuracy of hand position sense

Mean positions of the left index fingertip of individual subject are shown in Fig. 4.4. Since the data were scaled for 10 by 10 cm target locations, all the subjects share the same target locations. The accuracy of hand position sense, distance between the left fingertip and corresponding target location, was significantly affected by all three fixed factors: Task ($F(2, 2609)=453.752$, $p<0.001$), Target location ($F(3, 2609)=27.077$, $p<0.001$), and Vision $F(1, 2609)=94.998$, $p<0.001$). All interactions between two or three factors were significant (Target*Vision ($F(3, 2609)=28.059$, $p<0.001$), Target Task ($F(6, 2609)=79.119$, $p<0.001$), Vision*Task ($F(2, 2609)=9.310$, $p<0.001$), and Target* Vision* Task ($F(6, 2609)=30.681$, $p<0.001$).

When accuracy was compared excluding influence of target locations through a post-hoc analysis, the accuracy of the sighted was clearly higher than that of the blind subjects across all tasks (Fig 4.5A). Another post-hoc analysis for task comparisons revealed that both subject groups showed greater level of errors in asymmetric hand position matching tasks, and the accuracy of the other two tasks (JAM and MDDM) was not significantly different (Fig 4.5B).

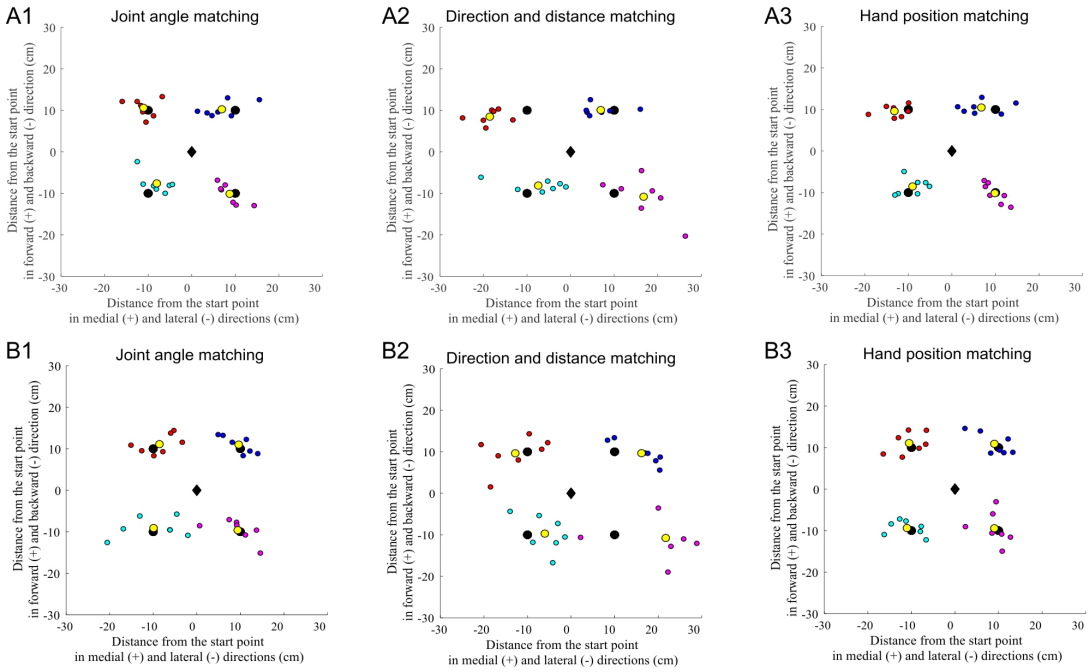

Figure 4.4: Mean left hand positions of individual subjects with respect to four targets (small color dots). Positions of targets T1-T4 (larger black circles) correspond to those shown in Fig. 4.1A and Fig. 4.1B by red asterisks. Black diamonds indicate the initial hand positions. A1, A2, and A3: Joint angle matching (JAM), asymmetric hand position matching (DDM), and symmetric hand position matching (MDDM) tasks, respectively, for normally sighted subjects. B1, B2, and B3: Joint angle matching, asymmetric hand position matching, and symmetric hand position matching tasks, respectively, for blind subjects. For each subject, the location of actual data and targets, arm segments lengths, and the distance from the left shoulder to the initial point were scaled to make the targets be located at $\pm$10 cm, $\pm$10 cm from the initial point.

4.3.2 Cued movement paradigm for evoking negative potentials

Measured EEG negative potentials in this study commonly presented CNV-like patterns across subject groups and tasks. They arose between two stimuli and started with brief positive potentials. Then, the potentials shifted to negative. It should be noted that artifacts caused by the audio beep were mixed with the potentials in 0-800 msec period though the beep lasted for 0-200 msec. However, measured EEG potentials were clearly affected by the subjects' visual experience and the tasks (Fig. 4.6, 4.7, and 4.8).

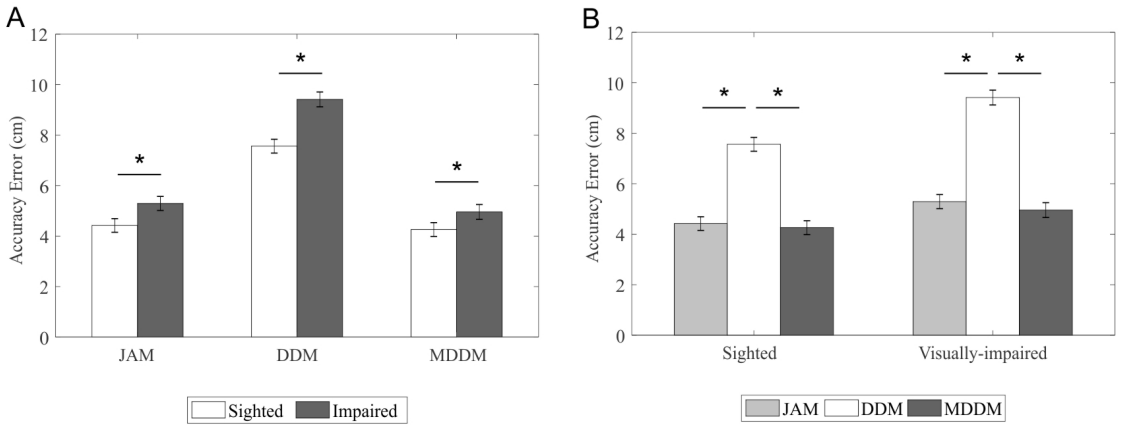

Figure 4.5: Comparisons of accuracy at four targets between subject groups and tasks. Error bars represent 95%-confidence intervals. The horizontal brackets indicate significant differences ($p<0.05$) between the tasks or subject groups. A: Accuracy comparisons between subject groups in each task. B: Accuracy comparisons among tasks in each subject group.

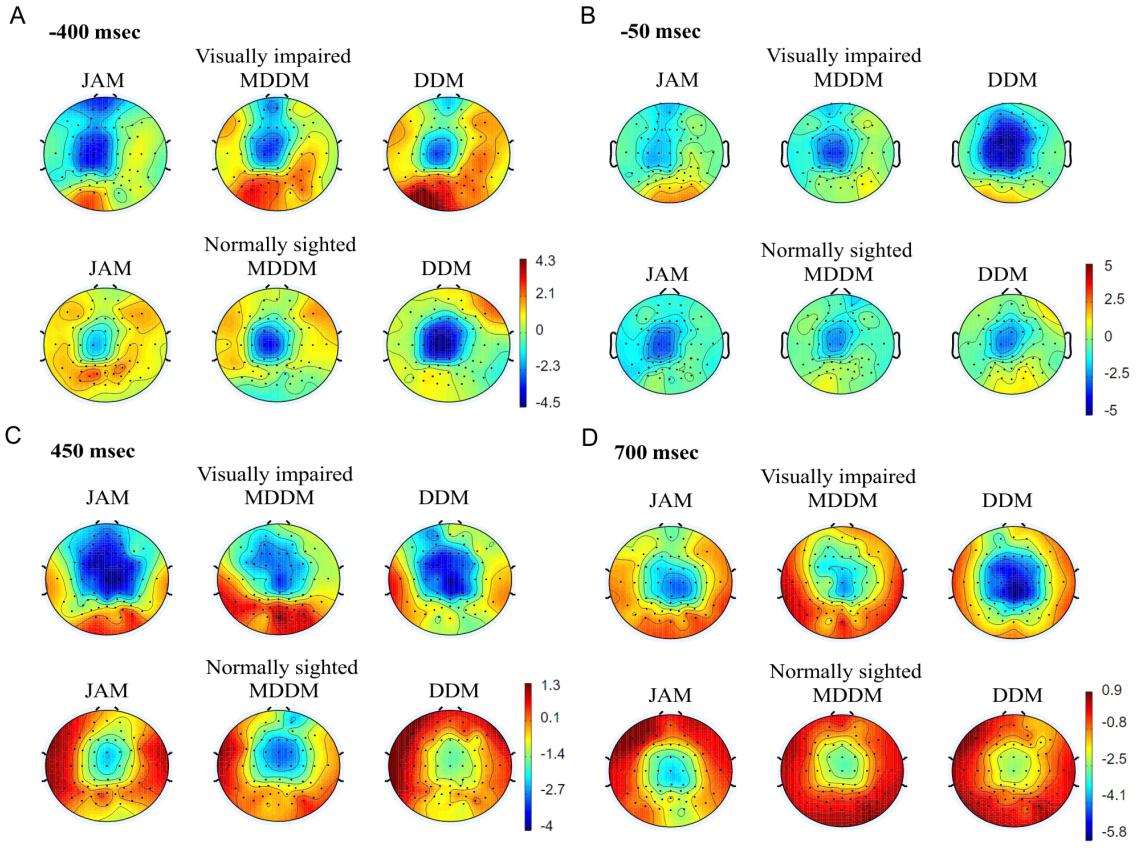

Figure 4.6: Head maps of EEG. A. at A) -400 msec, B) at -50 msec, C) 450 msec, and D) 700 msec, respectively.

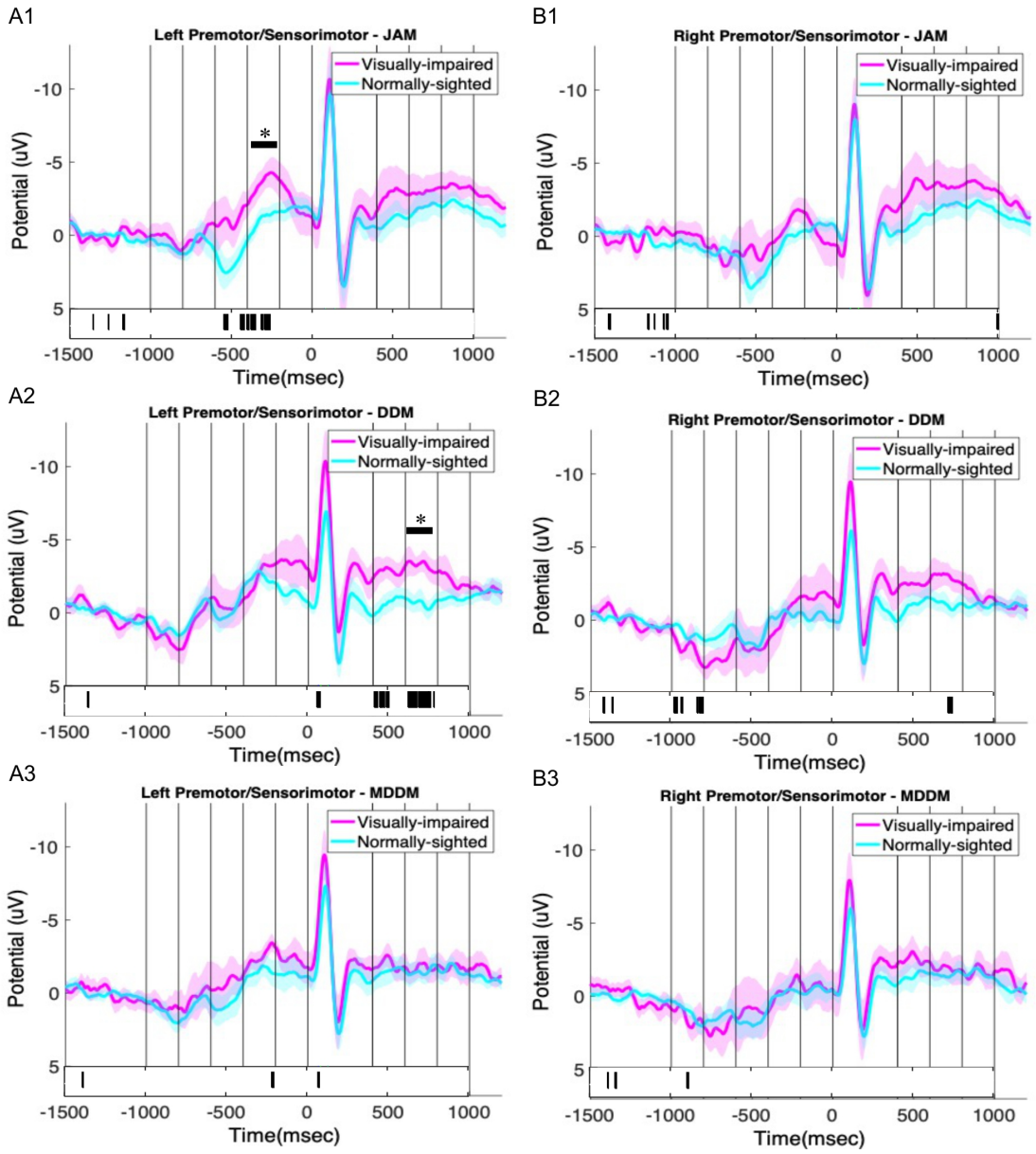

Figure 4.7: Comparisons of EEG negative potentials between subject groups.

When the potentials of two subject groups were compared, no significant difference was observed in the right hemisphere. On the other hand, in the left hemisphere, the visually-impaired subjects showed more negative potentials during passive movement period in JAM task, and the potential was more negative during active

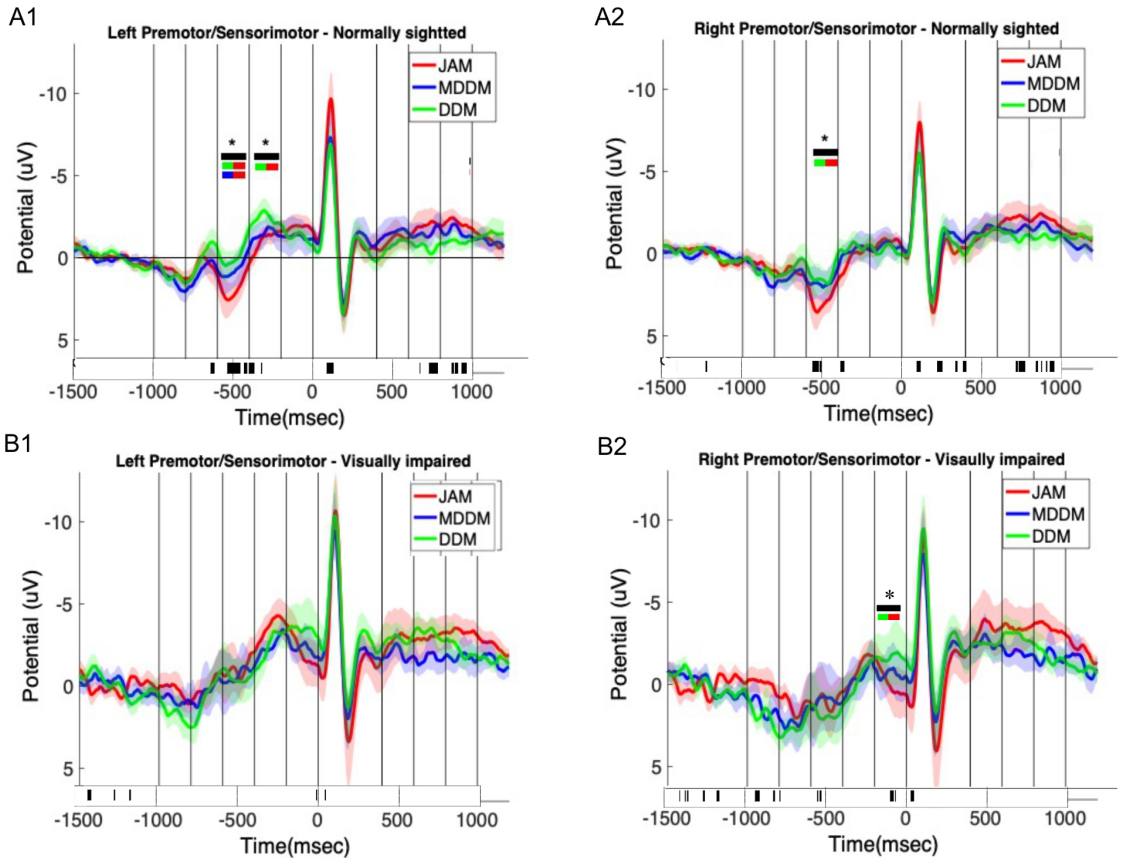

Figure 4.8: Comparisons of EEG negative potentials between tasks.

movement period in DDM task. Two subject groups did not display difference in MDDM task (Fig. 4.7).

In the task comparisons, both subject groups showed the greatest EEG activities in DDM task and the smallest in JAM task during passive movement period. However, during active movement period, JAM task showed the greatest level of EEG activities (Fig. 4.8).

4.4 Discussion

4.4.1 Similarities between EEG negative potentials and accuracy of limb position sense

In general, measured EEG negative potentials were consistent with the level of accuracy of arm matching tasks. The long-lasting greater level of negative EEG potentials in the left hemisphere of the visually-impaired group in JAM and DDM tasks can be associated with the larger arm matching accuracy errors of the visually impaired subjects in all tasks except MDDM, which did not have a group difference in the potentials (Fig. 4.7). Also, it can be seen that higher accuracy errors of both subject groups in DDM tasks are related to overall more negative EEG potentials of DDM task, whereas the EEG potentials for JAM task were less negative (Fig. 4.8). Therefore, task complexity reflected in the EEG negative potentials during the bilateral hand position matching tasks appear to affect the accuracy errors of hand position matching: task complexity is correlated with accuracy errors.

4.4.2 Possible preference of joint coordinate system in symmetric JAM and MDDM hand position matching tasks

One consisting result found in all hand position matching tasks was that both accuracy and the EEG negative potential levels of joint angle matching (JAM) and symmetric hand position matching (MDDM) tasks were similar even though the task instructions were different. On the other hand, symmetric (MDDM) and asymmetric hand position matching (DDM) tasks showed very different trends of accuracy and the EEG negative potentials in both subject groups, despite the subjects were instructed to use similar matching parameters that were defined in external Cartesian coordinate system: distance and direction from the initial point. In fact, joint angle matching and symmetric hand position matching tasks were kinematically identical, therefore, the latter can be performed either using joint or external coordinates. Also, obtained results suggest that the

task was less complex when the subjects performed joint angle matching (JAM task). Therefore, based on the similarities of accuracy and the EEG negative potential results, it is reasonable to think that the subjects preferably used either the joint coordinate system or external coordinate system for symmetric hand position matching tasks.

The current consensus on the mechanisms responsible for limb position sense is that signals generated by the muscle spindle afferents ascend to the somatosensory cortex and other cortical areas. These afferent signals generate sensations of position of limb segments with respect to each other (joint-based representation of position sense) and also sensations of position of the limb endpoint with respect to the body and external environment (Cartesian body-based representation) (Naito et al. 2016; Proske and Gandevia 2018). The latter representation requires the transformation from perceived joint angles to limb endpoint location, and this transformation is joint angle-dependent, nonlinear and requires an accurate estimation of the length of limb segments. Therefore, presumably, the subjects might prefer to use joint coordinate system in a situation where both coordinate systems are available.

4.4.3 Role of visual experience in hand position sense

Results of accuracy errors and the corresponding measured EEG negative potentials suggest that visual experience of the subject has positive effects on hand position sense in bilateral hand position matching regardless of the type of the tasks. In other words, the subjects with visual experience performed all types of hand position matching tests more accurately than the visually-impaired subject did, and for the sighted participants the matching tasks were less complex, as reflected in less negative EEG potentials (Fig. 4.7).

Therefore, our first hypothesis that visual experience improves hand position sense was supported by both accuracy errors and the EEG negative potentials.

Notably, the group differences in the EEG negative potentials were observed only in the left hemisphere. Also, the difference between the groups occurred during passive movement in JAM task and during active movement in DDM task. These results imply that visual experience of the subjects affects recognition of reference hand (the right hand) mainly. Also, it is probable that the subjects perceive position of the reference hand in joint coordinates and then convert it onto extrapersonal coordinates.

4.4.4 Task differences

Although the auditory (Kellogg 1962) and tactile (Postma et al. 2007) sensory modalities contribute importantly to the development of the spatial sense, individuals deprived of visual experience early in life might not be able to form an exact representation of the peripersonal space. This might affect the joint angle and hand position matching tasks in blind persons differently. The joint angle based task relies on the comparison of joint angle-related proprioceptive and tactile information from the left and right limbs, which does not require the knowledge of arm location in the external space (Proske 2015). On the other hand, hand positions in extrapersonal coordinates can be derived from the joint angle-related information, however, this derivation requires estimations of arm segment dimensions from body schema (Longo and Haggard 2010), which might be compromised in the blind because of the importance of visual experience for forming an accurate body schema (Cattaneo et al. 2008; Gross et al. 1974) and automatic remapping

between hand position in joint and external space by sighted individuals (Crollen and Collignon 2012).

Overall, during planning period (passive hand movement), both subject groups showed more negative EEG potentials in DDM task and the smallest in JAM task (Fig. 4.8). Therefore, our second hypothesis that hand position matching in external space would be a more complex task and lead to greater accuracy error was supported. However, according to Fig. 4.8, the task differences seem to be clearer in the sighted subjects wherein the difference occurred in both hemisphere and had many significant differences at each sampling point, marked as black bars.

4.5 Conclusion

The obtained results showed that the EEG negative potentials are highly associated with accuracy levels of hand position sense, which suggests task complexity the subject perceived is reflected in the EEG negative potentials. In addition, the results clearly suggest that visual experience affects hand position sense in positive way, by improving accuracy and reducing perceived task complexity. Therefore, the first hypothesis of this study that visual experience improves hand positioning sense was supported. The difference in EEG activities between two subject groups occurred in the left hemisphere, and it implies that the visual experience is closely connected with reference hand position recognition than active hand matching execution.

Another finding was that both symmetric matching tasks, JAM and MDDM, had very similar results in accuracy errors and task complexity even though they had different instructions for subjects. Since results of the same were quite different from an asymmetric

DDM task, we suggest that the subjects might prefer to use joint coordinates for both tasks. Since the two tasks are kinematically identical and arm matching using joint coordinates appear to be perceived as less complex, it is reasonable to think that the subjects preferably used joint coordinates.

CHAPTER 5. AIM 4: EFFECTS OF SELF-REINNERVATION OF HAMSTRINGS, QUADRICEPS AND SARTORIUS ON PRECISION OF HINDPAW POSITION CONTROL DURING THE SWING PHASE OF LEVEL WALKING IN THE CAT

5.1 Introduction

As described in Chapter 1, three major factors affect precision and accuracy of limb endpoint position sense: (i) limb posture, (ii) visual experience, and (iii) input from muscle spindle afferents. Specific Aims 1 through 3 determined the role of the first two factors in precision and accuracy of limb endpoint position sense in human blind and sighted participants. The third factor can be addressed using analysis of precision of hindpaw position control during the swing phase of walking in the cat after the monosynaptic input muscle spindle Ia afferents is removed by self-reinnervation of the major knee muscles (Cope et al. 1994).

It is well established that complete loss of proprioception in people with large-fiber sensory neuropathy severely disrupts limb position sense and motor performance during arm reaching movement (Ghez et al. 1995; Rothwell et al. 1982; Sainburg et al. 1993). These patients show uncoordinated, jerky, unsteady movements. Similar uncoordinated movements have been observed in locomoting transgenic mice with genetically removed muscle spindles (Akay et al. 2014) – these mice generally show loss of inter-joint coordination during the swing phase and changed activity patterns primarily in flexor

muscles. The above studies strongly suggest that proprioceptive sensory feedback is critical for proper movement control. One important component of proprioceptive feedback is responsible for limb position sense and originates from muscle spindle group Ia and II afferents (Proske and Gandevia 2018). Activation of these afferents in humans by tendon vibration evokes illusions of joint motion and changed joint position in the direction of stretch of the vibrated muscle (McCloskey 1978; Roll and Vedel 1982).

On the other hand, degrading input from the muscle spindles by muscle self-reinnervation that removes muscle stretch reflex (Cope et al. 1994; Lyle et al. 2016) does not appear to have a substantial effect on kinematics of level and upslope walking in the cat, but affects kinematics of only downslope walking in which self-reinnervated muscles undergo lengthening contraction (Abelew et al. 2000; Gregor et al. 2018; Maas et al. 2007). The lack of stretch reflex in self-reinnervated muscles is explained by failure of muscle spindle Ia afferents to activate motoneurons via monosynaptic connections (Bullinger et al. 2011). It is still possible that the limb position-related information contained in activity of spindle primary Ia and secondary II afferents from the self-reinnervated muscles reaches interneurons in the spinal cord and brain and is used for proper movement control.

Alternatively, removal of monosynaptic input from Ia afferents and possible degradation of input from the secondary spindle afferents after self-reinnervation of ankle extensors (Abelew et al. 2000; Gregor et al. 2018; Maas et al. 2007) do affect limb position sense but deficits of level and upslope walking are minor for other reasons. One such reason may be that ankle angle-related information can be supplied by intact ankle flexors, e.g. tibialis anterior. Another reason may be that ankle angle position information is less important for proper control of the whole hindlimb kinematics and paw position than

sensory information from more proximal joints, the knee and hip, due to a relatively short foot length.

According to the uncontrolled manifold analysis (Klishko et al. 2014), cats stabilize (control) their horizontal and vertical hindpaw positions during the swing phase of walking (especially immediately before and after the stance phase) by coordinated changes of limb segment angles. Since cats cannot see their hindpaws, this stabilization must be based on hindlimb position sense. Therefore, analysis of hindpaw position at the terminal and initial swing phase may reveal the effects of muscle spindle input disturbance on hindpaw position sense.

The experiments described below were conducted to investigate the effects of self-reinnervation of major knee flexors and extensors on precision of hindpaw position control during the swing phase of walking in the cat. If one assumes that self-reinnervation of major knee muscles substantially degrades hindlimb position sense, the following changes in locomotion kinematics should occur: (1) precision of paw placement at terminal and early swing during level walking should decrease (paw position variability should increase) and (2) the typical coordination of joint angles that maintains invariant hindlimb orientation and length (Chang et al. 2009) should be disrupted. These two expectations were tested.

5.2 Methods and materials

All surgical and experimental procedures were conducted in agreement with the Principles of Laboratory Animal Care (NIH publication No.86-23, revised 1985) as approved by the Georgia Tech Institutional Animal Care and Use Committee.

5.2.1 Animal characteristics and training

Four adult female cats (mass 3.1±0.59 kg; mean ± SD, Table 5.1) were investigated in this study. The animals were trained with food reinforcement to walk on a custom-made Plexiglas-enclosed walkway (3.0 m x 0.4 m) (Fig. 5.1). The walkway was equipped with three force plates (16 cm x 11 cm and 11 cm x 7 cm; Bertec Corporation, Columbus, OH, USA) and covered with a non-slip rubber mat; for more details see (Gregor et al. 2006; Prilutsky et al. 2011). Training period lasted between 2 and 4 weeks. In last several training sessions, the animals were trained to wear 28 small reflective markers. After training and before surgical procedures, full body kinematics during level, upslope (27^{o}) and downslope (-27^{o}) walking were recorded in each animal (see below).

5.2.2 Surgical procedures

All cats underwent two surgical procedures: (1) implantation of EMG electrodes in major hindlimb muscles and (2) self-reinnervation of hamstring, quadriceps and sartorius. Details of these procedures have been described elsewhere (Gregor et al. 2018; Prilutsky et al. 2011). All surgeries were performed in aseptic conditions under general isoflurane anesthesia. Teflon-insulated multi-stranded stainless-steel fine wires (CW5402; Cooner Wire, Chatsworth, CA, USA) were passed subcutaneously along the back from the skull to an incision in the right hindlimb. The other side of the wires connected to a multi-pin connector was fixed on the cat skull with screws and dental cement. A thin strip of insulation (~1 mm) was removed from the fine wires passed to the hindlimb, and a pair of wires was secured inside the muscle belly. Mild electrical stimulations were applied to the

Table 5.1 Cat characteristics.

Cat	Sex	Mass (kg)	Thigh length (cm)	Shank length (cm)	Tarsal length (cm)
Cat 1 (We)	Female	2.55	97	100.5	58.5
Cat 2 (Cr)	Female	3.02	94	95	61.5
Cat 3 (St)	Female	2.96	95.5	108.5	67
Cat 4 (Sq)	Female	3.94	103	102.5	63.5
Mean±SD	-	3.1±0.59	97.4±3.9	101.6±5.6	62.6±3.6

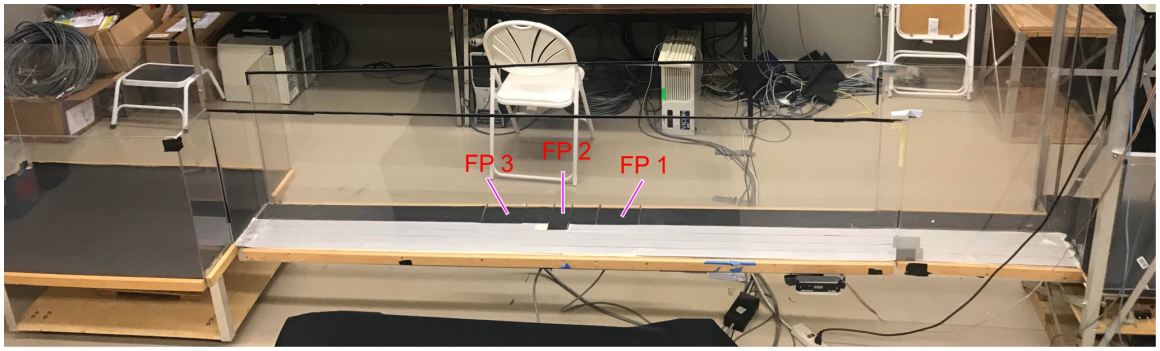

Figure 5.1: A custom-made Plexiglas-enclosed walkway with three force plates.

hindlimb muscles through the head connector to verify wire placements by observation of muscle twitches. The implanted muscles included biceps femoris posterior (hip extensor, knee flexor, BFP), biceps femoris anterior (hip extensor, BFA), rectus femoris (hip flexor, knee extensor, RF), vastus lateralis or vastus medialis (knee extensors, VA), medial gastrocnemius (knee flexor, ankle extensor, MG) and soleus (ankle extensor, SO). The cats received pain medicine for three days and antibiotics for ten days during the recovery. The animals recovered for 2 weeks.

After the cats fully recovered and recordings of baseline EMG and kinematics were finished (see below), second surgery was conducted to transect and reattach nerves innervating major muscles crossing the knee. These muscles were sartorius (anterior and medial heads), quadriceps (rectus femoris and vastus medial, lateral and intermedius heads), biceps femoris anterior and posterior heads, semimembranosus and semitendinosus. After incision of skin above the target muscle and nerve, the nerve was identified and carefully separated from surrounding tissues. The nerve was transected by sharp scissors and the denervation was verified by mild electrical stimulation of the proximal nerve stump. The transected nerve stumps were aligned with each other and attached together with fibrin glue (equal parts of thrombin and a 1:1 mixture of fibrin and fibronectin; Sigma-Aldrich, St. Louis, MO, USA). To relive stress on the reattached nerve stumps, several stitches were placed in the epineurium using absorbable vicryl 5-0 suture. The animals recovered after surgery for one week. Measurements of EMG and kinematics during level and slope walking were conducted periodically over the next 6-9 months to monitor recovery of EMG and locomotor mechanics.

5.2.3 Locomotion experiment

Locomotion experiments were conducted before and after the nerve transection/repair surgeries to measure walking kinematics of the cats along with EMG activities from the right hindlimb muscles. Baseline data collection was performed 3-5 days a week, 2 times a day for 4-5 weeks. After nerve transection and repair surgery, data collection was conducted periodically every 2-3 months to monitor recovery of locomotion and EMG activity. During the data collection, the cats received food reward right after they walked across the walkway in each direction. Each crossing of the walkway was considered as a single trial. The recording sessions continued until the cats stopped their self-initiated walking.

In order to record walking kinematics, 28 light-reflective markers were placed using double-sided adhesive on the anatomical landmarks indicated in Fig. 5.2; see details in (Farrell et al. 2014; Prilutsky et al. 2005). 3D marker positions were recorded using a motion capture system equipped with 6 cameras (Vicon Motion Systems Ltd, Oxford, UK) at a sampling rate of 120Hz. The three components of ground reaction force and its point of application were recorded at a sampling of 360 Hz by 3 small force plates (Bertec Corporation, Columbus, OH, USA) embedded in the walkway during cat walking. EMG signals were collected through a flexible shielded cable (Cooner Wire, Chatsworth, CA,

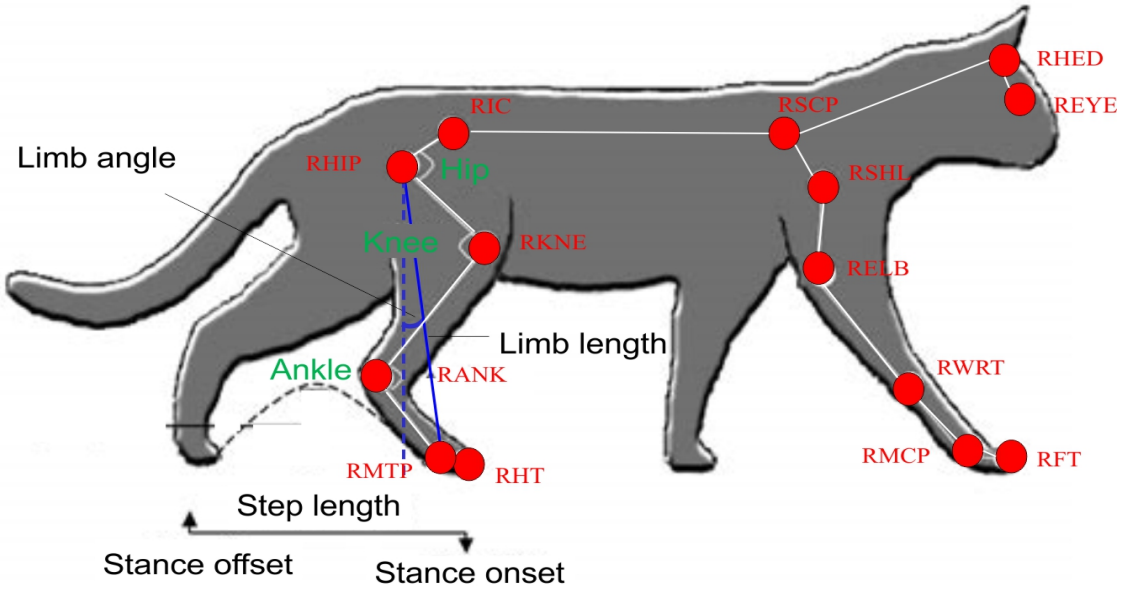

Figure 5.2: A schematic of cat biomechanical model and locations of reflective markers. Red circles represent reflective markers attached to the cat body on both sides (only right markers are shown). The corresponding body landmarks are: right and left iliac crest (RIC and LIC), right and left hip joints (RHIP and LHIP), right and left knee joints (RKNE and LKNE), right and left ankle joints (RANK and LANK), right and left metatarsophalangeal joints (RMTP and LMTP), right and left hindlimb toes (the distal end of the digits; RHT and LHT), right and left scapulars (RSCP and LSCP), right and left shoulder joints (RSHL and LSHL), right and left elbow joints (RELB and LELB), right and left wrist joints (RWRT and LWRT), right and left metacarpophalangeal joints (RMCP and LMCP), right and left forelimb toes (the distal end of the digits; RFT and LFT), right and left heads (near entrance to the ear canal, RHED and LHED), and right and left eyes (lateral corner of the eye; REYE and LEYE). The hindlimb length is defined as the distance from the hip marker to the MTP marker; the hindlimb angle is the angle of the hindlimb with respect to the vertical, angle is positive when the hindlimb line is in front of the vertical.

USA) attached to the head plug. EMG signals were samples at 3000 Hz, band-pass filtered (30-1000 Hz, 3dB), amplified (100x), and saved on a PC. Locomotor data collection was completed in 6-9 months after the animals recovered locomotion (no visible limping was observed) and EMG activity of recorded self-reinnervated muscles did not show changes

over several months, as assessed qualitatively. After completion of locomotion experiments, a terminal experiment was conducted on each animal to test stretch reflexes in selected self-reinnervated muscles (i.e., VA and RF) in the laboratory of Dr. T. Richard Nichols (Lyle et al. 2016; Nichols 2018).

5.2.4 Data Analysis

For the purpose of this study only level walking was analysed. Analysis included kinematics of joint angles, limb length and orientation of the right hindlimb with self-reinnervated knee muscles and the left intact hindlimb. In addition, interlimb interaction moments were computed during the swing phase. EMG activity was not analysed, however EMG recordings were used for monitoring the recovery process.

5.2.4.1 Joint angle parameters

To test effects of self-reinnervation of knee muscles on walking kinematics, several parameters of ankle and knee joint angle trajectories were analyzed for both reinnervated and intact hindlimbs. The joint angle parameters included (1) the swing flexion magnitude (joint angle change from toe off to maximum flexion during swing), (2) the joint yield (joint angle change from touchdown to the minimum angle in stance), and (3) the joint push-off (joint angle change from the minimum angle in stance to toe off). For the hip joint, (1) the flexion magnitude and (2) extension magnitude during the walking cycle were analyzed. For computing the above kinematic parameters, recorded positions of body markers were low-pass filtered (Butterworth zero phase lag, 4^{th} order filter with cutoff frequency of 6 Hz). Positions of the knee marker were recalculated using marker positions on the ankle and hip and measured lengths of the shank and thigh (Table 5.1) to reduce

errors caused by skin motion (Goslow Jr et al. 1973). Ankle, knee and hip joint angles, as well as hindlimb length and orientation (see Fig. 5.2) were computed for each recorded video frame. These mechanical variables were time normalized to the walking cycle duration and averaged for each percent of cycle time across cycles within each cat and across cats.

5.2.4.2 Hindlimb orientation and length

Hindlimb orientation and length were calculated to investigate changes in whole-limb kinematics. The hindlimb orientation was defined as the angle between the vertical and line connecting the hip and MTP markers. The hindlimb length was defined as the distance between the hip and MTP markers (Fig. 5.2). The minimum limb length during swing was determined.

5.2.4.3 Precision of hindlimb paw (MTP marker) positioning at stance onset and offset

To measure precision or repeatability of hindpaw positioning at the stance onset and offset during walking, relative location of the MTP joint with respect to the hip were calculated at stance onset and offset. Data from multiple trials were fitted by 95% confidence ellipse (Johnson and Wichern 2007), and area of the ellipse was used as an index of precision of paw positioning.

5.2.4.4 Interaction intersegmental moments

Interaction intersegmental moments were computed for qualitative analysis of hindlimb swing dynamics. The limb dynamics have been reported to depend on presence of proprioceptive feedback (Sainburg et al. 1995). The equations for computing

intersegmental interaction moments were adopted from (Hoy and Zernicke 1986). Computed moments at each joint include effects of hip linear acceleration, angular velocity and acceleration of the proximal and distal segments, and gravitational effects of the distal segments. The interaction joint moments were computed for the swing phase of walking. Inertial properties of the hindlimb segments (mass, moment of inertia, position of the center of mass) were computed from measured cat mass and segment length using the regression equations reported in (Hoy and Zernicke 1985). Resultant muscle moments at the ankle, knee and hip joints were also computed.

5.2.5 Statistical analysis

To investigate effects of muscle self-reinnervation one joint angle and whole hindlimb kinematics, a linear mixed model analyses (West et al. 2015) were performed for each dependent kinematic variable. Self-reinnervation (pre and post) and Hindlimb (right, self-reinnervated and left, intact) were considered within subject fixed independent factors; cats and trials were random factors.

Since multiple trials were needed to generate one precision ellipse for each condition and cat, statistical tests on paw positioning precision were conducted after combining stance offset and onset data to increase statistical power. The effects of self-reinnervation on the area of precision ellipses of paw positioning were analyzed with a two-way repeated measures ANOVA. Within subject independent factors were Self-Reinnervation (pre and post) and Hindlimb (right, self-reinnervated and left, intact).

To examine effects of self-reinnervation of right knee muscles on intersegmental and joint moments, the moment values for each joint were averaged over a 5%-swing time window. These values served as dependent variables in the linear mixed analysis with one fixed factor Self-reinnervation and random factors cats and trials, as described above.

All statistical tests were performed using IBM SPSS v21 software (Chicago, IL, USA). The significance level for all tests was set at an alpha level of 0.05, and the Bonferroni post-hoc test was used for pairwise comparisons.

5.3 Results

5.3.1 Joint angles parameters

Time-normalized hindlimb joint angle trajectories of all cats are presented in Fig. 5.3. Self-reinnervation of knee muscles had significant effects on all analyzed parameters of the ankle angle across both hindlimbs: (1) swing flexion ($F(1,178)=47.464$, $p<0.001$), (2) stance yield ($F(1,178)=7.101$, $p=0.008$), and (3) stance push-off ($F(1,178)=36.944$, $p<0.001$). As shown in Fig. 5.4A, all joint parameters of the right ankle (self-reinnervated side) decreased after self-reinnervation. Similar changes were observed in the left ankle of the intact hindlimb except the left ankle yield in stance did not change after self-reinnervation. Results of the corresponding pair-wise comparisons of ankle angle changes for the intact and self-reinnervated hindlimbs were: swing flexion: ($F(1,178)=12.340$, $p=0.001$; affected) and ($F(1,178)=25.837$, $p<0.001$; affected); stance yield: ($F(1,178)=2.591$, $p=0.109$; unaffected) and ($F(1,178)=4.660$, $p=0.032$; affected); stance push-off: ($F(1,178)=12.019$, $p=0.001$; affected) and ($F(1,178)=39.393$, $p<0.001$; affected).

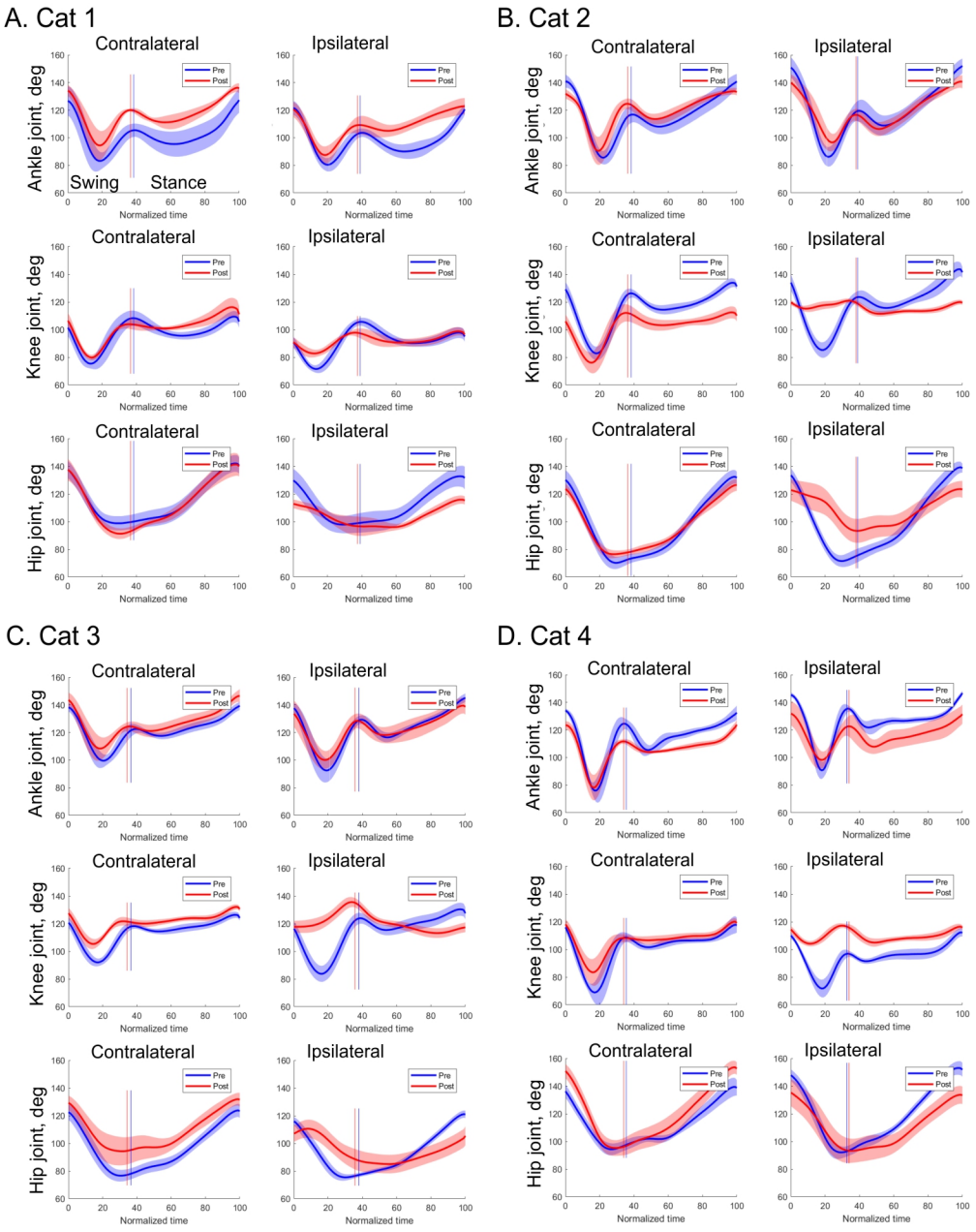

Figure 5.3: Time-normalized joint angle trajectories of left (intact) and right (affected) hindlimb during walking of each cat. The first, second, and third rows represent the ankle, knee, and hip joints, respectively. Intact condition data are plotted with blue lines and shades (mean±SD), and the data for self-reinnervation condition are plotted with red lines and shades.

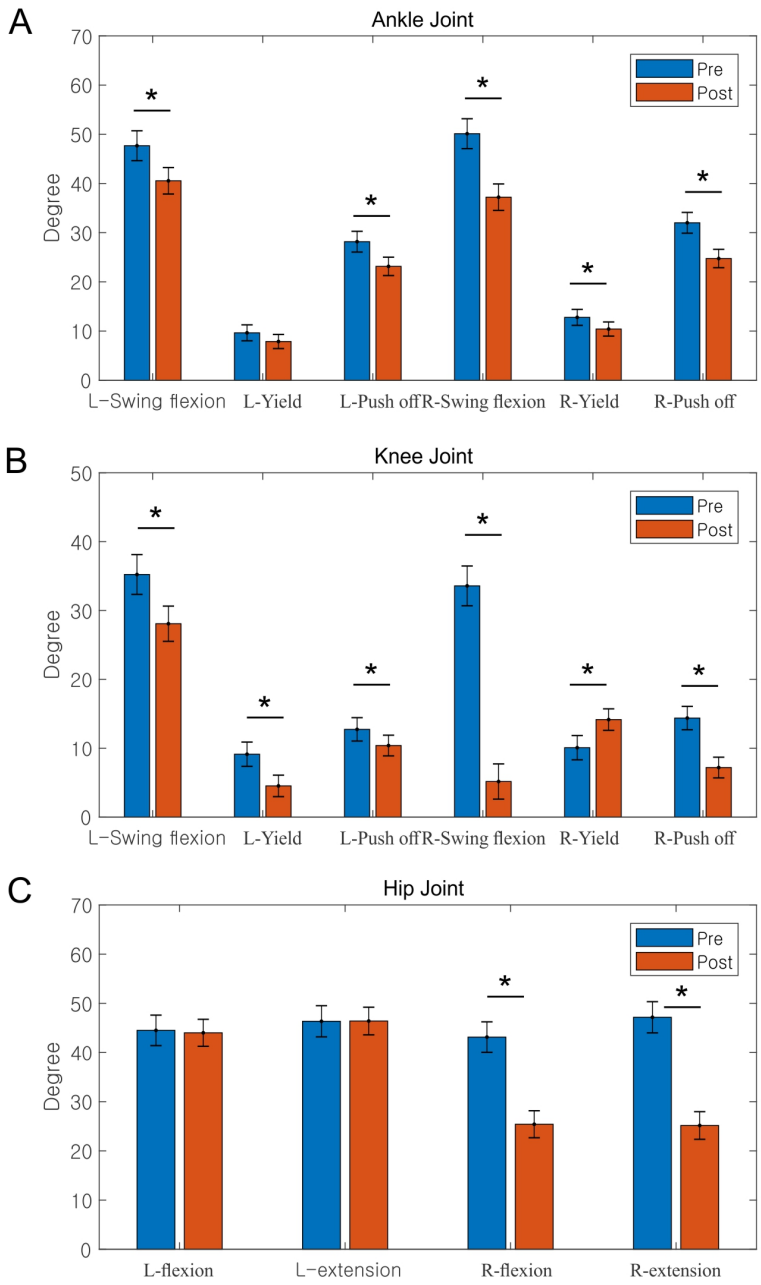

Figure 5.4: Comparisons of joint angle parameters for left (intact) and right (affected) hindlimbs between pre and post self-reinnervation of knee muscles of the right hindlimb. Joint angle parameters are swing flexion, stance yield, and stance push-off. The pre and post data are represented by blue and red bars, respectively. Error bars are 95% confidence intervals. *, p>0.05, linear mixed model, Bonferonni pairwise post-hoc comparison.

Self-reinnervation of knee muscles had similar effects on the knee joint angle parameters. Post self-reinnervation, all knee joint parameters of intact and self-reinnervated hindlimbs decreased as shown in Fig. 5.4B (swing flexion: ($F(1,178)=13.366$, $p<0.001$; affected) and ($F(1,178)=211.197$, $p<0.001$; affected); stance yield: ($F(1,178)=14.872$, $p<0.001$; affected) and ($F(1,178)=11.691$, $p=0.001$; affected); stance push-off: ($F(1,178)=4.183$, $p=0.042$; affected) and ($F(1,178)=39.132$, $p<0.001$, affected). There was significant interaction between Self-reinnervation and Hindlimb factors for the knee joint: $F(1,178)=26.468$, $p<0.001$). In the hip joint, muscle self-reinnervation affected both flexion and extension angles (($F(1,178)=47.464$, $p<0.001$) and ($F(1,178)=7.101$, $p=0.008$), respectively).

The hip flexion and extension magnitudes decreased after the self-reinnervation only on the affected side ($F(1,178)=71.297$, $p<0.001$) and ($F(1,178)=105.130$, $p<0.001$), respectively) (Fig. 5.4C).

5.3.2 Hindlimb orientation and length

Trajectories of whole-limb kinematic variables, hindlimb orientation and length, are displayed in Fig. 5.5. Qualitatively, patterns of the limb orientation angle of left and right hindlimbs did not change after self-reinnervation of the knee muscles. According to the linear mixed model analysis, Self-reinnervation had a significant effect on the hindlimb angle at stance offset ($F(1,178)=13.591$, $p<0.001$). Post-hoc analysis revealed that the stance offset limb angle decreased after self-reinnervation on the affected side but not in

the contralateral side (Fig. 5.6A). The hindlimb angle at stance onset, on the other hand, decreased after self-reinnervation on both affected and unaffected sides (Fig. 5.6A).

Patterns of hindlimb length changed markedly after self-reinnervation of right knee muscles (Fig. 5.5). Specifically, the limb length on both sides shifted to smaller values. Limb lengths at stance offset and onset, and the minimum limb length became shorter after self-reinnervation for both left and right hindlimb – limb length at stance offset ($F(1,178)=4.534$, $p=0.035$; decreased) and ($F(1,178)=6.585$, $p=0.011$; decreased); limb length at stance onset: ($F(1,178)=12.317$, $p=0.001$; decreased) and ($F(1,178)=35.395$, $p<0.001$; decreased); and the minimum limb length in swing ($F(1,178)=6.833$, $p=0.010$; decresed) and ($F(1,178)=70.909$, $p<0.001$; decreased) (Fig. 5.6B).

5.3.3 Precision of paw positioning at stance onset and offset

Distributions of paw positions with fitted ellipses at stance onset and offset with respect to the hip marker position are presented for each cat in Fig. 5.7. Precision of paw positioning at stance onset and offset were affected by Self-reinnervation ($F(1,7)=15.888$, $p=0.005$), but not by Hindlimb ($F(1,7)=0.111$, $p=0.749$) factor. There was no significant interaction between these factors ($F(1,7)<0.001$, $p=0.989$). Post-hoc analyses showed that precision level of paw positioning was increased after the muscle self-reinnervation in affected hindlimb ($F(1,7)=8.738$, $p=0.021$), whereas unaffected side did not show change after the self-reinnervation (Fig. 5.8).

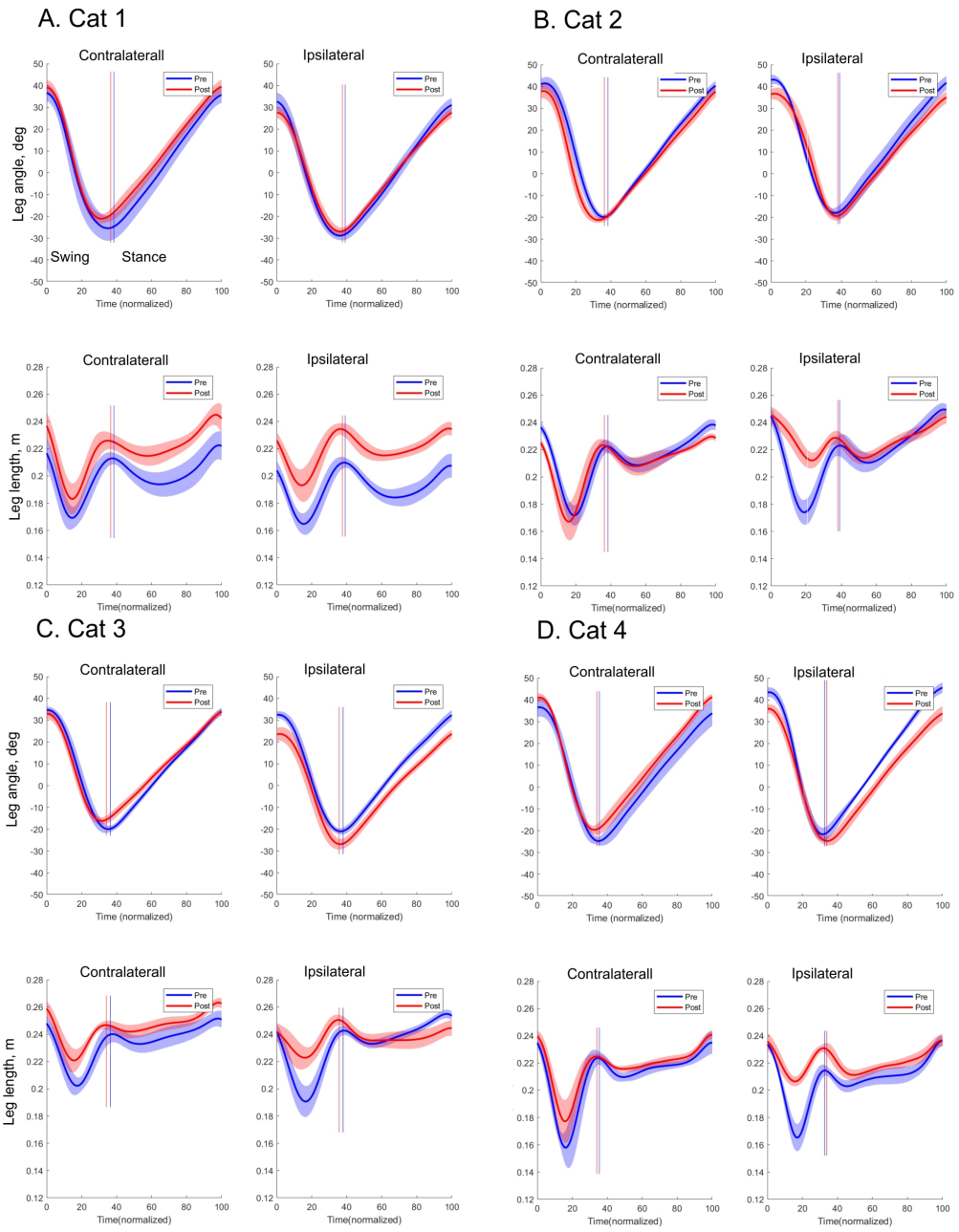

Figure 5.5: Time-normalized hindlimb angle and length during walking of each cat. The contralateral leg corresponds to the left (intact) hindlimb and the ipsilateral leg, to the right (affected) hindlimb. Pre self-reinnervation data are plotted with blue lines and shades (mean±SD) and Post self-reinnervation data are plotted with red lines and shades.

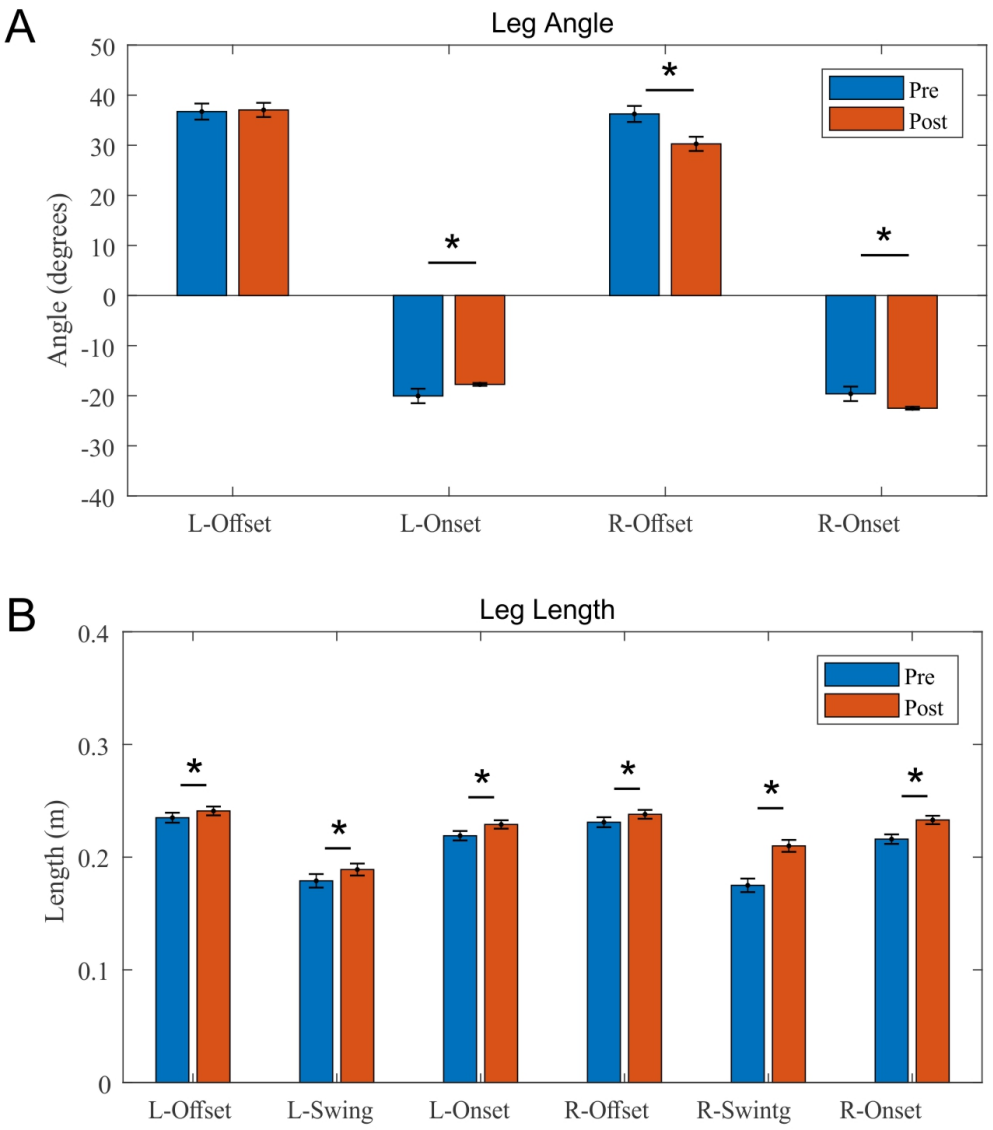

Figure 5.6: Hindlimb angle and length of left (L) and right (R) hindlimbs pre and post self-reinnervation of right knee muscles. Left and right hindlimbs are intact and affected hindlimbs. **A**: Hindlimb angles at stance onset and offset. **B**: Hindlimb length at stance onset and offset and at midswing. The pre and post data are represented by blue and red bars, respectively. Error bars are 95% confidence intervals. *, $p>0.05$, linear mixed model, Bonferonni pairwise post-hoc comparison.

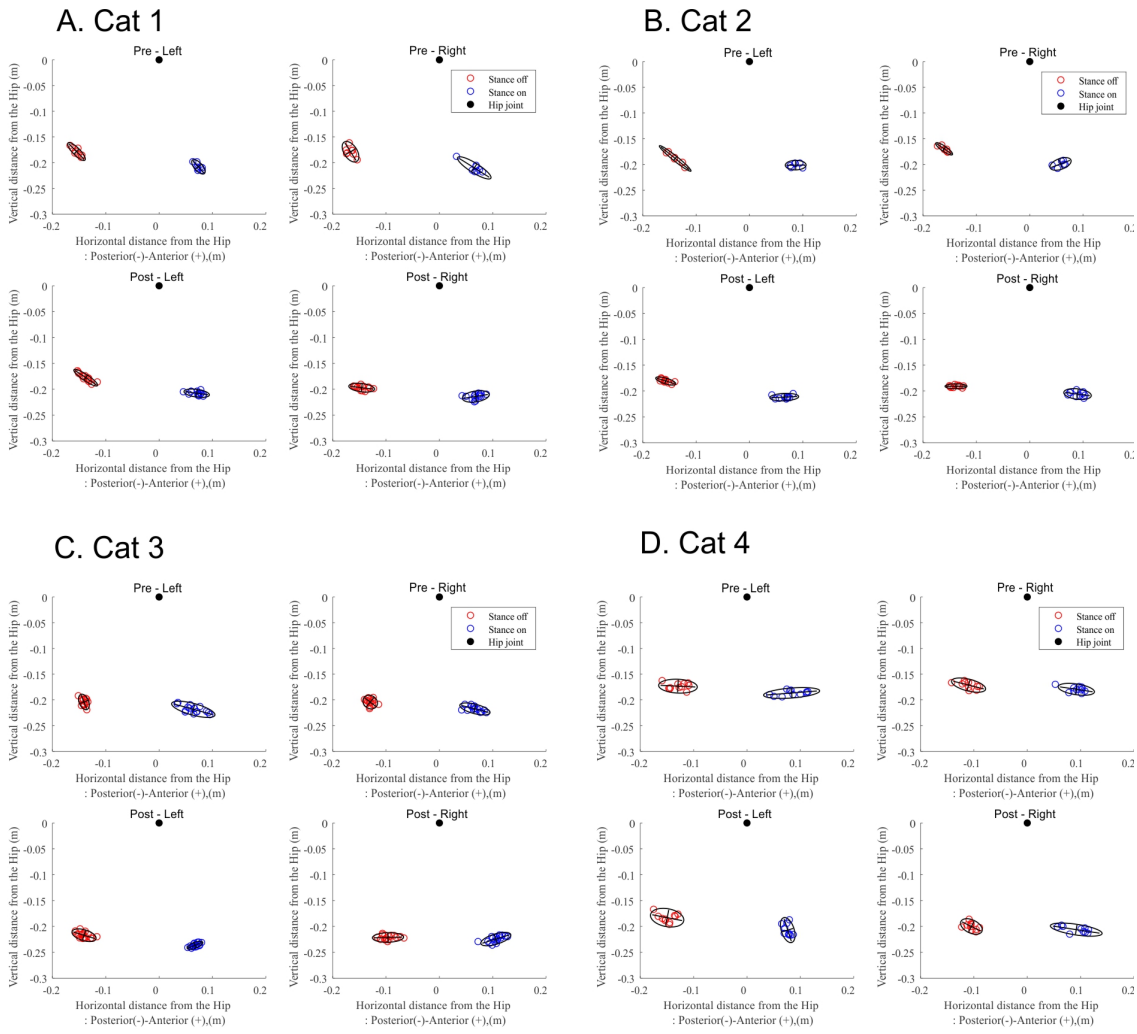

Figure 5.7: Distributions of paw positions (MTP marker locations) fitted with 95% confidence ellipses at stance onset and offset with respect to the hip joint. For each cat, the first and second columns display results of left (intact) and right (self-reinnervated) hindlimbs; the first and second rows present pre and post self-reinnervation conditions. Individual data from each trial is represented as red (stance offset) or blue (stance onset) circles. The black small circle at top center indicate the hip joint location.

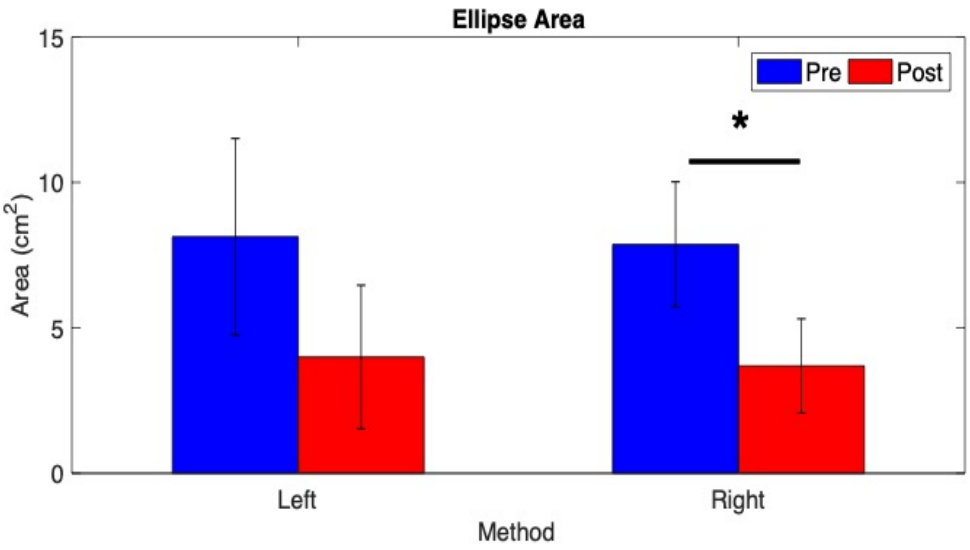

Figure 5.8: The area of the precision ellipse of paw positioning pre and post self-reinnervation of right knee muscles. The pre and post data are represented by blue and red bars. Error bars are 95% confidence intervals. *, p>0.05, repeated measures ANOVA, Bonferonni pairwise post-hoc comparison.

5.3.4 Intersegmental interaction moments of ipsilateral hindlimb

As follows from Fig. 5.9, interaction and muscle moments at each joint had opposite signs. That was especially apparent for the hip and ankle moments in the first half of the swing phase, as well as for all three joints in the last 30% of the swing period. Self-reinnervation of the right knee muscles changed the interaction and muscle moments at mid swing in the hip and ankle joints all cats but cat 1. For the knee joint, changes of the interaction moments occurred only in cats 2 and 4; whereas joint moments changed only in cat 4. No knee moment changes occurred in cats 1 and 3.

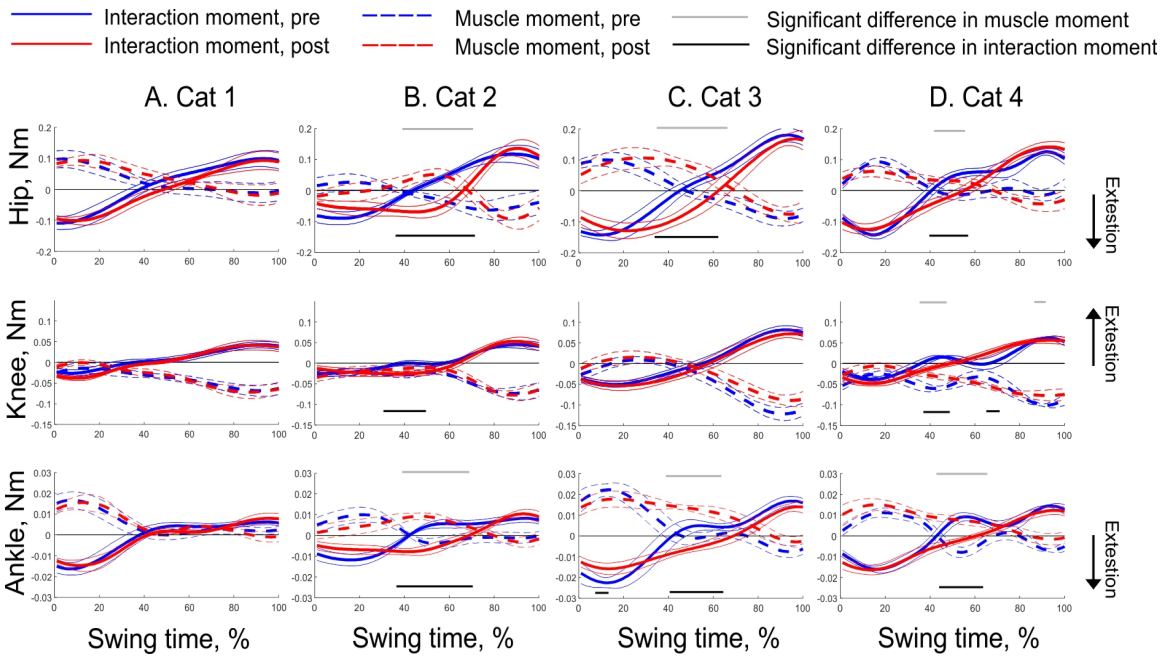

Figure 5.9: Intersegmental interaction and muscle moments at in the right (affected) hindlimb joints during swing phase. Solid and dotted lines represent interaction moment and muscle moments, respectively. Pre self-innervation condition data are plotted with blue lines and shades (mean±SD). Post self-reinnervation data are plotted with red lines and shades. Significant statistical difference between pre and post conditions are indicated by black (for interaction moment) or gray (muscle moment) horizontal lines in each panel.

5.4 Discussion

5.4.1 Tested hypotheses

The results of these experiments did not support the first hypothesis that self-reinnervation of major knee muscles would lead to lower precision of hindpaw placement at stance onset and offset. Contrary to expectations, the area of precision ellipse of the affected hindlimb decreased, while the area of the contralateral hindlimb ellipse had a tendency to decrease but did not reach significance (Fig. 5.8). The second hypothesis was

largely supported as the hindlimb length of both hindlimbs became longer over the walking cycle (Fig. 5.6B) and the leg orientation angle of the affected hindlimb changed its values at the stance onset and offset.

Previous studies have reported that self-reinnervation the cat ankle extensors did not cause noticeable changes in kinematics of level and upslope walking (Gregor et al. 2018; Maas et al. 2007), while Chang et al. (2009) showed that patterns of whole-limb kinematics such as limb length and orientation were conserved after self-reinnervation of ankle extensors. Thus, the results of this study suggest that self-reinnervation of more proximal muscles that include major antagonist muscles have greater effects on walking kinematics than those from distal joint muscles.

5.4.2 Possible adaptive mechanisms to improve precision of hindpaw placement in the affected hindlimb

The most unexpected result of this study was that self-reinnervation of major knee muscles improved precision of hindpaw position at terminal and early swing. Control of hindpaw position relies exclusively on limb position sense since visual or any other sensory information is unavailable. The nervous system appears to stabilize hindpaw position in the sagittal plane at terminal and early swing by coordinated changes of limb segment angles (Klishko et al. 2014). That is, the hindpaw position may be an important control variable during walking. The fact that the hindlimb kinematics during walking substantially changed after self-reinnervation of knee muscles suggests that hindlimb position sense was negatively affected. Given the above considerations, it is possible that the observed kinematic adaptations are aimed at improving stability of hindpaw placement. As I have

shown in Chapter 1, limb posture is capable of modulating precision of limb endpoint position. For example, although limb extension increases an overall area of the hindpaw precision ellipse, it significantly decreases the radial random error, the error in the direction of the limb line (see Fig. 2.2 C1). Thus, an extended hindlimb during walking after self-reinnervation of knee muscles (Fig. 5.6B) may reduce variability in this direction. The fact that the ellipse area of the hindpaw precision ellipse decreased post self-reinnervation suggests that additional factors apart from hindlimb may contribute.

One such factor may be co-activation of knee antagonists. Although, EMG activity was not quantitatively analyzed in this study, it appears from available raw EMG recordings that the knee extensor VA acquired an additional activity burst during the swing phase post self-reinnervation in all cats (Fig. 5.10). This burst coincided with an increased EMG burst of the knee flexor and hip extensor BFB. Note that no such co-activation occurred pre self-reinnervation. This co-activation of knee antagonists should increase knee stiffness and help reject perturbations arising from intersegment interaction moments and possible errors in control commands.

It is possible that these new EMG bursts were not consequences of purposeful motor adaptations to improve control of hindpaw position after muscle self-reinnervation. These new EMG bursts could simply originate from reinnervation of inappropriate targets,

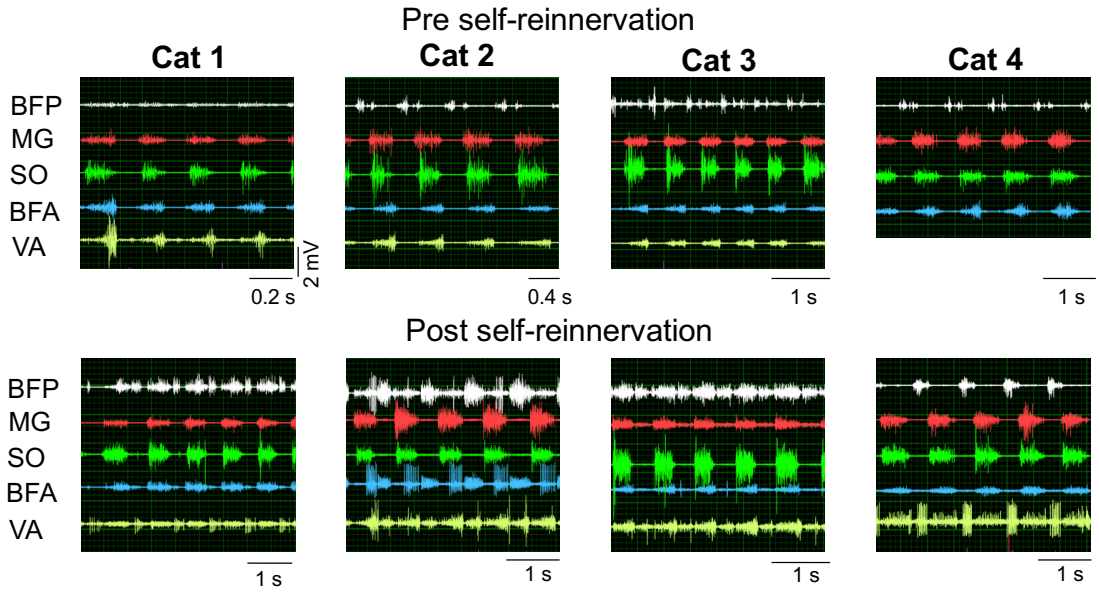

Figure 5.10: Examples of EMG recordings of right hindlimb muscles pre and post self-reinnervation of knee muscles during upslope walking.

e.g. VA muscle fibers could be partially reinnervated by the nerve of sartorius medial head. This possibility could not be excluded. On the other hand, self-reinnervation of ankle extensors soleus (SO), medial (MG) and lateral (LG) gastrocnemius did not change the differential activity of these muscles during paw shake responses – almost complete inhibition of SO and highly exaggerated activity of MG and LG (Mehta and Prilutsky 2014). If substantially inappropriate innervation occurred between SO and MG-LG nerves, the changes in activity patterns would have been apparent. Furthermore, co-activation of VA and BFP and an increased leg extension during the swing phase of walking has been reported in one subject who lost proprioception below the neck (Lajoie et al. 1996). Similar co-activation of elbow flexors and extensors was reported for hand movements in patients

lacking proprioception (Sainburg et al. 1995). This co-activation of antagonists may be useful to reject perturbations caused by interaction moments.

A reduced range of joint motion during the swing phase after self-reinnervation of knee muscles (Fig. 5.4), a more extended hindlimb (Fig. 5.6B) and co-activation of knee antagonist muscles (Fig. 5.10) appear to be advantageous for dealing with interaction moments when proprioceptive feedback is impaired. Pre self-reinnervation, the interaction and muscle moments change out of phase with each other in early and late stance. This is consistent with previous studies (Wisleder et al. 1990; Zubair et al. 2018). Post self-reinnervation, less coordinated changes between the interaction and muscle moments occurred at the ankle and hip joints; however, little changes can be seen at the knee (Fig. 5.9). Preservation of the knee moment patterns post self-reinnervation could result from the motor adaptations described above.

5.4.3 Role of spindle group Ia and II afferents in control of locomotion

Muscle self-reinnervation has been reported to remove stretch-reflex from the muscle (Cope et al. 1994; Cope and Clark 1993; Lyle et al. 2016). Stretch reflex removal has been explained by demonstrating retractions of monosynaptic connections of Ia afferents from motoneuron cell bodies (Alvarez et al. 2011). Loss of stretch reflex from ankle extensors after self-reinnervation has been implicated in the exaggerated ankle yield during stance of downslope walking, but the ankle yield in stance of level and upslope walking appeared to be normal (Abelew et al. 2000; Gregor et al. 2018; Maas et al. 2007). In this study, however, the stance knee yield increased post self-reinnervation, although the range of knee angle displacements decreased during the swing phase (Fig. 5.4B). These

results suggest that stretch reflex may play different roles in the knee extensors and flexors operating primarily during the stance and swing phases, respectively.

It is not currently known if polysynaptic pathways from spindle group Ia and II are intact post self-reinnervation and continue function properly. The role of these length-related afferents from muscles crossing knee and hip in the control swing-stance transitions has been well documented (Kriellaars et al. 1994; Lam and Pearson 2002; McVea et al. 2005; Stecina et al. 2005). It is shown in this study that post self-reinnervation, the swing onset started at a smaller hindlimb angle and stance onset, at a larger angle with respect to the vertical through the hip (Fig. 5.6 A). The latter result could be potentially explained by a reduced length feedback from hip extensors and sartorius (Lam and Pearson 2002; McVea et al. 2005; Stecina et al. 2005).

CHAPTER 6. SUMMARY AND CONCLUSIONS

6.1 Summary

Position sense is known to be affected by many factors (see Section 1.2). In this study, I have shown how limb posture, visual experience, and monosynaptic inputs from muscle spindle Ia afferents affect position sense. These factors are closely associated with position sense and are related to coordinate transformation from joint space to limb endpoint space. The coordinate transformation is an important part of limb endpoint perception in external space. The prior research to date has generated conflicting conclusions about the contribution of these factors to limb position sense. Therefore, I have identified the conflicting results, analyzed possible alternative interpretations of these results, formulated and tested new hypotheses. As a results, I obtained new information about the role of these factors in limb position sense by utilizing various theoretical and experimental approaches and was able to resolve some of the controversies in the literature.

In aim 1, I demonstrated that the better precision of hand position sense closer to the body than further away and in the radial direction than in the azimuth direction can be explained by the arm posture alone. The geometric model based on a nonlinear coordinate transformation from joint space to hand space reasonably predicted the experimentally obtained precision of hand position sense across a horizontal workspace. This result means that precision of hand position sense is affected by the transformation from joint to hand coordinates and thus by limb posture. Along with that, I showed that the direction of predicted arm precision ellipses is highly correlated with the direction of arm stiffness ellipses with nearly orthogonal relationship. This finding suggested a mechanistic

explanation for how the distribution of random errors of hand position sense is shaped by the arm stiffness.

In aim 2, I showed that visual experience improves position sense possibly due to developing a more accurate and precise representation of body schema and dimensions of body segments. Importantly, accuracy and precision of arm position sense of the sighted subjects was significantly better than that of the visually-impaired subjects. Both subject groups performed joint angle based position matching task (JAM) more accurately and precise than hand position based task (DDM). In term of precision, the sighted group displayed higher precision in JAM and MDDM tasks than in DDM task, whereas their precision of position sense was higher than in the blind. In task comparison, the sighted group had greater errors in DDM task compared to the other tasks, the blind did not display task differences. As a result, accuracy appears to be affected by visual experience more than precision.

In aim 3, it has been found that task complexity during hand position matching tasks, measured by an EEG event-related potential, is closely related to accuracy levels of hand position matching. This finding likely reflects the process of transformation of arm joint coordinates to hand external coordinates. Inspired from a previous study (Cui et al. 2000, a CNV-like negative EEG potential was measured in cued movement paradigm. In that paradigm, a warning signal was the onset of passive movement of the reference arm by robot and imperative stimulus was audio cue to start matching movement by the indicator arm. As a result, the measured negative potentials were more negative in the blind subjects who had greater accuracy errors. In addition, more negative potentials were

measured in DDM task than in JAM task, and result matched greater accuracy error in DDM task. Therefore, task complexity appeared to be related to accuracy errors.

Lastly, the role of monosynaptic input from muscle spindle Ia afferents from major knee muscles in control of hindpaw position during the swing phase was revealed in walking cats. Klishko et al. (2014) have reported that hindpaw position is stabilized by cats right before and after the stance phase by their coordinated changes in limb segment angles. Therefore, the hindpaw position control at these time instances of swing appeared a good model to address the role of muscle spindle input in precision of paw position control for the following reasons. First, this hindpaw position control must be based on proprioception and involve muscle spindle afferents, since the cat cannot see the hindpaw during walking. Second, monosynaptic input from muscle spindles can be disrupted by an invasive method such as muscle self-reinnervation. The analysis of precision of hindpaw position control revealed that the precision improved after self-reinnervation of knee muscles, even though joint kinematics and whole-limb kinematics have changed substantially. Specifically, joint angle ranges decreased across entire walking cycle and limb length became longer during the swing phase. I concluded that these changes were caused by a disruption of monosynaptic input from knee muscle spindle Ia inputs and achieved by adapting a new more extended hindlimb posture by the cat.

In this study, my goal was to investigate how limb posture, visual experience, and input from muscle spindle Ia afferents affect position sense. These three factors are important elements in coordinate transformation from joint space to limb endpoint space, and therefore in perception of the endpoint position in external space without vision. This research has contributed to deeper understanding of position sense.

6.2 Conclusions

6.2.1. Role of arm posture in hand position sense

The goal of aim 1 was to investigate role of arm posture in hand position sense. Previous studies have demonstrated that precision of hand position sense is non-uniform in a horizontal workspace. People perceive hand position more precisely in the radial than in azimuth direction and closer to the body than farther away. The reasons for this non-uniformity was not clear. Assuming that perception of hand position without vision requires a nonlinear transformation from the arm joint coordinates to hand Cartesian coordinates, I hypothesized that the arm posture contributes to the non-uniform precision of hand position sense. To test this hypothesis, I conducted a theoretical analysis of the transformation of random angle errors at shoulder and elbow joints into the corresponding hand position random errors for a two-joint arm model. The analysis revealed that hand precision ellipses were non-uniform in the horizontal workspace, their size increased with distance from the body, and they were oriented nearly orthogonal to the arm stiffness ellipses reported in the literature. I also measured precision of hand position sense in a bimanual hand position-matching task at four horizontal targets forming a square in front of the body in 11 right-handed healthy individuals. I found that the measured precision ellipses at all four targets were qualitatively similar to the predicted ones. The mean precision of hand position measured experimentally and predicted by the model was greater for the closer targets than for the distant ones and was greater in the radial and anterior-posterior direction than in the azimuth and left-right direction, respectively. I concluded that arm posture alone could explain the non-uniform precision of hand position sense in the horizontal workspace.

6.2.2. Role of visual experience in hand position sense

Position sense of arm segments with respect to each other originates from joint angle-related sensory information. Hand position sense with respect to external space can be derived from joint-related information using estimated dimensions of arm segments. Visual experience contributes to forming somatosensory representations of body segment dimensions and integration of somatosensory information encoded in joint-based and external coordinates. Thus, blindness may differentially affect the limb position sense in joint and external space coordinates. I examined the role of visual experience in arm position sense in joint angle matching and hand position matching tasks. Sighted (n=7) and age-matched blind participants (n=7) performed three arm matching tasks: joint angle matching (JAM), hand distance and direction matching (DDM), and hand distance and mirror direction matching (MDDM). In the latter two tasks, hand position was matched in external coordinates. The blind generally had lower accuracy and precision of arm position sense in joint angle and hand position matching than the sighted. I also found that the blind had the same precision of arm position sense in the joint angle matching and hand position matching tasks. I concluded that visual experience positively affects arm position sense possibly due to integration of visual and proprioceptive sensory information and the development of more accurate body schema. I suggested that similar precision of arm position sense in joint and external coordinates in the blind may result from a possible increase in perceptual acuity of other exteroceptors that could provide information about limb position in the peripersonal space.

6.2.3. Effects of visual experience on accuracy of hand position sense and task complexity during hand matching tasks in joint and external space.

The goal of my aim 3 was to determine the effects of visual experience on perception of task complexity during hand matching tasks in joint and external space. The task complexity was estimated by the magnitude of a negative EEG potential inspired by CNV. Two hypotheses were tested: (1) visual experience improves hand position sense (2) hand positioning in external space would be perceived as a more complex task and lead to lower accuracy. These hypotheses were tested using concurrent 64 channel EEG recordings and arm kinematic assessments derived from the KINARM robot. Accuracy of hand position sense and EEG activity in right-handed individuals with normal (n=7) and impaired (n=7) vision were measured during hand position matching tasks. Hand position matching tasks included (i) joint angle matching (JAM – hand position matching in joint coordinates), (ii) hand mirror direction and distance matching in external coordinates (MDDM) – kinematically identical to the JAM, and (iii) hand direction and distance matching in external coordinates (DDM) – kinematically different from the JAM and MDDM. It was found that measured EEG negative potentials showed substantial association with accuracy of hand position sense. Overall, the blind subjects demonstrated lower accuracy and perceived the tasks as more complex, i.e. had higher EEG negative potentials in the left parietal area. Both the blind and sighted subject groups demonstrated lower accuracy and perceived the DDM task as more complex. In addition, both symmetric matching tasks, JAM and MDDM (kinematically identical but based on different instructions), displayed very similar results in terms of accuracy and task complexity, which suggested that the subjects might use joint angle matching in both symmetric tasks.

6.2.4. Effects of self-reinnervation of major knee muscles on precision of hindpaw position control during the swing phase of level walking in the cat.

The goal of aim 4 was to determine the effects of self-reinnervation of hamstrings, quadriceps and sartorius muscles on hindpaw position control during walking in the cat. Since muscle self-reinnervation has been reported to substantially disrupt muscle-length dependent feedback from Ia afferents to motoneurons (Alvarez et al. 2011; Bullinger et al. 2011), I hypothesized that post self-reinnervation of knee muscles (1) precision of hindpaw position control at the terminal and initial swing during level walking should decrease (paw position variability should increase) and (2) the typical coordination of joint angles that maintains invariant hindlimb orientation and length (Chang et al. 2009) should be disrupted. Muscle nerves to the right hamstrings, quadriceps and sartorius muscles of 4 cats were surgically transected and repaired using fibrin glue. Mechanics and EMG activity of hindlimb muscles during level walking were recorded before and 6-9 months after surgery. Following self-reinnervation, the affected muscles recovered their EMG activity; however, hindlimb kinematics of both hindlimbs significantly changed. Range of motion decreased, bilaterally, during swing and stance at the ankle and hip, and at the knee during swing and the push-off phase of stance. Knee yield during stance increased in the affected and decreased in the sound hindlimb. Limb length during mid-swing and at stance onset (but not stance offset) increased bilaterally. The distribution area of random errors of hindpaw position (precision ellipse) at the terminal and initial swing phase decreased for both hindlimbs (precision increased). These results did not support hypothesis 1 but supported hypothesis 2. Given stabilization of paw position during the swing phase by coordinated changes of limb segment angles in intact cats (Klishko et al. 2014) and greater radial endpoint precision at longer limb lengths (see Chapter 2), I suggest that the observed kinematic adaptations improve precision of paw position of the affected hindlimb at the

terminal and initial swing. More extended hindlimb and greater knee flexor-extensor co-activation during swing could also help reduce knee interactive moments.

6.3. Future works

The central nervous system (CNS) represents the body in many coordinate systems and may choose among these representations during movement planning and execution (Kawato 1999). Interestingly, the accuracy and precision of kinematically identical tasks varies with task instructions, which implies that the CNS selects or weights multisensory information. For example, subjects more accurately judge fingertip position than elbow angle in the same one-joint position task in the horizontal plane; this was explained by possibly better access by the brain to the limb endpoint position information (Fuentes and Bastian 2010). The interactions among multisensory inputs are complicated: a slight change in shoulder posture disrupts the ability of deafferented monkeys to accurately reach a visual target by extending their elbow (Polit and Bizzi 1979). Therefore, further investigations of mechanisms by which CNS selects among multiple sensory inputs encoded in multiple coordinate frames can shed new light on fundamentals of position sense and accurate motor performance.

REFERENCES

Abelew TA, Miller MD, Cope TC, and Nichols TR. Local loss of proprioception results in disruption of interjoint coordination during locomotion in the cat. *J Neurophysiol* 84: 2709-2714, 2000.

Aimonetti JM, Hospod V, Roll JP, and Ribot-Ciscar E. Cutaneous afferents provide a neuronal population vector that encodes the orientation of human ankle movements. *J Physiol* 580: 649-658, 2007.

Aimonetti JM, Roll JP, Hospod V, and Ribot-Ciscar E. Ankle joint movements are encoded by both cutaneous and muscle afferents in humans. *Exp Brain Res* 221: 167-176, 2012.

Akay T, Tourtellotte WG, Arber S, and Jessell TM. Degradation of mouse locomotor pattern in the absence of proprioceptive sensory feedback. *Proceedings of the National Academy of Sciences of the United States of America* 111: 16877-16882, 2014.

Alary F, Goldstein R, Duquette M, Chapman CE, Voss P, and Lepore F. Tactile acuity in the blind: a psychophysical study using a two-dimensional angle discrimination task. *Exp Brain Res* 187: 587-594, 2008.

Alvarez FJ, Titus-Mitchell HE, Bullinger KL, Kraszpulski M, Nardelli P, and Cope TC. Permanent central synaptic disconnection of proprioceptors after nerve injury and regeneration. I. Loss of VGLUT1/IA synapses on motoneurons. *J Neurophysiol* 106: 2450-2470, 2011.

Batista AP, Santhanam G, Byron MY, Ryu SI, Afshar A, and Shenoy KV. Reference frames for reach planning in macaque dorsal premotor cortex. *Journal of neurophysiology* 2007.

Bhattacharyya R, Musallam S, and Andersen RA. Parietal reach region encodes reach depth using retinal disparity and vergence angle signals. *Journal of neurophysiology* 2009.

Bottasso CL, Prilutsky BI, Croce A, Imberti E, and Sartirana S. A numerical procedure for inferring from experimental data the optimization cost functions using a multibody model of the neuro-musculoskeletal system. *Multibody System Dynamics* 16: 123-154, 2006.

Bretscher O. *Linear Algebra with Application. 5th Edition*. Boston: Pearson, 2013.

Bullinger KL, Nardelli P, Pinter MJ, Alvarez FJ, and Cope TC. Permanent central synaptic disconnection of proprioceptors after nerve injury and regeneration. II. Loss of functional connectivity with motoneurons. *J Neurophysiol* 106: 2471-2485, 2011.

Buneo CA, Jarvis MR, Batista AP, and Andersen RA. Direct visuomotor transformations for reaching. *Nature* 416: 632, 2002.

Cappagli G, Cocchi E, and Gori M. Auditory and proprioceptive spatial impairments in blind children and adults. *Dev Sci* 20: 2017.

Casey KL. The somatosensory system. In: *Clinical examination of the nervous system*, edited by Gilman S. New York: McGraw-Hill, 1999, p. 175–211.

Cattaneo Z, Vecchi T, Cornoldi C, Mammarella I, Bonino D, Ricciardi E, and Pietrini P. Imagery and spatial processes in blindness and visual impairment. *Neuroscience and biobehavioral reviews* 32: 1346-1360, 2008.

Chang YH, Auyang AG, Scholz JP, and Nichols TR. Whole limb kinematics are preferentially conserved over individual joint kinematics after peripheral nerve injury. *J Exp Biol* 212: 3511-3521, 2009.

Clark F, Grigg P, and Chapin J. The contribution of articular receptors to proprioception with the fingers in humans. *Journal of Neurophysiology* 61: 186-193, 1989.

Clark FJ, Larwood KJ, Davis ME, and Deffenbacher KA. A metric for assessing acuity in positioning joints and limbs. *Experimental Brain Research* 107: 73-79, 1995.

Cohen DA, Prud'homme MJ, and Kalaska JF. Tactile activity in primate primary somatosensory cortex during active arm movements: correlation with receptive field properties. *J Neurophysiol* 71: 161-172, 1994.

Cole J, and Paillard J. Living without touch and peripheral information about body position and movement: Studies with deafferented subjects. *The body and the self* 245-266, 1995.

Collins DF, Refshauge KM, Todd G, and Gandevia SC. Cutaneous receptors contribute to kinesthesia at the index finger, elbow, and knee. *J Neurophysiol* 94: 1699-1706, 2005.

Cope TC, Bonasera SJ, and Nichols TR. Reinnervated muscles fail to produce stretch reflexes. *J Neurophysiol* 71: 817-820, 1994.

Cope TC, and Clark BD. Motor-unit recruitment in self-reinnervated muscle. *J Neurophysiol* 70: 1787-1796, 1993.

Crollen V, and Collignon O. Embodied space in early blind individuals. *Front Psychol* 3: 272, 2012.

Cui RQ, Egkher A, Huter D, Lang W, Lindinger G, and Deecke L. High resolution spatiotemporal analysis of the contingent negative variation. *Clin Neurophysiol* 111: 1847-1859, 2000.

Cuppone AV, Cappagli G, and Gori M. Audio feedback associated with body movement enhances audio and somatosensory spatial representation. *Frontiers in integrative neuroscience* 12: 37, 2018.

Delhaye BP, Long KH, and Bensmaia SJ. Neural Basis of Touch and Proprioception in Primate Cortex. *Comprehensive Physiology* 8: 1575, 2018a.

Delhaye BP, Long KH, and Bensmaia SJ. Neural Basis of Touch and Proprioception in Primate Cortex. *Compr Physiol* 8: 1575-1602, 2018b.

Denavit J, and Hartenberg RS. A kinematic notation for lower-pair mechanisms based on matrices. *Trans ASME J Appl Mech* 23: 215–221, 1955.

Edin B. Cutaneous afferents provide information about knee joint movements in humans. *J Physiol* 531: 289-297, 2001.

Farrell BJ, Bulgakova MA, Beloozerova IN, Sirota MG, and Prilutsky BI. Body stability and muscle and motor cortex activity during walking with wide stance. *J Neurophysiol* 112: 504-524, 2014.

Feldman AG. Space and time in the context of equilibrium-point theory. *Wiley Interdisciplinary Reviews: Cognitive Science* 2: 287-304, 2011.

Ferrell W, Gandevia S, and McCloskey D. The role of joint receptors in human kinaesthesia when intramuscular receptors cannot contribute. *The Journal of physiology* 386: 63-71, 1987.

Fiehler K, Reuschel J, and Rosler F. Early non-visual experience influences proprioceptive-spatial discrimination acuity in adulthood. *Neuropsychologia* 47: 897-906, 2009.

Flash T, and Mussa-Ivaldi F. Human arm stiffness characteristics during the maintenance of posture. *Experimental brain research* 82: 315-326, 1990.

Franklin DW, Liaw G, Milner TE, Osu R, Burdet E, and Kawato M. Endpoint stiffness of the arm is directionally tuned to instability in the environment. *The Journal of neuroscience : the official journal of the Society for Neuroscience* 27: 7705-7716, 2007.

Fuentes CT, and Bastian AJ. Where is your arm? Variations in proprioception across space and tasks. *J Neurophysiol* 103: 164-171, 2010.

Fujiwara Y, Lee J, Ishikawa T, Kakei S, and Izawa J. Diverse coordinate frames on sensorimotor areas in visuomotor transformation. *Scientific reports* 7: 14950, 2017.

Galletti C, Fattori P, Kutz DF, and Gamberini M. Brain location and visual topography of cortical area V6A in the macaque monkey. *European Journal of Neuroscience* 11: 575-582, 1999.

Gandevia SC, and Phegan CM. Perceptual distortions of the human body image produced by local anaesthesia, pain and cutaneous stimulation. *J Physiol* 514 (Pt 2): 609-616, 1999.

Gardner EP, Martin JP, and Jessell TP. The bodily senses. In: *Principles of neural science*, edited by Kandel. E. R.; Scwartz JHJ, T. M. New York: McGraw-Hill, 2000, p. 430-450.

Gaunet F, and Rossetti Y. Effects of Visual Deprivation on Space Representation: Immediate and Delayed Pointing toward Memorised Proprioceptive Targets. *Perception* 35: 107-124, 2006.

Gilman S. Joint position sense and vibration sense- anatomical organisation and assessment>. *J Neurol Neurosurg Psychiatry* 73: 473-477, 2002.

Goble DJ. Proprioceptive acuity assessment via joint position matching: from basic science to general practice. *Phys Ther* 90: 1176-1184, 2010.

Goble DJ, Coxon JP, Wenderoth N, Van Impe A, and Swinnen SP. Proprioceptive sensibility in the elderly: degeneration, functional consequences and plastic-adaptive processes. *Neuroscience and biobehavioral reviews* 33: 271-278, 2009.

Goslow Jr GE, Reinking RM, and Stuart DG. The cat step cycle: hind limb joint angles and muscle lengths during unrestrained locomotion. *Journal of Morphology* 141: 1-41, 1973.

Gregor RJ, Maas H, Bulgakova MA, Oliver A, English AW, and Prilutsky BI. Time course of functional recovery during the first 3 mo after surgical transection and repair of nerves to the feline soleus and lateral gastrocnemius muscles. *J Neurophysiol* 119: 1166-1185, 2018.

Gregor RJ, Smith DW, and Prilutsky BI. Mechanics of slope walking in the cat: quantification of muscle load, length change, and ankle extensor EMG patterns. *J Neurophysiol* 95: 1397-1409, 2006.

Gross Y, Webb R, and Melzack R. Central and peripheral contributions to localization of body parts: evidence for a central body schema. *Exp Neurol* 44: 346-362, 1974.

Hall LA, and McCloskey D. Detections of movements imposed on finger, elbow and shoulder joints. *The journal of physiology* 335: 519-533, 1983.

Held R, and Rekosh J. Motor-sensory feedback and the geometry of visual space. *Science* 141: 722-723, 1963.

Howard IS, Ingram JN, Kording KP, and Wolpert DM. Statistics of natural movements are reflected in motor errors. *J Neurophysiol* 102: 1902-1910, 2009.

Hoy MG, and Zernicke RF. Modulation of limb dynamics in the swing phase of locomotion. *J Biomech* 18: 49-60, 1985.

Hoy MG, and Zernicke RF. The role of intersegmental dynamics during rapid limb oscillations. *J Biomech* 19: 867-877, 1986.

Iandolo R, Squeri V, De Santis D, Giannoni P, Morasso P, and Casadio M. Proprioceptive bimanual test in intrinsic and extrinsic coordinates. *Front Hum Neurosci* 9: 72, 2015.

Itaguchi Y, and Fukuzawa K. Effects of arm stiffness and muscle effort on position reproduction error in the horizontal plane. *Perceptual and motor skills* 114: 757-773, 2012.

Jammalamadaka SR, Sengupta A, and ebrary Inc. Topics in circular statistics. In: *Series on multivariate analysis 5*. River Edge, N.J.: World Scientific, 2001.

Johnson RA, and Wichern DW. *Applied Multivariate Statistical Analysis*. Upper Saddle River, NJ 07458: Pearson Education, Inc, 2007.

Kawato M. Internal models for motor control and trajectory planning. *Curr Opin Neurobiol* 9: 718-727, 1999.

Kellogg WN. Sonar system of the blind. *Science* 137: 399-404, 1962.

Kennett S, Taylor-Clarke M, and Haggard P. Noninformative vision improves the spatial resolution of touch in humans. *Current biology : CB* 11: 1188-1191, 2001.

Kistemaker DA, Van Soest AKJ, Wong JD, Kurtzer IL, and Gribble PL. Control of position and movement is simplified by combined muscle spindle and Golgi tendon organ feedback. *American Journal of Physiology-Heart and Circulatory Physiology* 2012.

Klishko AN, Farrell BJ, Beloozerova IN, Latash ML, and Prilutsky BI. Stabilization of cat paw trajectory during locomotion. *J Neurophysiol* 112: 1376-1391, 2014.

Kriellaars DJ, Brownstone RM, Noga BR, and Jordan LM. Mechanical entrainment of fictive locomotion in the decerebrate cat. *J Neurophysiol* 71: 2074-2086, 1994.

Laboissiere R, Lametti DR, and Ostry DJ. Impedance control and its relation to precision in orofacial movement. *J Neurophysiol* 102: 523-531, 2009.

Lajoie Y, Teasdale N, Cole JD, Burnett M, Bard C, Fleury M, Forget R, Paillard J, and Lamarre Y. Gait of a deafferented subject without large myelinated sensory fibers below the neck. *Neurology* 47: 109-115, 1996.

Lam T, and Pearson KG. Sartorius muscle afferents influence the amplitude and timing of flexor activity in walking decerebrate cats. *Exp Brain Res* 147: 175-185, 2002.

Lametti DR, and Ostry DJ. Postural constraints on movement variability. *J Neurophysiol* 104: 1061-1067, 2010.

Lessard N, Pare M, Lepore F, and Lassonde M. Early-blind human subjects localize sound sources better than sighted subjects. *Nature* 395: 278-280, 1998.

Longo MR, and Haggard P. An implicit body representation underlying human position sense. *Proc Natl Acad Sci U S A* 107: 11727-11732, 2010.

Longo MR, Mancini F, and Haggard P. Implicit body representations and tactile spatial remapping. *Acta psychologica* 160: 77-87, 2015.

Lyle MA, Prilutsky BI, Gregor RJ, Abelew TA, and Nichols TR. Self-reinnervated muscles lose autogenic length feedback, but intermuscular feedback can recover functional connectivity. *J Neurophysiol* 116: 1055-1067, 2016.

Maas H, Prilutsky BI, Nichols TR, and Gregor RJ. The effects of self-reinnervation of cat medial and lateral gastrocnemius muscles on hindlimb kinematics in slope walking. *Exp Brain Res* 181: 377-393, 2007.

Makin TR, Holmes NP, and Zohary E. Is that near my hand? Multisensory representation of peripersonal space in human intraparietal sulcus. *Journal of Neuroscience* 27: 731-740, 2007.

Maravita A, Spence C, and Driver J. Multisensory integration and the body schema: close to hand and within reach. *Current biology : CB* 13: R531-539, 2003.

Matthews PB. Proprioceptors and their contribution to somatosensory mapping; complex messages require complex processing. *Canadian journal of physiology and pharmacology* 66: 430-438, 1988.

McCloskey DI. Kinesthetic sensibility. *Physiol Rev* 58: 763-820, 1978.

McVea DA, Donelan JM, Tachibana A, and Pearson KG. A role for hip position in initiating the swing-to-stance transition in walking cats. *J Neurophysiol* 94: 3497-3508, 2005.

Medina J, and Coslett HB. From maps to form to space: touch and the body schema. *Neuropsychologia* 48: 645-654, 2010.

Mehta R, and Prilutsky BI. Task-dependent inhibition of slow-twitch soleus and excitation of fast-twitch gastrocnemius do not require high movement speed and velocity-dependent sensory feedback. *Front Physiol* 5: 410, 2014.

Merlet J-P. Jacobian, Manipulability, Condition Number, and Accuracy of Parallel Robots. *Journal of Mechanical Design* 128: 199, 2006.

Milner TE. Contribution of geometry and joint stiffness to mechanical stability of the human arm. *Exp Brain Res* 143: 515-519, 2002.

Mon-Williams M, Wann JP, Jenkinson M, and Rushton K. Synaesthesia in the normal limb. *Proceedings Biological sciences / The Royal Society* 264: 1007-1010, 1997.

Mussa-Ivaldi FA, Hogan N, and Bizzi E. Neural, mechanical, and geometric factors subserving arm posture in humans. *Journal of Neuroscience* 5: 2732-2743, 1985.

Naito E, Morita T, and Amemiya K. Body representations in the human brain revealed by kinesthetic illusions and their essential contributions to motor control and corporeal awareness. *Neurosci Res* 104: 16-30, 2016.

Nardone A, Tarantola J, Miscio G, Pisano F, Schenone A, and Schieppati M. Loss of large-diameter spindle afferent fibres is not detrimental to the control of body sway during upright stance: evidence from neuropathy. *Experimental brain research* 135: 155-162, 2000.

Nava E, Steiger T, and Roder B. Both developmental and adult vision shape body representations. *Sci Rep* 4: 6622, 2014.

Nichols TR. Distributed force feedback in the spinal cord and the regulation of limb mechanics. *J Neurophysiol* 119: 1186-1200, 2018.

Oh K, and Prilutsky BI. Contributions of arm posture to non-uniform precision of hand position sense in a horizontal workspace. *J Neurophysiol*, in review, 2019.

Oldfield RC. The assessment and analysis of handedness: the Edinburgh inventory. *Neuropsychologia* 9: 97-113, 1971.

Perreault EJ, Kirsch RF, and Crago PE. Voluntary control of static endpoint stiffness during force regulation tasks. *J Neurophysiol* 87: 2808-2816, 2002.

Pesaran B, Nelson MJ, and Andersen RA. Dorsal premotor neurons encode the relative position of the hand, eye, and goal during reach planning. *Neuron* 51: 125-134, 2006.

Plooy A, Tresilian JR, Mon-Williams M, and Wann JP. The contribution of vision and proprioception to judgements of finger proximity. *Exp Brain Res* 118: 415-420, 1998.

Polit A, and Bizzi E. Characteristics of motor programs underlying arm movements in monkeys. *J Neurophysiol* 42: 183-194, 1979.

Postma A, Zuidhoek S, Noordzij ML, and Kappers AM. Differences between early-blind, late-blind, and blindfolded-sighted people in haptic spatial-configuration learning and resulting memory traces. *Perception* 36: 1253-1265, 2007.

Prilutsky BI. Coordination of two- and one-joint muscles: functional consequences and implications for motor control. *Motor control* 4: 1-44, 2000.

Prilutsky BI, Maas H, Bulgakova M, Hodson-Tole EF, and Gregor RJ. Short-term motor compensations to denervation of feline soleus and lateral gastrocnemius result in preservation of ankle mechanical output during locomotion. *Cells Tissues Organs* 193: 310-324, 2011.

Prilutsky BI, Sirota MG, Gregor RJ, and Beloozerova IN. Quantification of motor cortex activity and full-body biomechanics during unconstrained locomotion. *J Neurophysiol* 94: 2959-2969, 2005.

Prochazka A, and Gorassini M. Ensemble firing of muscle afferents recorded during normal locomotion in cats. *The Journal of physiology* 507: 293-304, 1998.

Proske U. The role of muscle proprioceptors in human limb position sense: a hypothesis. *J Anat* 227: 178-183, 2015.

Proske U, and Gandevia SC. Kinesthetic senses. *Compr Physiol* 8: 1157-1183, 2018.

Proske U, and Gandevia SC. The proprioceptive senses: their roles in signaling body shape, body position and movement, and muscle force. *Physiol Rev* 92: 1651-1697, 2012.

Ribot-Ciscar E, Bergenheim M, Albert F, and Roll JP. Proprioceptive population coding of limb position in humans. *Exp Brain Res* 149: 512-519, 2003.

Roll JP, and Vedel JP. Kinaesthetic role of muscle afferents in man, studied by tendon vibration and microneurography. *Exp Brain Res* 47: 177-190, 1982.

Rossetti Y, Gaunet F, and Thinus-Blanc C. Early visual experience affects memorization and spatial representation of proprioceptive targets. *NeuroReport* 7: 1219-1225, 1996.

Rossetti Y, Meckler C, and Prablanc C. Is there an optimal arm posture? Deterioration of finger localization precision and comfort sensation in extreme arm-joint postures. *Experimental Brain Research* 99: 131-136, 1994.

Sainburg RL, Ghilardi MF, Poizner H, and Ghez C. Control of limb dynamics in normal subjects and patients without proprioception. *J Neurophysiol* 73: 820-835, 1995.

Sainburg RL, Poizner H, and Ghez C. Loss of proprioception produces deficits in interjoint coordination. *J Neurophysiol* 70: 2136-2147, 1993.

Sainburg RL, and Schaefer SY. Interlimb differences in control of movement extent. *J Neurophysiol* 92: 1374-1383, 2004.

Sandwell DT. Biharmonic spline interpolation of GEOS-3 and SEASAT altimeter data. *Geophysical research letters* 1987.

Sarlegna FR, Gauthier GM, Bourdin C, Vercher JL, and Blouin J. Internally driven control of reaching movements: a study on a proprioceptively deafferented subject. *Brain Res Bull* 69: 404-415, 2006.

Scott SH, and Loeb GE. The Computation of Position Sense from Spindles in Mono- and Multiarticular Muscles. *J Neurosci* 14: 7529-7540, 1994.

Shadmehr R, and Wise SP. *Computational neuroscience. The computational neurobiology of reaching and pointing: A foundation for motor learning.* Cambridge, MA, US: MIT Press, 2005.

Sherrington CS. On the proprio-ceptive system, especially in its reflex aspect. *Brain* 29: 467-482, 1907.

Slinger RT, and Horsley V. Upon the orientation of points in space by the muscular, arthrodial, and tactile senses of the upper limbs in normal individuals and in blind persons. . *Brain* 29: 1-27, 1906.

Soechting JF. Does position sense at the elbow reflect a sense of elbow joint angle or one of limb orientation? *Brain Res* 248: 392-395, 1982.

Soechting JF, and Terzuolo CA. An algorithm for the generation of curvilinear wrist motion in an arbitrary plane in three-dimensional space. *Neuroscience* 19: 1393-1405, 1986.

Spong MW, and Vidyasagar M. *Robot dynamics and control*. New York: Wiley, 1989, p. xvi, 336 p.

Stecina K, Quevedo J, and McCrea DA. Parallel reflex pathways from flexor muscle afferents evoking resetting and flexion enhancement during fictive locomotion and scratch in the cat. *J Physiol* 569: 275-290, 2005.

Stevens JC, Foulke E, and Patterson MQ. Tactile acuity, aging, and braille reading in long-term blindness. *J Exp Psychol Appl* 2: 91-106, 1996.

Sturnieks DL, Wright JR, and Fitzpatrick RC. Detection of simultaneous movement at two human arm joints. *J Physiol* 585: 833-842, 2007.

Thinus-Blanc C, and Gaunet F. Representation of Space in Blind Persons: Vision as a Spatial Sense? *Psychological Bulletin* 121: 20-42, 1997.

Tsay AJ, Giummarra MJ, Allen TJ, and Proske U. The sensory origins of human position sense. *J Physiol* 594: 1037-1049, 2016.

van Beers RJ, Sittig AC, and van der Gon JJD. The precision of proprioceptive position sense. *Exp Brain Res* 122: 367-377, 1998.

Walter WG, Cooper R, Aldridge VJ, McCallum WC, and Winter AL. Contingent Negative Variation: An Electric Sign of Sensorimotor Association and Expectancy in the Human Brain. *Nature* 203: 380-384, 1964.

Watson D. *Contouring: a guide to the analysis and display of spatial data*. Elsevier, 2013.

West BT, Welch KB, and Gatecki AT. *Linear Mixed Models. A Practical Guide using Statistical Software*. Boca Raton, FL: CRC Press, 2015.

Wilson ET, Wong J, and Gribble PL. Mapping Proprioception across a 2D Horizontal Workspace. *PLoS One* 5: 2010.

Wise A, Gregory J, and Proske U. Detection of movements of the human forearm during and after co-contractions of muscles acting at the elbow joint. *The Journal of physiology* 508: 325-330, 1998.

Wisleder D, Zernicke RF, and Smith JL. Speed-related changes in hindlimb intersegmental dynamics during the swing phase of cat locomotion. *Exp Brain Res* 79: 651-660, 1990.

Wong J, Wilson ET, Malfait N, and Gribble PL. Limb stiffness is modulated with spatial accuracy requirements during movement in the absence of destabilizing forces. *J Neurophysiol* 101: 1542-1549, 2009.

Zubair HN, Stout EE, Dounskaia N, and Beloozerova IN. The role of intersegmental dynamics in coordination of the forelimb joints during unperturbed and perturbed skilled locomotion. *J Neurophysiol* 120: 1547-1557, 2018.

VITA

Kyunggeune Oh

Kyunggeune Oh was born in Chonan, South Korea. He received his B.S. and M.S. in mechanical and aerospace engineering from Seoul National University in Seoul, South Korea. During his five years of work experience at the Korea Institute of Science and Technology in Seoul, he conducted advanced research pertaining to the development of the heads and faces of humanoid robots for human-robot interaction. In the last two years, his research has focused on biomedical robotics and the development of a lower-limb rehabilitation robot and robotic instruments for brain surgery. He has published two journal papers and nine conference papers and registered four US patents. He is currently a doctoral candidate in the School of Biological Science at the Georgia Institute of Technology, where he is investigating neurobiomechanical mechanisms of position sense and motor control in human upper limbs and the hindlimb of the cat. His study was funded by the National Science Foundation and the National Institutes of Health.